Contract Report 655

Dynamic Modeling and Monitoring of Water, Sediment, Nutrients, and Pesticides in Agricultural Watersheds during Storm Events

by

Deva K. Borah, Maitreyee Bera, Susan Shaw, and Laura Keefer

Prepared for the
Illinois Groundwater Consortium

September 1999

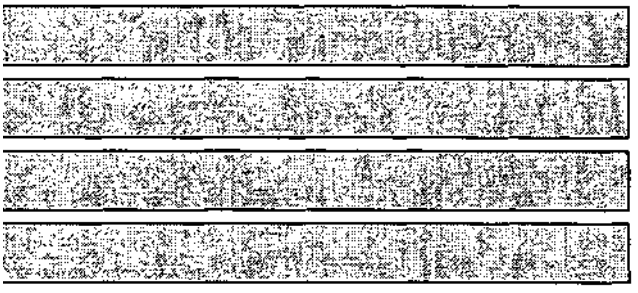

Illinois State Water Survey
Watershed Science Section
Champaign, Illinois

A Division of the Illinois Department of Natural Resources

Dynamic Modeling and Monitoring of Water, Sediment, Nutrients, and Pesticides in Agricultural Watersheds during Storm Events

by

Deva K. Borah, Maitreyee Bera, Susan Shaw, and Laura Keefer

Illinois State Water Survey
Watershed Science Section
2204 Griffith Drive
Champaign, Illinois 61820-7495

A Division of the Illinois Department of Natural Resources

Prepared for the
Illinois Groundwater Consortium
Southern Illinois University at Carbondale
Carbondale, Illinois 62901-4709

Subcontract Numbers: 97-03 & 98-06
Project Numbers: 1-5-28718 & 1-5-28923

September 1999

The Illinois Groundwater Consortium was funded by Congressional appropriations through the U.S. Department of Agriculture to Southern Illinois University at Carbondale. Members are the Illinois State Geological Survey, Illinois State Water Survey, Southern Illinois University at Carbondale and at Edwardsville, and University of Illinois Agricultural Experiment Station and Cooperative Extension Services.

The findings and recommendations in this report are not necessarily those of the funding agencies.

ISSN 0733-3927

Executive Summary

Each year large quantities of fertilizer and herbicides are applied to Midwestern farm fields. In a recent investigation, the White House Committee on Environment and Natural Resources (Goolsby et al., 1999) found elevated concentrations of nitrate-nitrogen (nitrate-N) in Midwestern streams and rivers. Some central Illinois drinking water supplies (Decatur, Danville, Pontiac, and Georgetown) periodically exceed the drinking water standard of 10 milligrams per liter (mg/L) of nitrate-N that was set to prevent incidence of methemoglobinemia (blue baby syndrome). Fertilizer application is not the only source of these elevated nitrate-N concentrations, other manmade and natural sources such as atmospheric deposition and fixation of N, and mineralization of organic N contribute significantly to the problem. Other drinking water sources, such as Lake Springfield, require expensive water treatments when they periodically exceed 3 micrograms per liter (µg/L) maximum concentration level (MCL) for atrazine, a commonly used herbicide.

Upland soil and streambank erosion, and sediment deposition are also critical water quantity and quality issues in Illinois. Erosion causes loss of fertile soil, streambank erosion causes loss of valuable lands, and both contribute large quantities of sediment in water flowing through streams and rivers that cause turbidity in sensitive biological resource areas and fill streambeds and banks, lakes, and reservoirs. Lake Decatur, Lake Springfield, and Peoria Lake are a few of the examples. Eroded soil and sediment also carry chemicals that pollute water bodies and stream/reservoir beds.

Runoff water from farm fields, collected in creeks or streams through tile drains or small ditches, contains significantly high concentrations of sediment and agricultural chemicals that pollute receiving water bodies during early stages of planting (late spring or early summer). Agricultural chemicals include chemicals applied through fertilizer, herbicides, and pesticides, and chemicals produced naturally most importantly atmospheric deposition, fixation, and mineralization. Understanding and dealing with these complex hydrologic, soil erosion, and sediment and contaminant transport processes and the associated problems have been quite a challenge for scientists and engineers. Mathematical models are becoming invaluable tools to analyze these complex processes and to evaluate land use and best management practices (BMPs) in reducing the damaging effects of flooding, soil erosion, sedimentation, and contamination on drinking water supplies and other valuable water resources. Existing and commonly used models are limited because they are not physically based and cannot simulate the dynamic behaviors of the water and its constituents' movements.

In a 1999 report, *New Strategies for America's Watersheds*, published by the National Research Council, the Committee on Watershed Management analyzed the current status of watershed modeling for decision making. The Committee concluded that the available models and methods are outdated, and "a major modeling effort is needed to develop and implement state-of-the-art models for watershed evaluation." Existing physically based models are computational and data intensive, and too cumbersome for

practical use in large watersheds. Therefore, new physically based and efficient models must be developed to simulate the spatially and temporarily varying physical and chemical processes in watersheds ranging in size from farm fields to river basins.

An effort is underway at the Illinois State Water Survey (ISWS) in which a dynamic watershed simulation model (DWSM) is being developed using physically based governing equations to simulate propagation of flood waves, entrainment and transport of sediment, and all agricultural chemicals commonly used in agricultural and rural watersheds. The model has three major components: hydrology, soil erosion and sediment transport, and nutrient and pesticide transport. These model components, adopted from earlier work of the lead author, have efficient routing schemes based on approximate analytical solutions of the physically based governing equations, and preserving the dynamic behaviors of the water, sediment, and accompanying chemical movements. These and other model formulations and procedures are described in this report. The nutrient and pesticide component is limited to transport of these chemicals with surface runoff and sediment considering adsorption and desorption and based on initial chemical concentrations dissolved with pore water and adsorbed with soil particles on the ground surface and in the near surface soil matrix. Reactions and transformations of the chemicals are not simulated.

During this two-year study, the first two components of the DWSM were tested on subwatersheds of the 925-square-mile Upper Sangamon River basin in east-central Illinois that drains into Lake Decatur, using data previously collected by the ISWS and intensive storm data collected during this study. The ISWS established an extensive monitoring network in this watershed, from which it has been collecting streamflow and nitrogen data since 1993. Monitoring was conducted in response to a legal commitment by the city of Decatur to the Illinois Environmental Protection Agency (IEPA) to reduce concentrations of nitrate-N in the lake to levels below the drinking water standard by the year 2001.

The hydrology component of the DWSM was tested on the entire Upper Sangamon River basin using data collected earlier by the ISWS. The model performed well in predicting peak flows and time to peak flows in the five monitored subwatersheds ranging in size from 38 to 112 square miles. However, the model underpredicted the recession and base flow portions of the hydrographs, as well as the runoff volumes from the larger subwatersheds due to the lack of tile drain and base flow simulation capabilities.

Detailed flow and concentrations of suspended sediment, nitrate-N, phosphate-phosphorous (phosphate-P), atrazine, and metolachlor were collected during 1998 spring storm events at the Big Ditch station, draining a 38-square-mile subwatershed of the Lake Decatur watershed. During 1999, the same types of data, except metolachlor, were collected at Big Ditch and two other stations on the main stem of the Sangamon River: Fisher and Mahomet draining, respectively, 240 and 360 square miles of the Upper Sangamon River or Lake Decatur watershed. Rainfall data were collected from newly established raingages: one at Big Ditch during 1998 and five others throughout the Upper

Sangamon River watershed above Mahomet during 1999. Rainfall data from the six stations varied noticeably from station to station, especially between the three eastern and three western stations.

In the above monitored data, all the constituents closely followed the flow hydrograph except nitrate-N. The nitrate-N concentration varied inversely with water discharge, decreasing drastically during rising and peak flows and increasing with the recession and base flow portions of the hydrographs. Such variations may be due to runoff pathways. For example, runoff through subsurface soil and the tile drain contains more nitrate-N than runoff over the ground surface (surface runoff). Therefore, peak flows contributed primarily by surface runoff contain less nitrate-N concentrations than water in the recession and base flows contributed primarily by the tile drain and subsurface flows flowing through the soil matrix. Another reason could be a limited release of nitrate-N from the soil where the threshhold could be reached before the peak flow and beyond dilution until the flow decreases to a level that is lower than the threshhold.

The monitored constituent data were analyzed to confirm consistencies within different sampling methods, and to develop statistical relationships of suspended sediment and chemical concentrations with the observed flow. The results confirmed consistencies of grab and automatic ISCO sampling procedures while monitoring suspended sediment, nitrate-N, and phosphate-P. Both grab and ISCO sampling were further confirmed using depth-width-integrated sampling methods to monitor suspended sediment.

The correlation equations of suspended sediment, nitrate-N, phosphate-P, atrazine, and metolachlor concentrations with flow are consistent with the observations made above. The relationships showed exponential increase in suspended sediment and exponential decay in nitrate-N, power, and logarithmic functions for phosphate-P, atrazine, and metolachlor with respect to water discharge. In addition to a combined relation for each of the constituents with respect to water discharge, separate equations were developed for each month during the monitoring period. These relationships suggest that concentrations of the constituents have different strong correlations with water discharge in different months representing different times in the growing season with varying climate and ground cover conditions.

The flow data monitored at the Big Ditch station were used to test and compare two different hydrologic algorithms of the DWSM: runoff curve number and interception-infiltration procedures. Both algorithms performed well in predicting peak and time to peak flows of intense storms, but the curve number algorithm performed better in predicting less intense storms. Sediment data monitored at Big Ditch were used to test the sediment component of the DWSM. The model performed well in predicting intense storms but poorly for less intense storms, probably due to model inability to simulate tile and base flows. Testing the nutrient and pesticides component of the DWSM is in progress and will continue in followup studies.

The study provides a valuable database of continuous rainfall, runoff, sediment, nitrogen, phosphorous, atrazine, and metolachlor in an east-central Illinois watershed collected during storm events. These data help us understand some of the complex physical and chemical processes in the watershed. Complete understanding would require more research and intensive data collection. The study also provides the model as an advanced tool for engineers, scientists, and public policy makers on watershed protection issues involving both the surface and ground waters and to help make environmentally and economically sound watershed management decisions.

Due to its extensive water, sediment, and pollutant routing schemes incorporating most of the dynamic behaviors, the DWSM provides a sound base for further development. For Illinois hydrologic conditions, the model must be further developed with tile drain and base flow routines, which will help improve the predictions of recession and base flow portions of the hydrographs, and also sediment discharges. The model also provides a sound base for further development in the simulations of streambank erosion and detailed stream sediment transport, major problems in many Illinois watersheds. Additional model testing is recommended in various watersheds in Illinois with different hydrologic and climatic conditions.

CONTENTS

FIGURES

Page

Page

TABLES

Introduction

Large quantities of fertilizer and herbicides are applied to Midwestern farm fields each year. Illinois annually applies one million tons of nitrogen fertilizer (IDOA, 1987) and 60 million pounds of herbicides (Pike, 1985). Illinois has 38 million acres of land, of which 28 million acres are farmland that receives agricultural chemicals (IDOA, 1987), including nitrogen (N), phosphorus (P), herbicides, insecticides, and fungicides.

Runoff water from farm fields, collected in creeks or streams through tile drains or small ditches, contains significantly high concentrations of agricultural chemicals during early stages of planting (late spring or early summer). Many Midwestern streams and rivers draining agricultural watersheds have elevated concentrations of nitrate-N (Smith et al., 1993; Goolsby et al., 1999). Forty percent of the rivers, 51 percent of the lakes, and 57 percent of the estuaries surveyed in the United States in 1994 (Doering et al., 1999) were found to be impaired by nutrient enrichment, and nonpoint source pollution; agriculture was identified as the most widespread source of water pollution. In Illinois, some drinking water supplies, such as Decatur (Demissie et al., 1996), Pontiac (Keefer et al., 1996), and Georgetown (Mitchell et al., 1994), periodically exceed the drinking water standard of 10 milligrams per liter (mg/L) of nitrate-N that was set to prevent incidence of methemoglobinemia (blue baby syndrome). Fertilizer application is not the only source of these elevated nitrate-N concentrations, other manmade and natural sources such as atmospheric deposition and fixation of N, and mineralization of organic N contribute significantly to the problem. Other drinking water sources, such as Lake Springfield, require expensive water treatments when they periodically exceed 3 micrograms per liter (µg/L) maximum concentration level (MCL) for atrazine, a commonly used herbicide.

The amount of atrazine released from the Mississippi River basin and passing through the river at Baton Rouge, Louisiana, during the flood of 1993, between July 7 and August 12, was estimated to be 175 metric tons or 193 tons (Rajagopal, 1993). This was more than the average annual load of 160 metric tons (176 tons). Goolsby et al. (1993) reported that from April-August 1993, atrazine and nitrate loads to the Gulf of Mexico through the Mississippi River were 539 metric tons (594 tons) and 827,000 metric tons (912,000 tons), respectively. The atrazine load, significantly higher than the loads in 1991 and 1992, was attributed to the 1993 flooding. The flood also increased the daily loads of nitrate in July and August, a period when nitrate concentrations in streams are generally lower than in late spring.

Concentrations of contaminants with respect to time varying water discharge shown in hydrographs are of great importance in preparing for the worst contamination scenario and developing the best management plans. Data for streamflow and the concentrations of triazine and alachlor herbicides (Liszewski and Squillace, 1991; Coupe and Johnson, 1991; Goolsby et al., 1993; Wang and Squillace, 1994) indicate no clear

trend between the flow and chemical constituent peaks. However, the timing of the flow peak does appear to have an influence on peak concentrations. Coupe and Johnson (1991) monitored total triazine herbicides in river waters at three watersheds in Illinois in spring 1990: Iroquois River at Chebanse, Sangamon River at Monticello, and Silver Creek at Freeburg. Drainage areas ranged from 464 to 2091 square miles. Peak concentrations of the total triazine herbicides ranged from 20 to 40 µg/L. Chemical peaks in the Iroquois River and at Silver Creek preceded the flow peaks; however, much smaller chemical peaks were observed soon after the flow peaks. In the Sangamon River, the chemical peak lagged behind the flow peak. Studies in Iowa (Liszewski and Squillace, 1991) indicate a much higher chemical peak during a relatively small flooding event in May-June 1989 than a larger flood event in March 1990. The chemical peak during the second flood coincided with the flow peak.

In a recent study, Ray et al. (1998) collected and analyzed water samples from four stations, Henry, Lacon, Naples/Jacksonville, and Hardin, in a 175-mile stretch of the Illinois River during and after flood events. The concentrations of total dissolved solids, nitrate-N, and atrazine observed during spring floods of 1995-1997 showed some scattered patterns with respect to flood stage, with nitrate-N having the most scattered pattern. No clear trend between the flow and chemical concentration peaks was noticed. However, due to an intense flooding event at the midsection of the study reach in spring 1996, the lower two stations showed high concentrations of atrazine (13.2 µg/L at Hardin) preceding the flow peaks.

A review of the literature (Brezonik et al., 1999; Goolsby et al., 1999; Mitsch et al., 1999; Vagstad et al., 1997; Gast et al., 1978; Azam et al., 1993; Lowrance, 1992; Patni et al., 1996; Gentry et al., 1998; Jordan et al., 1995; Jordan et al., 1997; USEPA, 1997) reveals that a number of factors affect the nutrient concentrations in runoff waters from agricultural watersheds: fertilizer application, organic soil mineralization, and transferability between forms of nitrogen, organic nitrogen, tile drainage, atmospheric deposition, and precipitation. Three interesting findings in those investigations are: (1) a nitrate mass balance for the Mississippi River basin shows atmospheric deposition to be comparable to the total amount of nitrate in the river; (2) heavy rainfall causes brief episodes of high discharge that make up a significant fraction of the total discharge and may flush out the nutrients to the receiving stream; and (3) nitrogen export from agricultural watersheds via nitrate leaching through tile drainage is strongly associated with high flow events, which result from frequent heavy rainfalls.

Upland soil and streambank erosion, and sediment deposition are critical water quantity and quality issues in Illinois (Demissie et al., 1988,1992; Roseboom et al., 1982; Fitzpatrick et al., 1985, 1987). Erosion causes loss of fertile soil, streambank erosion causes loss of valuable lands, and both contribute large quantities of sediment in the water flowing through streams and rivers causing turbidity in sensitive biological resource areas, filling streambeds and banks, lakes, and reservoirs. Lake Decatur (Fitzpatrick et al., 1987), Lake Springfield (Fitzpatrick et al., 1985), and Peoria Lake (Demissie et al., 1988) in Illinois are a few examples of serious lake sedimentation. Court

Creek and its major tributaries above Dahinda, Illinois (Roseboom et al., 1982) are examples of serious streambank erosion. Eroded soil and sediment also carry chemicals that pollute water bodies and stream/reservoir beds.

Understanding and dealing with the above complex hydrologic, soil erosion, and sediment and contaminant transport processes, and the associated problems have been quite a challenge for the scientists and engineers, especially due to the spatial and temporal variability of these processes within a watershed. Mathematical models are becoming invaluable tools to analyze those complex processes, and to evaluate land use and best management practices (BMPs) in reducing the damaging effects of flooding, soil erosion, sedimentation, and contamination on drinking water supplies and other valuable water resources. Developing or selecting a model from the public and private domain to simulate and deal with all those complex processes and problems is a difficult task.

Some of the well-known nonpoint source pollution models include: Agricultural NonPoint Source pollution or AGNPS model (Young et al., 1987, 1989), Hydrological Simulation Program - Fortran or HSPF (Bicknell et al., 1993), Simulator for Water Resources in Rural Basins or SWRRB (Williams et al., 1985; Arnold et al., 1990), Chemical, Runoff, and Erosion from Agricultural Management Systems or CREAMS (Knisel, 1980), Groundwater Loading Effects on Agricultural Management Systems or GLEAMS (Leonard et al., 1987), Erosion-Productivity Impact Calculator or EPIC (Williams et al., 1984), Areal Nonpoint Source Watershed Environment Response Simulation or ANSWERS (Beasley et al., 1980), KINematic runoff and EROSion or KINEROS model (Woolhiser et al., 1990), Water Erosion Prediction Project or WEPP (Lane and Nearing, 1989), Cascade based 2-Dimensional watershed rainfall-runoff or CASC2D model (Julien and Saghafian, 1991; Julien et al., 1995), and a European Hydrological System or MIKE SHE model (Abbott et al., 1986a,b). Recently, a new model, Soil and Water Assessment Tool or SWAT (http://www.brc.tamus.edu/swat/swatfact.html), emerged mainly from SWRRB, and features from CREAMS, GLEAMS, EPIC, and Routing Outputs To Outlets or ROTO, another channel-reservoir routing program (Arnold et al., 1995).

Very few of the above models are commonly used to analyze hydrology and nonpoint source pollution in a watershed. The AGNPS and HSPF models are among those few with AGNPS being used for its simplicity and HSPF for its comprehensiveness. Both models are empirically based with some physically based features. The AGNPS model was used in a recent ISWS study (Demissie et al., 1996; Borah et al., 1996a,b). The model generated only the runoff volume, peak flow, yields and average concentrations of sediment and nutrients during a single rainfall event. Such results may be useful to determine the overall effect of the storm but lack sufficient details of temporal variations (hydrograph, and sediment and pollutant graphs) for effective evaluation of BMPs. The HSPF model, a continuous simulation model, uses many parameters due to its empirical structure, which prevented its wide use in the past. Most

of its major applications were made with the assistance of the model developers (Donigian et al., 1986; Imhoff et al, 1983).

The above models are limited in many ways developed to perform specific tasks. Most of these models (AGNPS, HSPF, SWRRB, CREAMS, GLEAMS, and EPIC) are empirically based and cannot simulate the dynamic behaviors of water and its constituents' movements. The physically based models (ANSWERS, KINEROS, CASC2D, and MIKE SHE) are computation intensive with numerical solutions of the governing equations, performance seriously affected by the associated numerical instabilities. These models are also data intensive, making them too cumbersome for practical use in large watersheds.

In a recent report *New Strategies for America's Watersheds,* published by the National Research Council, the Committee on Watershed Management (1999) analyzed the current status of watershed modeling for decision making. The Committee concluded that the available models and methods are outdated, and "a major modeling effort is needed to develop and implement state-of-the-art models for watershed evaluation." Therefore, new physically based and efficient models must be developed to simulate the spatially and temporarily varying physical and chemical processes in watersheds ranging in size from farm fields to river basins.

The primary objective of this study was to develop a dynamic watershed simulation model using physically based governing equations to simulate propagation of flood waves, soil erosion, and entrainment and transport of sediment and all commonly used agricultural chemicals in agricultural and rural watersheds. Objectives also included monitoring and collection of data from Illinois watersheds that were used to test validity and usefulness of the model in Illinois.

A dynamic watershed simulation model (DWSM) is being developed using physically based governing equations to simulate propagation of flood waves, soil erosion, and entrainment and transport of sediment and all commonly used agricultural chemicals in agricultural and rural watersheds. The model has three major components: (1) hydrology, (2) soil erosion and sediment transport, and (3) nutrient and pesticide transport. Formulations and procedures of these components are adopted from earlier work of the lead author (Borah, 1989a,b; Ashraf and Borah, 1992). Each model component has efficient routing schemes based on approximate analytical solutions of the physically based governing equations, preserving the dynamic behaviors of the water, sediment, and the accompanying chemical movements, which none of the other nonpoint source pollution models have.

The DWSM was tested on the 925-square-mile Upper Sangamon River basin in east-central Illinois, which drains into Lake Decatur (Figure 1), using data already collected by the ISWS and intensive storm data collected during this project. The ISWS (Demissie et al., 1996) established an extensive monitoring network in this watershed, from which it has been collecting streamflow and nitrogen data since 1993. Monitoring

was in response to a legal commitment by the city of Decatur to the Illinois Environmental Protection Agency (IEPA) to reduce concentrations of nitrate-N in the lake below the 10 mg/L drinking water standard by the year 2001.

The DWSM hydrology component was tested on the entire Lake Decatur watershed using data collected earlier by the ISWS. The model component and the application results, along with some monitored data described below were reported earlier (Borah et al., 1998). Detailed flow and concentrations of suspended sediment, nitrate-N, phosphate-P, atrazine, and metolachlor were collected at the Big Ditch station (106 in Figure 1), draining a 38-square-mile subwatershed, during the 1998 spring storm events. During 1999, the same types of data, except metolachlor, were collected at Big Ditch and two other stations on the main stem of Sangamon River: Fisher and Mahomet (112 and 105 in Figure 1), draining respectively 240 and 360 square miles of the Upper Sangamon River or Lake Decatur watershed. Rainfall data were collected from newly established raingages, one at Big Ditch during 1998, and five others in 1999 throughout the upper watershed above Mahomet.

The monitored constituent data were analyzed to confirm consistencies of different sampling methods, and to develop statistical relationships between suspended sediment, chemical concentrations, and observed flow. The flow data monitored at the Big Ditch station were used to test and compare two different hydrologic algorithms of the DWSM. Sediment data monitored at Big Ditch were used to test the DWSM sediment component. Most of these data, analyses, and modeling results, along with the formulations of the sediment model component were reported earlier (Borah et al., 1999). Testing of the DWSM nutrient and pesticides component is in progress and will continue in foliowup studies.

The study provides a valuable database of continuous rainfall, runoff, sediment, nitrogen, phosphorous, atrazine, and metolachlor in an east-central Illinois watershed collected during storm events. These data will help us understand the complex physical and chemical processes in a watershed. The study also provides the DWSM as an advanced tool for engineers, scientists, and public policy makers to deal with watershed protection issues involving both surface and ground waters and to make environmentally and economically sound watershed management decisions.

This report presents and discusses formulations of all the three model components, test results of the hydrology and sediment components, data collection methods, the collected data, and some analyses.

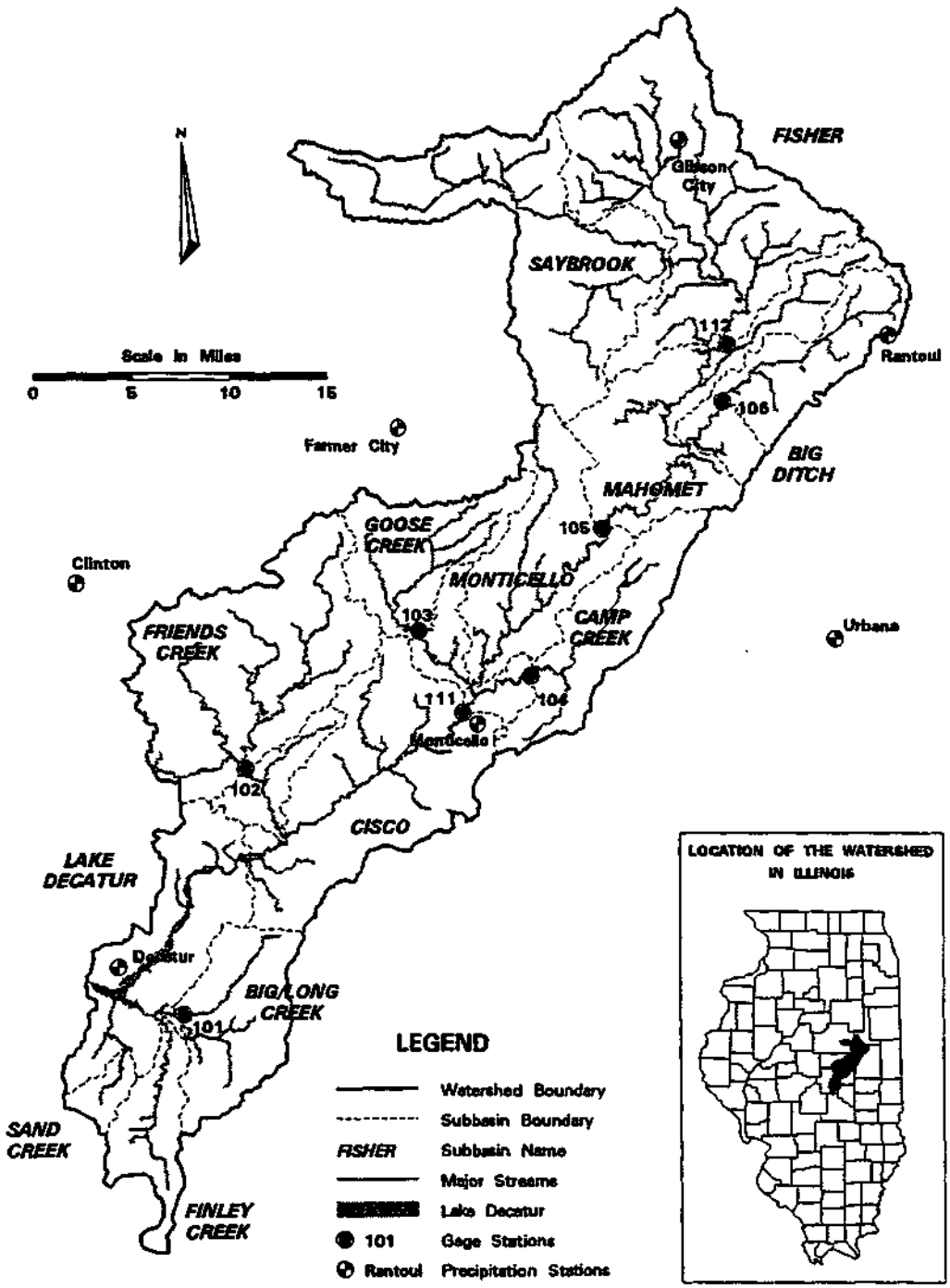

Figure 1. Upper Sangamon River basin draining into Lake Decatur (after Demissie et al., 1996)

Acknowledgments

The authors acknowledge the financial support from the Illinois Groundwater Consortium to conduct this study. The Illinois Groundwater Consortium is funded by Congressional appropriations through the U.S. Department of Agriculture to Southern Illinois University at Carbondale. Members include: Illinois State Geological Survey, Illinois State Water Survey, Southern Illinois University at Carbondale and at Edwardsville, and University of Illinois Agricultural Experiment Station and Cooperative Extension Services. The findings and recommendations in this report are not necessarily those of the funding agencies.

We thank ISWS Chief Derek Winstanley and Watershed Science Section Head Nani Bhowmik (former) and Manoutchehr Heidari (currently acting) for their support and permission to use ISWS resources in this study, special thanks to Chief Winstanley for his critical and useful comments on the report. We also thank Misganaw Demissie for his guidance in initial formulation of the study; Loretta Skowron, Lauren Sievers, Daniel Webb, Sofia Lazousky, and Yi Han for performing laboratory analyses of the monitored water samples; Michael Myers and Amy Russell for their assistance in field data collection; Kathleen Brown for preparing the Geographic Information System maps; and Renjie Xia and George Roadcap for critically reviewing the report. Eva Kingston edited the report, and Linda Hascall reviewed and formatted the graphics.

Hydrologic Model Formulations

The driving force of the DWSM comes from a dynamic hydrologic model in which hydrologic processes are simulated for a given rainfall event, and time and space varying flow depths and flow rates of surface runoff are computed. These processes are simulated by subdividing the watershed into subwatersheds, specifically, into one-dimensional overland, channel, and reservoir flow elements. Such divisions take into account the nonuniformities in topographic, soil, and land-use characteristics. These characteristics are treated as being uniform within each of the elements. Overlands are represented by rectangular areas with representative length, slope, width, soil, cover, and roughness. Channels are described by representative cross-sectional shape, slope, length, and roughness. Reservoirs are represented by stage-storage-discharge relations.

Figure 2 shows the general computational operations of the hydrologic model in the form of a flow diagram. Rates of rainfall excess on the overland elements are computed from a given breakpoint rainfall record using two alternative algorithms described below. Excess rainfall is routed over the overland elements as a cascading process. The water reaching the channels is routed through the channel-reservoir network. The same kinematic wave-based routing scheme, described below, is used to route water over the overlands and through the channels. The standard storage-indication method, described below, is used to route floodwater through reservoirs. Gravity flow logic is used to determine the computational sequence, starting from the uppermost overland and ending in a channel or a reservoir at the watershed outlet. An efficient sequencing scheme is used in which the outflow hydrograph from a flow element is stored until it is used as inflow while routing through the following downstream element. Once a hydrograph has been used, it is erased to make the storage space available for the hydrograph of another element.

Rainfall Excess by SCS Runoff Curve Number

Soil Conservation Service or SCS (1972) runoff curve number method is the simpler of the two alternative methods used to compute rainfall excess. This method requires estimation of only one parameter, the curve number, for each overland. Rainfall excess is computed using the following relations:

$$Q_r = \frac{(P - 0.2S_r)^2}{P + 0.8S_r} \tag{1}$$

$$S_r = \frac{25400}{CN} - 254 \tag{2}$$

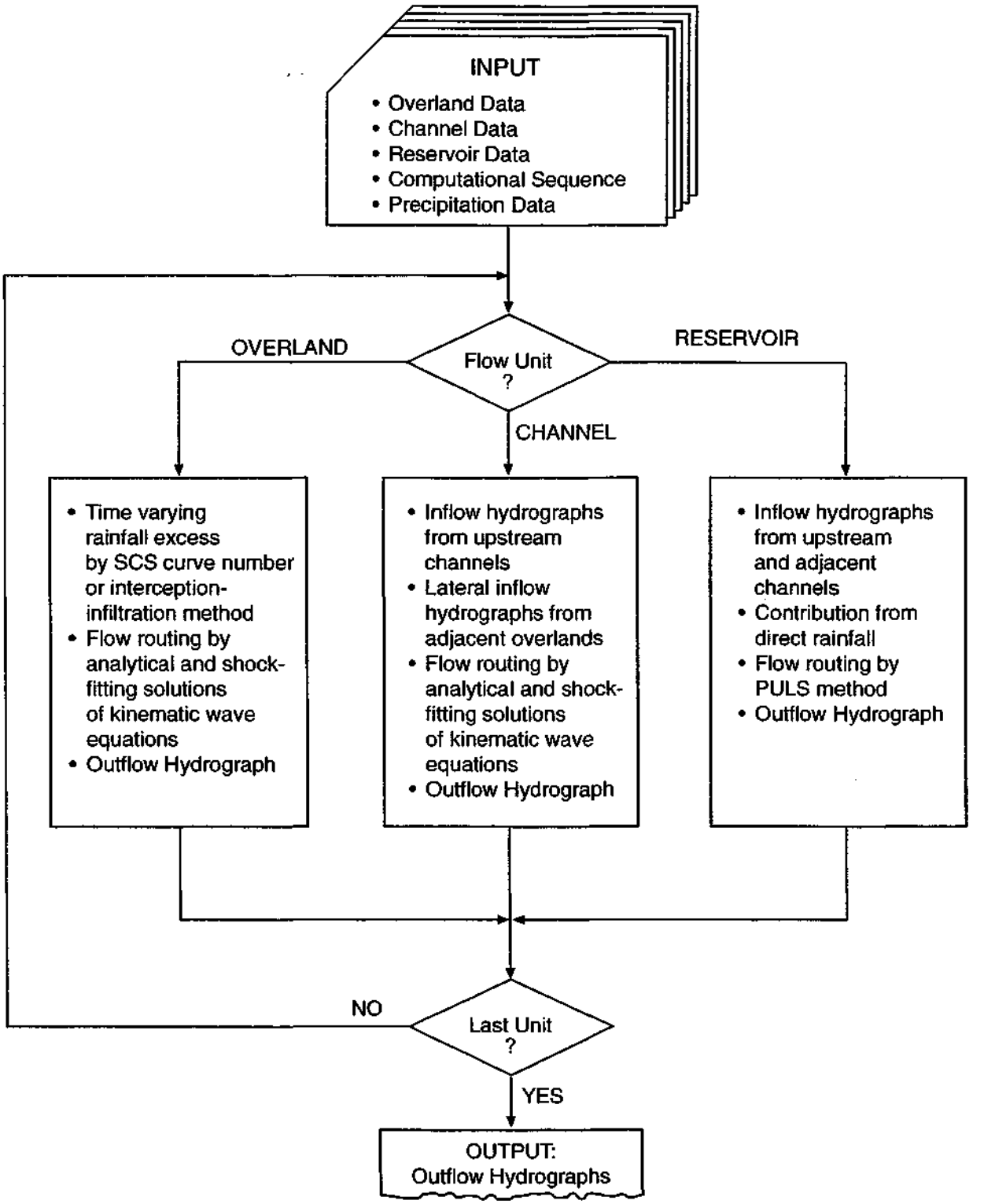

Figure 2. Flow diagram of hydrologic model

where Q_r = direct runoff or rainfall excess (millimeters or mm), P = accumulated rainfall (mm), S_r = potential difference between rainfall and direct runoff (mm), and CN = curve number representing runoff potential of a surface (values 2-100). The CN for each overland is estimated based on its soil type, land use, management practices, and antecedent moisture conditions. Accumulated rainfall excess at each breakpoint time interval is computed using the above two equations, estimated CN, and the accumulated rainfall at the breakpoint. Increments of rainfall excess during the breakpoint time intervals are computed by subtracting each accumulated rainfall excess from its successive value. Rainfall intensities are computed by dividing the rainfall excess increments by the corresponding time intervals.

Rainfall Excess Considering Interception-Infiltration Losses

This method computes the rate of rainfall excess by deducting the rate of rainfall losses due to interception at tree canopies and ground covers and due to infiltration through the ground surface from the rainfall intensity. Ground covers include low vegetation, grasses, rocks, and litter. The water balance equation is written as:

$$I_e = I - D_c I_c - D_g I_g - f \quad \textbf{(3)}$$

where I_e = rate of rainfall excess, I = rainfall intensity, D_c = canopy cover density, I_c = rate of canopy interception, D_g = ground cover density, I_g = rate of ground-cover interception, and f = rate of infiltration. The canopy and ground cover densities for each overland are the ratios of the areas covered by the respective covers to the surface area.

The rates of interception I_c and I_g are computed using the following relations (Simons et al., 1975):

$$I_c = I, \qquad \text{if } \Sigma I\Delta t \le (1-I_s)V_c \quad (4)$$

$$I_c = ES_c, \qquad \text{if } \Sigma I\Delta t > (1-I_s)V_c \quad (5)$$

$$I_g = I - D_c I_c, \qquad \text{if } \Sigma(I-D_c I_c)\Delta t \le (1-I_s)V_g \quad (6)$$

$$I_g = ES_g, \qquad \text{if } \Sigma(I-D_c I_c)\Delta t > (1-I_s)V_g \quad (7)$$

where V_c and V_g = interception storage capacities of canopy and ground cover, respectively, per horizontal area of the cover, I_s = ratio of initial storage to the storage capacity of canopy or ground cover assuming the same for both covers, S_c and S_g = ratios of evaporating surface to horizontal area of a representative canopy and a ground cover, respectively, E = mean evaporation rate from interception storage, and At = time interval.

At the beginning of a storm, the net rainfall (rainfall intensity minus interception losses) reaching the ground passes through the surface into the soil, because the initial infiltration capacity rate exceeds the initial net rainfall rate for all practical purposes. In this case, the infiltration rate is equal to the net rainfall rate, and there is no runoff. Once the net rainfall rate exceeds the infiltration rate, water starts accumulating on the ground surface as depression storage. After satisfying the required depression storage, water starts flowing downstream as surface runoff. Time elapsed until the beginning of excess rainfall producing runoff is ponding time. It is very difficult to describe depression storage and, therefore, it is implicitly combined with interception storage capacity and treated as initial loss.

In computing the ponding time and the infiltration rate after ponding, an algorithm developed by Smith and Parlange (1978) was used. The algorithm is based on a simplified solution of the equation for one-dimensional diffusion of water under gravity. The ponding time t_p and the infiltration rate f are computed by numerically solving the following expressions resulting from the above solution.

$$\int_0^{t_p} I_n dt = \frac{B}{(I_{np} - K_s)} \tag{8}$$

$$K_s(t - t_p) = \int_0^{t_p} I_n dt \left[\frac{I_{np} - f}{f - K_s} - \frac{I_{np} - K_s}{K_s} \ln \frac{(I_{np} - K_s)f}{(f - K_s)I_{np}} \right] \tag{9}$$

where I_n = net rainfall rate (I-D_cI_c-DgIg), I_{np} = net rainfall rate at ponding time, B = a parameter dependent on soil type and moisture content, and K_s = saturated hydraulic conductivity. The parameter B was found to be a function of soil sorptivity and can be roughly estimated as $B \cong S^2/2$, where S is soil sorptivity (Smith and Parlange, 1978).

Water Routing through Overland and Channel

The water routing algorithm for both overland and channel flow elements is based on kinematic wave approximations (Lighthill and Whitham, 1955) of the Saint-Venant or shallow water wave equations governing unsteady free surface flow. The governing equations are:

$$\frac{\partial A}{\partial t} + \frac{\partial Q}{\partial x} = q \tag{10}$$

$$Q = \alpha A^m \tag{11}$$

where A = flow cross-sectional area, Q = flow rate of water discharge, q = rate of lateral inflow per unit length, t = time, x = downslope position, a = kinematic wave parameter,

and m = kinematic wave exponent. These equations are written for a channel, and are also used for overlands simply by substituting A, Q, and q with flow depth, rate of water discharge per unit width, and rate of rainfall excess, respectively. The kinematic wave parameter a and the exponent m are assumed independent of time and piecewise uniform in space (constant within each flow element), and are expressed as:

$$\alpha = \frac{S^{1/2}}{na^{2/3}} \tag{12}$$

$$m = (5-2b)/3 \tag{13}$$

$$P = a\,A^{b} \tag{14}$$

where S = longitudinal bed slope of the flow element, n = Manning's roughness coefficient, P = wetted perimeter of the flow element, and a and b = coefficient and exponent, respectively, in wetted perimeter versus flow area relation. For overland conditions, a = 1.0 and b = 0.0. For a channel, a and b are estimated from cross-sectional measurements. The lateral inflow q is assumed piecewise uniform in space and piecewise constant in time (constant over a time interval).

Equations 10 and 11 were solved analytically by the method of characteristics, and the solutions were expressed in the following discretized form (Borah et al., 1980):

$$A_{i,j} = A_{i-1,j-1} + q_j \Delta t_j \tag{15}$$

$$Q_{i,j} = Q_{i-1,j-1} + q_j \Delta x_i \tag{16}$$

where i = subscript representing a discrete point along the x-axis, j = subscript representing a discrete point along the t-axis, Atj = time increment, and ΔX_i = space increment, as shown in Figure 3, which illustrates the water routing algorithm. A constant computational time interval is chosen. The initial flow condition is assumed uniform within the flow elements. Routing is carried out by tracing characteristics and shock paths, starting with the characteristic Co, in the x-t domain. A characteristic is traced starting from the t-axis (x = 0) and continued until it intersects the downstream end of the flow element by using the above analytical solution (Equations 15 and 16) and Equation 11. Equation 15 is used to compute Ay and Equation 11 to compute Qi,j. Equation 16 is used to solve for Δxi, which is added to Xi-I to compute a new coordinate (xj,tj) of the characteristic. When there is no lateral inflow (qj = 0), the flow values A and Q remain unchanged along the characteristic, and the space increment is computed as $Axi=amA^{m-1}\Delta t_j$.

Since the initial flow condition is assumed to be uniform, all characteristics emanating from the x-axis (t = 0) are parallel to Co and the outflow conditions at times t_1, t_2, t_3, .. are equal to those computed at the points 1, 2, 3, . . . on C_0 (Figure 3). After the

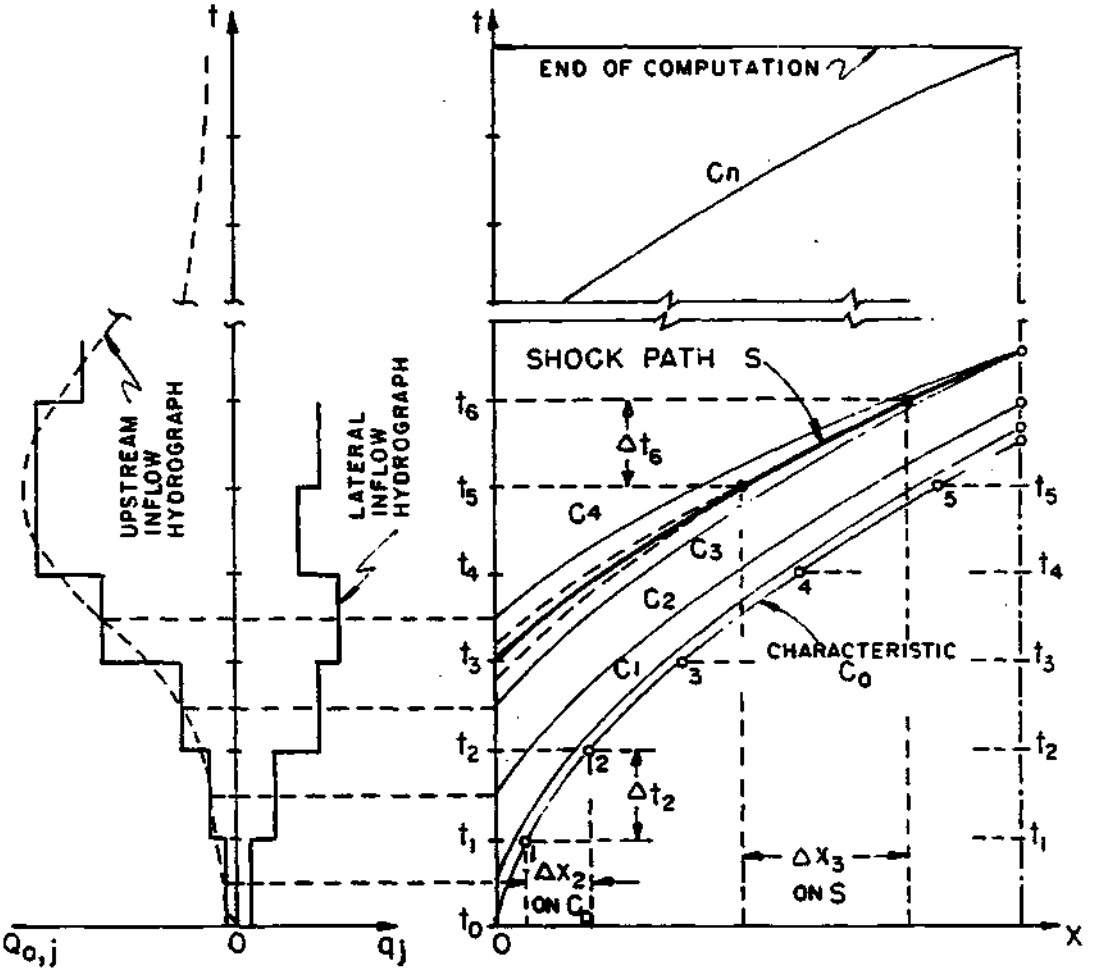

Figure 3. Tracing characteristics and shock paths in kinematic wave routing (after Borah et al., 1980)

initial characteristic Co, the characteristics are traced once from each time interval emanating from the midpoints. Before tracing a characteristic, a shock-forming condition, where two characteristics meet and the solution fails, is checked. The condition is:

$$A_{0,j} - A_{0,j-1} > \frac{1}{2}(q_j + q_{j-1})\Delta t \tag{17}$$

If this condition is satisfied, a shock wave (discontinuous water surface or abrupt flow depth) is introduced at time t_{j-i}. The shock wave is a discontinuity where the initial flow values before and behind the shock are $A_{oj-1}{}^{a}=A_{oj-1}$ and $A_{oj-1}{}^{b}=A_{oj,}$ respectively. Here, the superscripts a and b indicate conditions before (ahead) and behind the shock. The shock path is traced by updating the flow values before and behind the shock at the end of each time interval using Equations 15 and 11, and computing the corresponding space increment using the following expression given by Borah et al. (1980):

$$\Delta x_i = \alpha \frac{(A_{i,j}{}^{b})^{m+1} - (A_{i,j}{}^{a})^{m+1} - (A_{i-1,j-1}{}^{b})^{m+1} + (A_{i-1,j-1}{}^{a})^{m+1}}{(m+1)(A_{i-1,j-1}{}^{b} - A_{i-1,j-1}{}^{a})q_j} \tag{18}$$

Similar to the characteristics (Figure 3), the procedure of tracing shock path continues until the shock intersects the downstream boundary. A single outflow value at the arriving time interval is computed by averaging the flow depths or flow areas before and behind the shock and converting this to flow using Equation 11. When qj=0, the flow values before and behind the shock remain unchanged and the space increment is computed as $Ax_i = \Delta t_j(Q^b-Q^a)/(A^b-A^a)$.

Introduction of the shock wave and routing it with the above procedure is called the "approximate shock-fitting solution" (Borah et al., 1980). Equations 11, 15, and 16 constitute the analytical solution. Equations 11, 15, and 18 constitute the approximate shock-fitting solution.

Discharges existing for all characteristics and shock paths at the time of arrival at the downstream boundary define an outflow distribution. Flow values at intermediate time intervals are computed by linear interpolation. Flow values are averaged when characteristics and/or shock paths arrive downstream during the same time interval.

Borah et al. (1980) demonstrated advantages of this water routing scheme based on the analytical and approximate shock-fitting solutions of the kinematic wave equations over finite difference numerical solutions.

Water Routing through Reservoir

Water routing through a reservoir is performed by using the storage-indication method (SCS, 1972) or Puls method, which assumes a level water surface within the reservoir, invariable storage-discharge relation, and steady-state flow during small time intervals. The method is based on the continuity equation, and may be expressed in the following descretized form:

$$\frac{2S_{t+\Delta t}}{\Delta t} + O_{t+\Delta t} = (I_t + I_{t+\Delta t}) + \left(\frac{2S_t}{\Delta t} - O_t\right) \quad (19)$$

where S = reservoir storage, O = outflow rate, I = inflow rate, t = time, and At = time interval. Initially, the depth of water (or elevation of the water surface) in the reservoir and the outflow from the reservoir are known. The inflow hydrograph is known or estimated. Therefore, the terms on the right-hand side of Equation 19 are also known. The outflows, and thus the outflow hydrograph, are computed by repeatedly using Equation 19 and the storage-discharge relation for the reservoir.

Soil Erosion and Sediment Transport Model Formulations

The soil erosion and sediment transport model component uses the same division of a watershed as the hydrologic component described above in which the watershed is divided into several representative overland and channel flow elements. Similar to the hydrologic simulations, sediment processes are simulated in each of these elements using unit width for overlands and the entire cross section for channels. Currently, the model does not simulate sediment processes in a reservoir.

Sediment transport is a complex process of detaching soil particles, transporting these downslope and depositing at some downslope locations through the actions of raindrops and flowing water. Erosion begins when raindrops strike the land surface and detach soil particles. Flowing water detaches more soil particles and carries them downslope. Erosion by flow on overlands usually occurs in rills. For modeling simplicity, erosion is assumed to be uniform over the overland and the channel beds. Similarly, sediment deposition is assumed to be uniform over the overland and the channel beds.

In this model, the flow of sediment-laden water is treated as a one-dimensional unsteady phenomenon in each flow element. The amount of sediment transported or deposited is the result of interactions between the transport capacity of the flow and the amount of sediment entering and moving along the flow. Imbalances between sediment supply and transport capacity cause erosion and deposition. These processes are all interrelated and must satisfy locally the conservation principle of sediment mass expressed by the sediment continuity equation. This equation is solved to keep track of erosion, deposition, and sediment discharges along the flow elements, which is called sediment routing.

The entire sediment size distribution is divided into several size groups represented by their median sizes, and each group is dealt with individually during simulation of each of the above processes. The total response, in the form of sediment concentration, discharge, or yield, is obtained by adding the responses of all size groups.

Soil Detachment

The model uses a detached soil depth on the bed of each flow element, as shown in Figure 4a, to track loose soil accumulated from bed materials detached by raindrop impact and from deposited sediments. Soil detachment by raindrop impact depends on soil cover and soil properties. Past research suggests that the rate of detachment is proportional to the square of the rainfall intensity. Ponded water, deeper than a critical depth, cushions the impact of raindrops and diminishes erosion. Based on existing research in the literature, the rate of soil detachment due to raindrop impact may be expressed as:

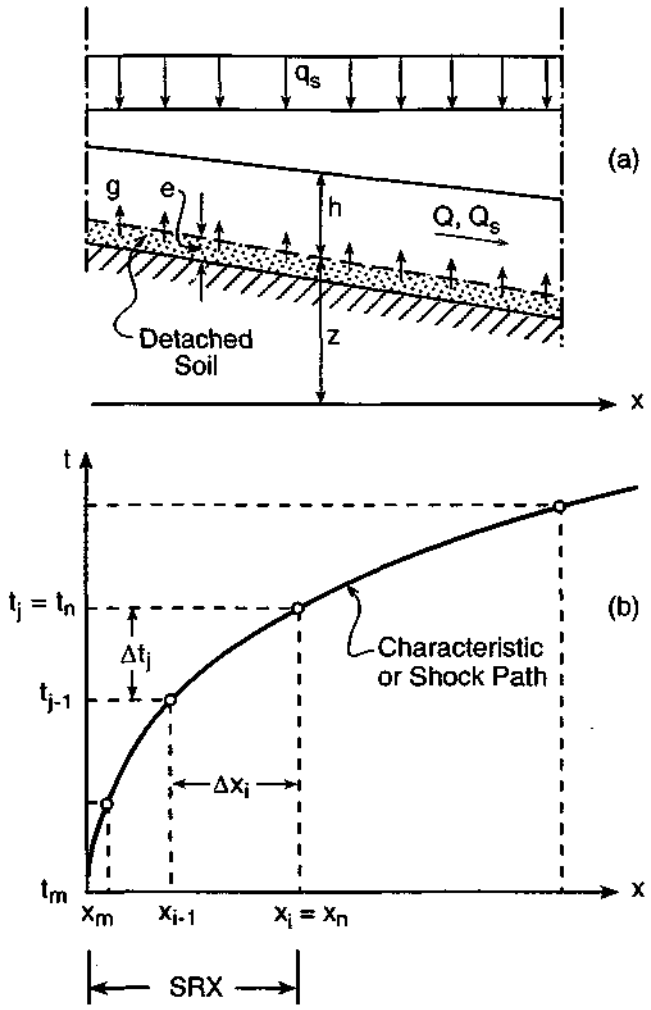

Figure 4. Sediment routing in a flow element: (a) schematic flow element: (b) tracing characteristic or shock path (after Borah, 1989b)

$$E_r = a_r I^2 (1 - D_c)(1 - D_g)(1 - \frac{h + e}{3d_{50}}), \quad \text{if } (h + e) < 3d_{50} \tag{20a}$$

$$E_r = 0, \quad \text{if } (h + e) \geq 3d_{50} \tag{20b}$$

where E_r = rate of soil detachment due to raindrop impact, a_r = raindrop detachment coefficient (RDC), I = rainfall intensity, D_c = canopy cover density, D_g = ground cover density, h = water depth, e = thickness of existing detached soil on the bed (Figure 4a), and d_{50} = median raindrop diameter. Equation 20 gives the detachment rate for the entire size distribution used in the simulation. Rate for each size group is calculated by multiplying this rate by the fraction of the corresponding size group in the distribution.

Sediment Routing

Sediment routing is based on the conservation of mass for the sediment load and material on the overland or the channel bed. Figure 4 illustrates the routing concept schematically. Figure 4a shows the different terms used in the sediment continuity equation, and Figure 4b shows the routing procedure using the method of characteristics. The continuity equation for a sediment size group may be written as:

$$\frac{\partial Q_s}{\partial x} + \frac{\partial CA}{\partial t} = q_s + g \tag{21}$$

where Q_s = volumetric sediment discharge, C = volumetric concentration of sediment, A = cross-sectional area of flow, q_s = volumetric rate of lateral sediment inflow per unit length, g = volumetric rate of material exchange with the bed per unit length, x = downslope distance, and t = time. Assuming sediment moves with the same velocity of water V, and water discharge Q remains constant within time and space intervals, Equation (21) may be written as:

$$\frac{\partial A_s}{\partial t} + V \frac{\partial A_s}{\partial x} = q_s + g \tag{22}$$

where A_s = sediment load, volume of sediment present in the flow per unit length ($A_s = CA = Q_s/V$), and V = average water velocity. Equation (22) is a quasi-linear hyperbolic equation governing the propagation of sediment load wave and is solved by the method of characteristics. By assuming q_s and g constants within space and time intervals, the solution (Borah et al., 1981; Borah, 1989b) may be expressed as:

$$\Delta x = V \Delta t \quad (23)$$

$$A_s = (A_s)_0 + (q_s + g) \Delta t \quad (24)$$

where Δx = space interval, Δt = time interval, and $(A_s)_0$ = initial value of sediment load. Sediment is routed along with the water, which is also routed based on the method of characteristics. In this scheme, a constant computational time interval is chosen, and characteristics and shock paths are traced in the x-t domain. Tracing is accomplished by computing flow depth or flow area, flow rate, and space increment for a characteristic or shock path at the end of each time interval, and accumulating the space increments. Similar characteristics and shock paths are used to route the sediment. Figure 4b shows such a characteristic or a shock path. Sediment is routed within the time interval and the corresponding space increment by following the steps described below.

Potential Exchange Rate

Based on existing research (Alonso et al., 1981), the bed load formula of Yalin (1963) is used to compute sediment transport capacities in overlands under any flow condition and for all size groups. In computing capacities in the channels, the total load formula of Yang (1973) is used for sediment sizes > 0.1 mm (fine to coarse sands) and the total load formula of Laursen (1958) is used for sediment sizes < 0.1 mm (very fine sands and silts). Based on the flow conditions within the above space and time intervals, and the representative size of the sediment size group, one formula is selected and the sediment transport capacity C^p for the size group is computed. Substituting this value in Equation (24), $A_s = AC^P$, this equation is solved for potential sediment exchange rate, which may be expressed as:

$$g^p = [AC^p - (A_s)_{i-1,j-1}]/\Delta t_j - q_s \quad (25)$$

where i = subscript representing a discrete point along the x-axis (Figure 4b), j = subscript representing a discrete point along the t-axis, p = superscript representing potential value, g^p = volumetric potential sediment exchange rate per unit length, and C^p = volumetric sediment concentration at potential (capacity) rate. The sign of g^p serves as an indicator of the deposition or erosion mode.

Deposition

If $g^p < 0$, the transport capacity of the flow is less than the sediment present in the flow. Consequently, g^p is the potential rate of sediment deposition, the actual amount of

sediment reaching the bottom during Δtj depends on fall velocity of the sediment particle. Therefore, the deposition rate is computed as:

$$D = -g^p, \quad \text{if } (2w\Delta t_j/h) \geq 1 \tag{26a}$$

$$D = -(2w\Delta t_j/h)g^p, \quad \text{if } (2w\Delta t_j/h) < 1 \tag{26b}$$

where D = volumetric rate of sediment deposition per unit length, w = particle fall velocity, and h = water depth.

Erosion

If $g^p > 0$, the transport capacity exceeds the amount of material in transport and, therefore, the flow will tend to pick up additional material from the bed. If the detached soil available on the bed is not sufficient to fulfill the capacity, the flow will erode soil from the parent bed material by expending more energy. Therefore, two erosion cases are considered depending on the volume of detached soil available on the bed. An available soil volume per unit length is calculated by adding soil detachment from raindrop impact [Equation (20)], if any, during At_j to the volume left from interval At_{j-1} as:

$$v_{i,j} = Pf(e_{i,j-1} + E_r\Delta t_j)(1 - \lambda) \tag{27}$$

where v = volume of detached soil on the bed per unit length, P = wetted perimeter (1 for overland elements), f = fraction of the sediment size group in the distribution, E_r = rate of soil detachment due to raindrop impact, and X = bed porosity. The potential exchange rate is converted into an equivalent volume of soil per unit length as:

$$\Delta v^p = g^p\Delta t_j \tag{28}$$

where Av^p = equivalent volume of potential exchange. If $v_{i,j} \geq Av^p$, the available detached soil is sufficient to supply sediment to flow. In this case, no additional erosion from undetached soil occurs, and the rate of erosion (entrainment) from the detached soil volume is computed as:

$$E_f = \frac{\Delta v^p}{\Delta t_j} \tag{29}$$

where E_f = rate of soil erosion, per unit length, due to flow. If $v_{i,j} < Av^p$, the available detached soil is less than the potential entrainment, and additional soil is detached from the parent bed material. Erosion from the parent bed material requires additional energy,

and, therefore, a flow detachment coefficient is used to compute the additional erosion from the undetached soil. In this case, the erosion rate due to flow is computed as:

$$E_f = \frac{1}{\Delta t_j}(v_{i,j} + a_f[\Delta v^p - v_{i,j}]) \quad \textbf{(30)}$$

where a_f = flow detachment coefficient (FDC).

Sediment Discharge and Bed Elevation

The net sediment exchange rate for the size group within Δx_i and At is computed as:

$$g = E_f - D \quad (31)$$

The current sediment load for the size group is computed from Equation (24) as:

$$(A_s)_{i,j} = (A_s)_{i-1,j-1} + (q_s + g)\Delta t_j \quad \textbf{(32)}$$

The sediment discharge for the size group is computed as:

$$(Q_s)_{i,j} = V(A_s)_{i,j} \quad \textbf{(33)}$$

The total sediment discharge is computed by adding discharges of all size groups. Discharges on all the characteristics and shock paths reaching a location, such as the downstream end of an element, define the sediment discharge hydrograph.

Within the space increment Ax_i and at the end of time interval At_j, the detached soil depth and the bed elevation are updated by summing the net material exchanges of all size groups.

Grouping Time and Space Intervals

The time interval selected for the characteristic and shock-fitting solutions may yield a cluster of small space increments. Repeating the above calculations for each of these increments may not be necessary. Therefore, the model has the option of combining a number of space and time intervals used in the solutions into larger intervals for the above sediment routing computations. Figure 4b shows such an interval (SRX). The user selects a value for SRX based on desired accuracy and computer time usage.

Nutrient and Pesticide Transport Model Formulations

The nutrient and pesticide transport model component also uses the same division of a watershed as the hydrology and sediment components described above, in which the watershed is divided into representative overland and channel flow elements. Similar to the hydrologic and sediment simulations, nutrient and pesticide transport processes are simulated in each of these elements, in a unit width for overlands, and in the entire cross section for channels.

Chemicals at the soil surface can be transferred to runoff in solution form through mixing of rainwater with soil solution, dissolution of chemicals present in the solid form, desorption of chemicals adsorbed to the soil, or adsorption of chemicals to eroded soil or sediment (Baily et al., 1974). Contamination of runoff occurs only when water ponding and initiation of runoff occur. Prior to initiation of runoff, chemicals are mixed with infiltrating rainwater and migrate downward into the soil matrix (Ingram and Woolhiser, 1980). When water ponding occurs and runoff begins, part of the rainwater infiltrates and another part becomes runoff. During this process, rainwater mixes with a mixing layer of the soil matrix, located at the ground surface, with degrees of interaction dependent upon depth, a concept known as nonuniform mixing (Ahuja, 1982; Heathman et al., 1985). The model component needs input from the hydrologic component on time of ponding, and infiltration and runoff rates.

Model formulations are based on the following assumptions:

1) The soil profile consists of small homogeneous soil increments (layers) as shown in Figure 5 for a mixing layer of the profile.

2) Initial water content, porosity, and chemical concentrations in each soil increment are known.

3) All rainwater infiltrates into the soil during the early part of a rainfall event, before water ponding occurs.

4) All soil pores participate sequentially in solute and water movement.

5) Water entering the soil surface mixes with soil (pore) water initially present in each increment and displaces it to the next increment.

6) Except for adsorption and desorption, other chemical reactions are negligible.

7) In case of adsorbed chemicals, dissolved and adsorbed phases of the chemicals are in equilibrium, governed by linear adsorption isotherm, which is expressed as:

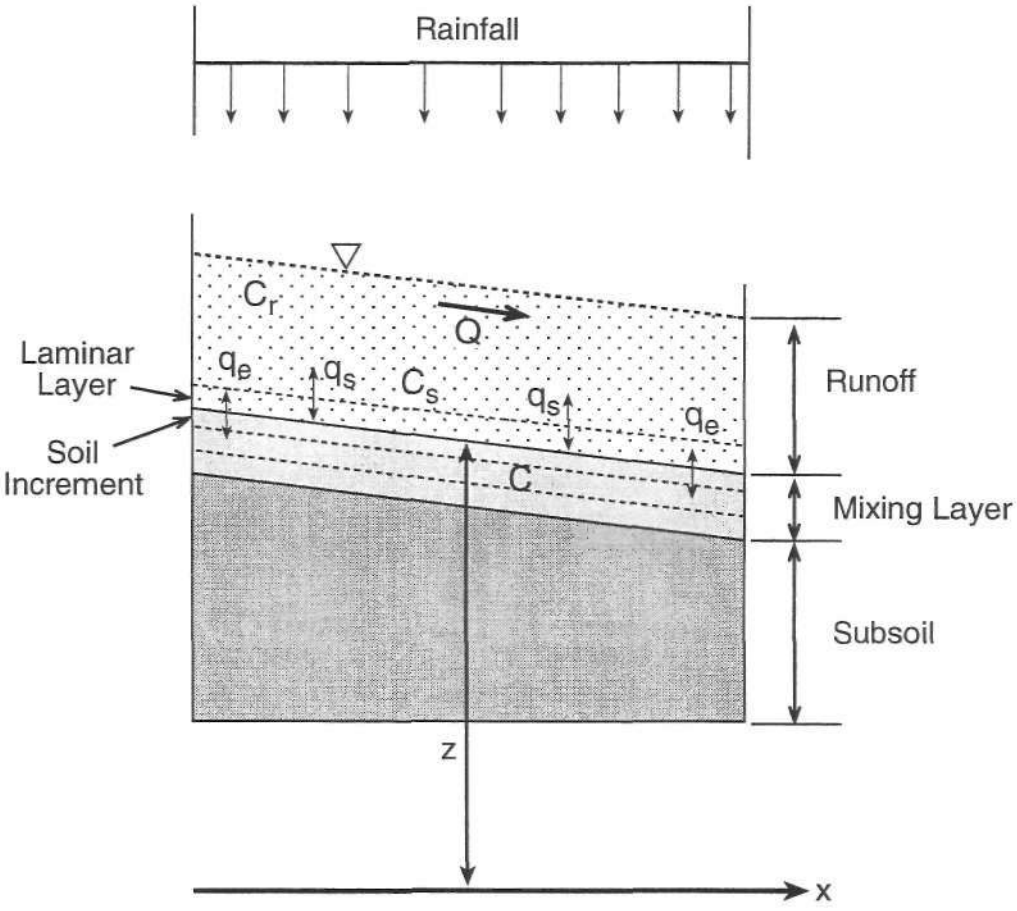

Figure 5. Schematic of chemical transport through rainfall-runoff and soil-chemical interactions (after Ashraf and Borah, 1992)

$$C_d = K\,C \quad \textbf{(34)}$$

where C_d = adsorbed chemical in soil particles (ug/g), K = partition coefficient (cm^3/g), and C = dissolved chemical concentration in soil solution (ug/cm^3).

Chemical Movement with Infiltrating Water

The model routes infiltrating water and chemicals through each soil increment using the concept of complete mixing (Ingram and Woolhiser, 1980). Based on initial water content in an increment, depth of water required to saturate that increment can be computed as:

$$D(i, j) = [\rho - \theta(i, j-1)]d \quad (35)$$

where D(i, j) = depth of water needed to saturate soil increment i during time step j (cm), p = soil porosity (cm /cm), 0(i, j) - water content in soil increment i during time step j (cm^3/cm^3), and d = thickness of each soil increment (cm).

Based on water available and water needed to saturate the upper soil increment, depth of water available for a soil increment during a time interval AT to saturate or infiltrate through the increment is given by:

$$Y(i, j) = Y(i-1, j) - D(i-1, j) \quad (36)$$

where Y(i, j) = depth of water available for soil increment i during time step j (cm).

In these formulations, flowing time through the soil increment is ignored and, therefore, valid for only small incremental depth and time interval. At the first soil increment (ground surface), available water is the infiltrating water, which is given as:

$$Y(i, j) = I(j)\,\Delta T \quad \textbf{(37)}$$

where I(j) = rate of infiltration during time step j (cm/s), and AT = time interval during each time step j (s).

If the available water depth is greater than or equal to the depth needed to saturate a soil increment, the water content in that increment becomes the saturated water content which is equal to the soil porosity. If available water is less than the amount needed to saturate a soil increment, the water content is computed based on initial water content plus the available water. Therefore,

$$\theta(i,j) = \rho, \quad \text{for } Y(i,j) \geq D(i,j) \tag{38}$$

$$\theta(i,j) = \theta(i,j-1) + \frac{Y(i,j)}{d}, \quad \text{for } Y(i,j) < D(i,j) \tag{39}$$

Based on mass conservation, chemical concentration in a soil increment due to the movement of the chemical with the infiltrating water is computed as:

$$C(i,j) = \frac{C(i,j-1)[\theta(i,j-1)d + K M_s] + Y(i,j) C(i-1,j)}{\theta(i,j) d + K M_s + Y(i,j)} \tag{40}$$

where C(i, j) = chemical concentration of soil solution in soil increment i during time step j (ug/cm^3), K = partition coefficient (cm^3 /g), and M_s = soil mass per unit area of a soil increment (g/cm).

Equation 40 includes adsorption and desorption of chemicals with soil particles. For nonadsorbed chemicals, such as nitrate, the partition coefficient K is zero.

Based on computational stability and success in preliminary applications (Ashraf and Borah, 1992), Equation 40 is modified when water available for an increment is more than water needed to saturate the increment, $Y(i,j) > D(i,j)$. In this case, it is assumed that the water needed to saturate a soil increment $D(i,j)$ passes through all the upper increments affecting concentrations in each increment. Therefore, while considering a soil increment i for computing water content and chemical concentration, concentrations in all the upper increments, $1,2,\ldots, i-1$, are updated, and then concentration in increment i is computed using Equation 40 and replacing Y(i, j) by D(i, j). This procedure may have accounted for the flowing time through the soil increments ignored in the formulations. Since the main purpose of this model was to simulate pollutant movement with surface runoff and sediment, detailed modeling of flow and pollutant movement through the unsaturated soil zone was not attempted at that time.

After considering all soil increments during a time interval, excess infiltrating water if any, percolates through deeper soil layers. The excess water passes through soil increments while affecting their chemical concentrations. Therefore, chemical concentration in each increment is updated using Equation 40.

For soil increment 1 (at the surface), contributing chemical concentration $C(i-1, j) = C(0, j)$ is the concentration of that chemical in rainwater if the ground surface has no existing water depth. In case of existing water depth on the ground surface (Figure 5), C(0, j) is the concentration of the infiltrating water resulting from overall mixing of existing surface water with the chemical flux from the mixing soil layer, as discussed below, during the previous computational time step.

Runoff Mixing with Soil Layer and Chemical Exchange

Once runoff begins (after ponding), rainfall is divided into infiltration contributing to subsurface flow and rainfall excess contributing to runoff. The infiltrated water and accompanying chemicals are routed through soil increments as previously described. The rainfall excess, in combination with the existing runoff, mixes and exchanges chemicals with a mixing soil layer consisting of several soil increments, as shown in Figure 5. At present, thickness of the mixing soil layer is a parameter, determined through model calibration using observed data. For the experimental boxes of Hubbard et al. (1989 a,b), Ashraf and Borah (1992) found the thickness of the layer to be 0.75 and 1.00 cm.

At the beginning of ponding, only the rainfall depth, during a computational time step, mixes with the soil layer. Once water starts accumulating on the ground, rainwater mixes with this existing water before mixing with the soil layer. In this case, the entire runoff depth does not necessarily interact with the soil layer, only a fraction of this depth in contact with the layer interacts (Parr et al., 1987). Based on Kay and Nedderman (1985), this mixing runoff depth is taken as the stagnant boundary layer thickness (laminar layer, Figure 5), and derived by equating the expressions of shear stress of the viscous layer ($\mu V/\delta$) and the hydrostatic shear stress at the bed (yhS) as:

$$\delta(j) = \frac{\mu V(j)}{\gamma\, h(j)\, S} \tag{41}$$

where 8 = mixing runoff depth or thickness of laminar flow layer (Figure 5) (cm), j = time step, μ = viscosity (dyne-s/cm), V= average runoff velocity (cm/s), *y* = specific weight of water (dyne/cm^3), h = runoff depth (cm), and S = ground slope, or hydraulic gradient (cm/cm).

The laminar layer (mixing runoff depth) interacts with the individual soil increments of the mixing soil layer with varying degrees of interaction. Based on Ahuja and Lehman (1983) and Heathman et al. (1985), degree of interaction is expressed as:

$$\beta(i) = e^{-bz(i)} \tag{42}$$

where P(i) = degree of interaction for soil increment i, b = constant, and z(i) = depth of soil increment i from the ground surface (cm).

Degree of interaction is calculated at the upper and lower ends of each increment and averaged. The constant b determines degree of interaction and is responsible for chemical transfer to surface runoff. Values of b may depend on soil characteristics, ground cover, rainfall characteristics (Ingram and Woolhiser, 1980), land grade (Wiese et al., 1980; Ingram and Woolhiser, 1980), and hydraulic conductivity of the mixing soil layer and the subsoil (Sharpley et al., 1981; Ahuja and Lehman, 1983). Values for degree

of interaction (P) range from zero to one, indicating absence of mixing and complete mixing, respectively. At the surface, **p** = 1, indicating complete mixing. At present b is a parameter determined through model calibration. Values of b ranged from 1.00 to 3.50 for the different experimental boxes where the model was initially tested (Ashraf and Borah, 1992).

Runoff water mixes with a soil increment in the mixing soil layer depending upon the degree of interaction for the increment. The resultant concentration in a soil increment is computed as:

$$C(i,j) = \frac{C(i,j-1)[\theta(i,j-1)d + K M_s] + \beta(i-1)\,\delta(j)\,C(i-1,j)}{\theta(i,j)\,d + K M_s + \beta(i)\,\delta(j)} \quad \textbf{(43)}$$

Starting at the ground surface, Equation 43 is used to compute chemical concentration in pore water of a soil increment as a result of mixing with runoff. For increment 1 (at the surface), contributing chemical concentration C(i - 1, j) = C(0, j) is the concentration of the existing water depth resulting from overall mixing with the chemical flux from the mixing soil layer during the previous computational time step.

After runoff of depth 8 interacts with an increment i, the resultant concentration of the mixing water during time step j becomes P(i) C(i, j). As a result of the mixing process, a chemical mass of P(i) 50) C(i, j) per unit area, represented by the last term in the numerator of Equation 43, enters the next soil increment and interacts with the existing chemical in that increment affecting the concentration of that increment as given by Equation 43. The procedure continues until the mixing water reaches the last increment of the mixing soil layer continuously changing the concentrations of the mixing water and the soil increments. The resultant concentration of the mixing water is computed after considering mixing with the last soil increment. Thus the rate of chemical mass entrainment to runoff is computed as:

$$q_e(j) = \beta(N)\,\delta(j)\,C(N,j)\,\frac{1}{\Delta t} \quad \textbf{(44)}$$

where $q_e(j)$ = chemical mass entrainment rate from mixing soil layer to surface runoff during time step j (µg/cm^2-s), and N = last soil increment (total number of increments) in the mixing soil layer.

Chemical Routing along Slope Length

Chemical routing along slope length is simulated by considering conservation of chemical mass in soluble form in runoff, conservation of chemical mass in adsorbed form with sediment and exchange of these dissolved and adsorbed chemical masses using

linear adsorption isotherm (Equation 34). Chemical exchange due to soil erosion, and sediment deposition are also considered.

Conservation of chemical mass in dissolved form in runoff and in adsorbed form in sediment may be respectively represented by the following continuity equations:

$$\frac{\partial(VC_r)}{\partial X} + \frac{\partial C_r}{\partial T} = q_e \tag{45}$$

$$\frac{\partial(VC_s)}{\partial X} + \frac{\partial C_s}{\partial T} = q_s \tag{46}$$

where V = average velocity of runoff water (cm/s), C_r= chemical mass load in runoff (µg/cm), C_s = chemical mass load adsorbed with sediment (µg/cm), q_s = chemical mass exchange rate (source/sink) with sediment (µg/cm^2-s), X = down slope position (cm), and T = time (s).

The contaminant mass exchange rate with sediment at time step j is computed as:

$$q_s(j) = C(1,j)\sum_{m=1}^{M}(P_m KE_m) - \frac{C_r(j-1)}{h(j-1)}\sum_{m=1}^{M}(P_m KD_m) \tag{47}$$

where $C(1,j)$ = chemical concentration in the first soil increment (fig/cm), j = time step, m = subscript representing sediment size class (group), M = total sediment size classes, P = preference factor of chemical to adsorb in a size class or aggregate, E = soil erosion rate (g/cm -s), D = sediment deposition rate (g/cm -s), K = partitioning coefficient of linear adsorption isotherm (cm /g), and h = depth of runoff water (cm).

The depth of runoff (h), soil erosion rate (E), and sediment deposition rate (D) are obtained from the hydrologic and sediment transport model components described above.

Based on Foster et al. (1985), the composition of sediment from the soil matrix consists of five particle classes: clay, silt, sand, small aggregate, and large aggregate. Clay, silt, and sand are primary particles having representative sizes 0.002, 0.01, and 0.2 mm, respectively, with specific gravity of 2.65. The small and large aggregates have specific gravity of 1.8 and 1.6, respectively. Sizes and distribution of particles in these aggregates are computed based on Foster et al. (1985).

The preference factor (P) depends on surface area of the particle or aggregate class. Preference factor is computed during a time interval from rates of erosion (E) and deposition (D) for each particle and aggregate class. Total surface area for the eroded or deposited sediment is computed by multiplying specific areas of the particle classes, as given by Foster et al. (1985), with their respective simulated weights, and summing all the products. For an individual class, P is obtained by dividing the surface area of the

particle class by the total surface area. Since the eroded and deposited particles/aggregates have the same physical and chemical properties as the original soil, the same value of partitioning coefficient (K) is used in computing equilibrium concentrations in different sediment classes.

Equations 45 and 46 are nonlinear hyperbolic equations. Assuming constant water velocity (V) in small space and time increments, these equations are solved by using the method of characteristics. The solutions are similar to the solutions of kinematic wave and sediment continuity equations (Borah et al., 1980; Borah, 1989a, b). Dissolved and adsorbed contaminant masses at a discrete point on a characteristic may be respectively expressed as:

$$C_r(i,j) = C_r(i-1,j-1) + q_e(j)\Delta T \tag{48}$$

$$C_s(i,j) = C_s(i-1,j-1) + q_s(j)\Delta T \tag{49}$$

where i = a discrete point on a characteristic along the X-axis, j = a discrete point on a characteristic along the T-axis, and AT = time interval during a computational time step (s).

As a result of chemical mass exchanges between runoff and sediment, the total chemical concentration at a discrete point and time is computed as:

$$C_t(i,j) = \frac{C_r(i,j) + C_s(i,j)}{h(i,j)\left(1 + \sum_{m=1}^{M} KA_m(j)P_m\right)} \tag{50}$$

where $C_t(i,j)$ = total chemical concentration in runoff and sediment ($\mu g/cm^3$), and $A_m(j)$= sediment load for size group m (g/cm^3).

The sediment load for each size group (A_m) is obtained from the hydrologic and sediment transport model components presented earlier.

Monitoring Lake Decatur Watershed

Lake Decatur Watershed: the Upper Sangamon River Basin

Figure 1 shows the 925-square mile Upper Sangamon River basin draining into Lake Decatur in east-central Illinois. The basin lies in the Till Plains section of the Central Lowland physiographic province. Agriculture is the dominant land use with row crops (corn and soybeans) covering 87 percent of the basin (Demissie et al., 1996). Bed slope of the main stem Upper Sangamon River varies from 0.00017 to 0.00084 with an average of 0.00049. Slopes in the major tributaries vary mostly from 0.00053 to 0.00088, rarely up to 0.00538. The soils are mostly silt loams and silty clay loams, poorly drained, and are very fertile with high organic content and high resistance to drought. Lake Decatur, the water supply reservoir for the city of Decatur, receives water from the entire Upper Sangamon River basin. The lake, having a maximum capacity of 28,000 acre-feet, has been experiencing water quality problems with nitrate-N concentration exceeding the 10 mg/L drinking water standard of the IEPA, as indicated earlier.

The ISWS (Demissie et al., 1996) completed a two-year monitoring and modeling study of the above basin to develop land-use management alternatives that would eventually bring the nitrate-N concentration in the lake below 10 mg/L. In that study, the ISWS established an extensive monitoring network throughout the watershed to continuously monitor flow and concentrations of nitrate-N, ammonium, total Kjeldahl nitrogen (TKN) at eight monitoring stations: five tributary stations, and three main stem stations along the Sangamon River (Figure 1). The AGNPS model was used to evaluate the effects of alternative management practices on nitrate-N loading into Lake Decatur (Borah et al., 1996a, b). Monitoring of flow and nitrate-N continued for six years till present (1999). Some data were used to test the hydrologic component of the DWSM in this study.

Monitoring Protocols

Monitoring involved measurements of water discharges and collection of water samples for analyses of nitrate-N, orthophosphate, total suspended solids (TSS), and three pesticides (atrazine, metolachlor, and alachlor) at selected monitoring stations established earlier by the ISWS. The 1998 monitoring was conducted at Big Ditch station, while the 1999 monitoring was conducted at Big Ditch, Fisher, and Mahomet (Figure 1). Storm events were targeted during the spring and early summer months, ideally before and after the applications of fertilizers and pesticides.

Water discharges were measured from continuous stage records and using stage-discharge rating curves. Stage-discharge rating curves were developed from many physical measurements of velocities and water cross-sectional areas at each monitoring

station during many different flow conditions and water levels. Velocities were measured using a current meter.

Samples for the analyses of nitrate-N, orthophosphate, and TSS or suspended sediment were collected using a time-integrated automatic water sampler at specified time intervals. Grab (point) samples were taken manually on visits to the station during a storm event for additional data points, and to compare suspended sediment and chemical concentrations with the concentrations from automatic sampler for quality control and quality assurance purposes. Samples for pesticide analyses were taken manually at the same time as the grab samples. Due to their higher degradable properties and possibilities of cross contamination, automatic samples were not used for pesticide analyses. Depth-width-integrated samples were collected during field visits for more accurate TSS analysis, and to compare suspended sediment concentrations with the measurements from grab (point) and automatic samples.

Sample Collection and Handling

All grab samples were initially collected in a 1-liter glass jar held inside an aluminum frame basket that was lowered on a rope into the stream at the thalweg, usually the midpoint of the stream where velocity is expected to be the greatest. The glass jar was first rinsed with deionized water and then once with the resident (stream) water before the samples were taken and transferred to the appropriate storage container. Table 1 lists the container types, sample sizes, and storage practices used for each type of analysis. The sample number and date and time of collection were recorded on the storage bottles for each parameter and then the bottles were placed in a cooler kept at less than 4°C and transported to the laboratory for analyses.

Table 1. Grab Sample Collection and Handling

Parameter	*Container*	*Sample size*	*Recommended holding time*
Nitrate-Nitrogen	Polyethylene bottle	60 ml	2 days/ 4°C
Orthophosphate	Polyethylene bottle	60 ml	2 days/ 4°C
Total Suspended Solids	Glass bottle	500 ml	7 days
Pesticides (atrazine, alachlor, metolachlor)	Amber glass bottle with teflon-lined cap (solvent-washed)	1000 ml	7 days until extraction, 4°C, 40 days after extraction

Most samples were collected by a time-integrated automatic water sampler (ISCO, 1975). Samples were collected in two 500 milliliter (ml) polyethylene bottles at specified time intervals, generally 3 hours during the rising, peak, and immediately after the peak of a storm hydrograph, and up to 6 hours during recession and base flow periods. Each tray of 28 samples was retrieved within three days of setup. Samples from the trays were labeled in the same manner as the grab samples. One sample was sent to the laboratory for analysis for nitrate-N and orthophosphate analysis, and the other sample (in a pre-weighed bottle) was analyzed for TSS. There was the possibility for exceeding of the holding times recommended by the U.S. Environmental Protection Agency (USEPA, 1983, 1993) for the samples to be analyzed for nitrate-N and orthophosphate. Therefore, grab samples were collected at the time of setup of the automatic sampler. Immediately after the grab sample was collected, the sampler was triggered to collect its first sample. The analytical results of the grab sample and the sampler-collected sample were compared for both parameters (nitrate-N and orthophosphate) and any evidence of sample degradation in the sampler-collected sample was noted. Experience had shown that little to no degradation of nitrate-N occur in samples analyzed a few days beyond recommended holding times.

For verifying accuracy of TSS concentrations measured by grab and time-integrated automatic samples, a U.S. Geological Survey (USGS) depth-integrated suspended sediment sampler DH-59 (Guy and Norman, 1970) was used to collect depth-width-integrated samples from the stream cross section at the monitoring station. The stream cross section was divided into several intervals. The sampler with an empty sample bottle was lowered to near the bottom of the stream and raised back to the surface in each cross-sectional interval at a constant speed collecting a sediment-laden water sample. The sample bottle inside the DH-59 sampler gradually filled as it was being lowered and raised. The sample bottle must be filled only up to a specified level, without which the procedure must be repeated with adjusted lowering and raising speed and/or with different nozzle size. The concentrations of all the samples from the cross-sectional intervals measured using the analytical procedure mentioned below were weighted to compute the average concentration based on the cross-sectional areas of the intervals.

Analytical Procedures

The analyses for the parameters of nitrate-N, orthophosphate, and pesticides were performed at the Analytical Chemistry Laboratory of the ISWS. The laboratory is IEPA certified for the chemical analyses of samples for nitrate-N and the pesticide species alachlor, atrazine, and metolachlor. The sediment laboratory of the ISWS performed the analysis for TSS. Table 2 lists the analytes, IEPA method number, and specifies the procedures used by the laboratories.

Table 2. Methodologies for Chemical and Sediment Analyses of Water Samples

Analyte	*IEPA method number*	*Methodology*
Nitrate-Nitrogen	300.0	Ion Chromatography USEPA(1993)
Orthophosphate	365.1	Colorimetric USEPA(1983)
Pesticides (atrazine, alachlor, and metolachlor)	507	Gas Chromatography USEP A(1991)
Total Suspended Solids		USGS (Guy, 1969)

Monitoring 1998 Spring Storms at Big Ditch Station

During 1997-1998, the first year of the project, intensive monitoring of the Big Ditch station (106 in Figure 1), draining a 38-square-mile subwatershed of the Lake Decatur watershed was carried out. As shown in Figure 1, monitoring station 106 on Big Ditch is located approximately 5 miles upstream of its confluence with the Sangamon River, where the drainage area is approximately 50 square miles. Continuous flow and concentrations of TSS or suspended sediment, nitrate-N, phosphate-P, atrazine, metolachlor, and alachlor were monitored during the spring and early summer storm events of 1998. A new tipping bucket type raingage with electronic data logger was installed in April 1998 near the Big Ditch monitoring station where continuous measurements of rainfall were recorded.

Figure 6 shows daily rainfall and suspended sediment concentrations, both with continuous measurements of hourly water discharges (hydrograph) at the Big Ditch station throughout the 1998 monitoring period. Rainfall measurements were recorded starting from the end of April. As shown by the hydrograph and rainfall records, major storm events occurred during March, May, and June. The storms during March were associated with snow and freezing rain, when water sampling and constituent monitoring ceased. Extensive samples were collected only during and after intense rainfall events, a few grab samples were collected during the dry and remaining portions of the monitoring period. As shown in Figure 6b, sediment concentrations followed closely the water discharge hydrograph, although varying significantly from time to time with respect to the growing season, as discussed later.

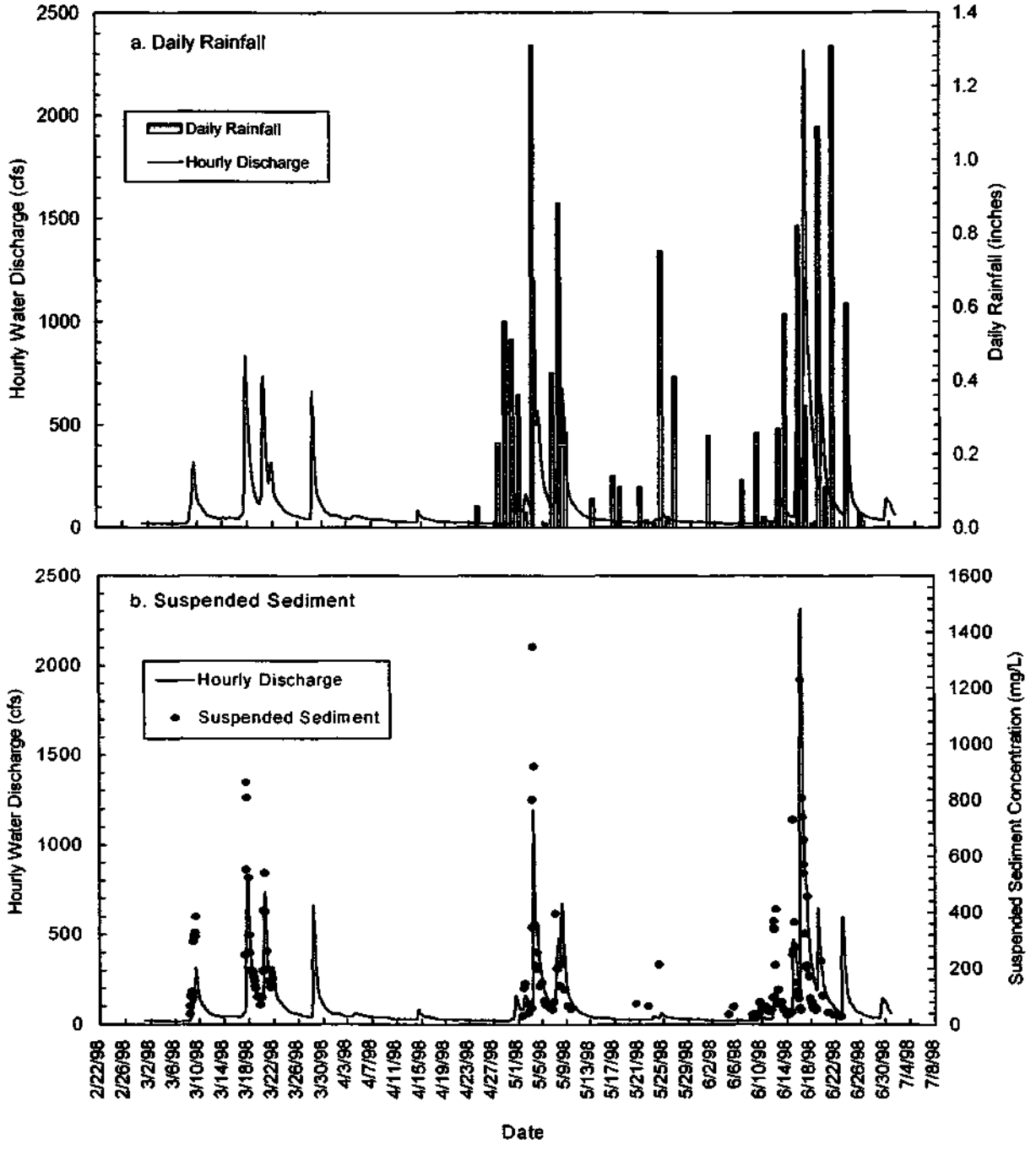

Figure 6. Observed data at Big Ditch monitored during the Spring 1998 storms: (a) hourly discharge and daily rainfall and (b) hydrograph and concentrations of suspended sediment

Figure 7 shows concentrations of nitrate-N (NO3-N), and phosphate-P (PO4-P) along with the hydrographs at the Big Ditch station throughout the 1998 monitoring period. As shown in Figure 7a, nitrate-N concentration generally varies inversely with water discharge, decreasing drastically during rising and peak flows, and increasing with the recession and base flow portions of the hydrographs. Such variations may be due to the pathways of runoff. Runoff through subsurface soil and tile drain contains more nitrate-N than runoff over the ground surface (surface runoff). Therefore, peak flows, primarily contributed by surface runoff contain less nitrate-N concentrations than water in the recession and base flows contributed by tile drain and subsurface flows flowing through the soil matrix. Another reason could be a limited release of nitrate-N from the soil, where the threshhold could be reached before the peak flow and beyond dilution until the flow becomes lower than the threshhold. Statistical relationships were developed, which are discussed later. As shown in Figure 7b, phosphate-P concentration follows the hydrograph similar to the sediment, which may be due to its adhesive properties with sediment.

Figure 8 shows the concentrations of atrazine and metolachlor along with the hydrograph at the Big Ditch station during the 1998 monitoring period. Since these two herbicides were monitored based on grab samples, data points for these constituents are not as intense as the sediment and nutrients. Similar to sediment and phosphate-P, concentrations of these herbicides also follow the hydrograph. Extreme concentration of about 30 µg/L was observed for both atrazine and metolachlor in May 1998. Analyses for alachlor did not detect this herbicide in water samples. Therefore, monitoring of alachlor was discontinued.

Monitoring 1999 Spring Storms above Mahomet

During 1998-1999, the second year of the project, monitoring was expanded to monitor two additional stations in the Upper Lake Decatur watershed. These stations were Fisher (112 in Figure 1) and Mahomet (105 in Figure 1), both located in the main stem of the Sangamon River and draining respectively 240 and 360 square miles of the Upper Sangamon (Lake Decatur) watershed. Monitoring was continued at the Big Ditch station (106 in Figure 1), draining a 38-square-mile subwatershed of the Lake Decatur watershed. Flow and concentrations of suspended sediment, nitrate-N, phosphate-P, and atrazine were monitored at all three stations during the spring and early summer storm events of 1999. Due to budgetary constraints, only one herbicide (atrazine) was monitored, and metolachlor was not monitored this year. Similar to Big Ditch station, Mahomet was equipped with an automatic ISCO sampler; however, Fisher did not have one due to installation difficulties at this location.

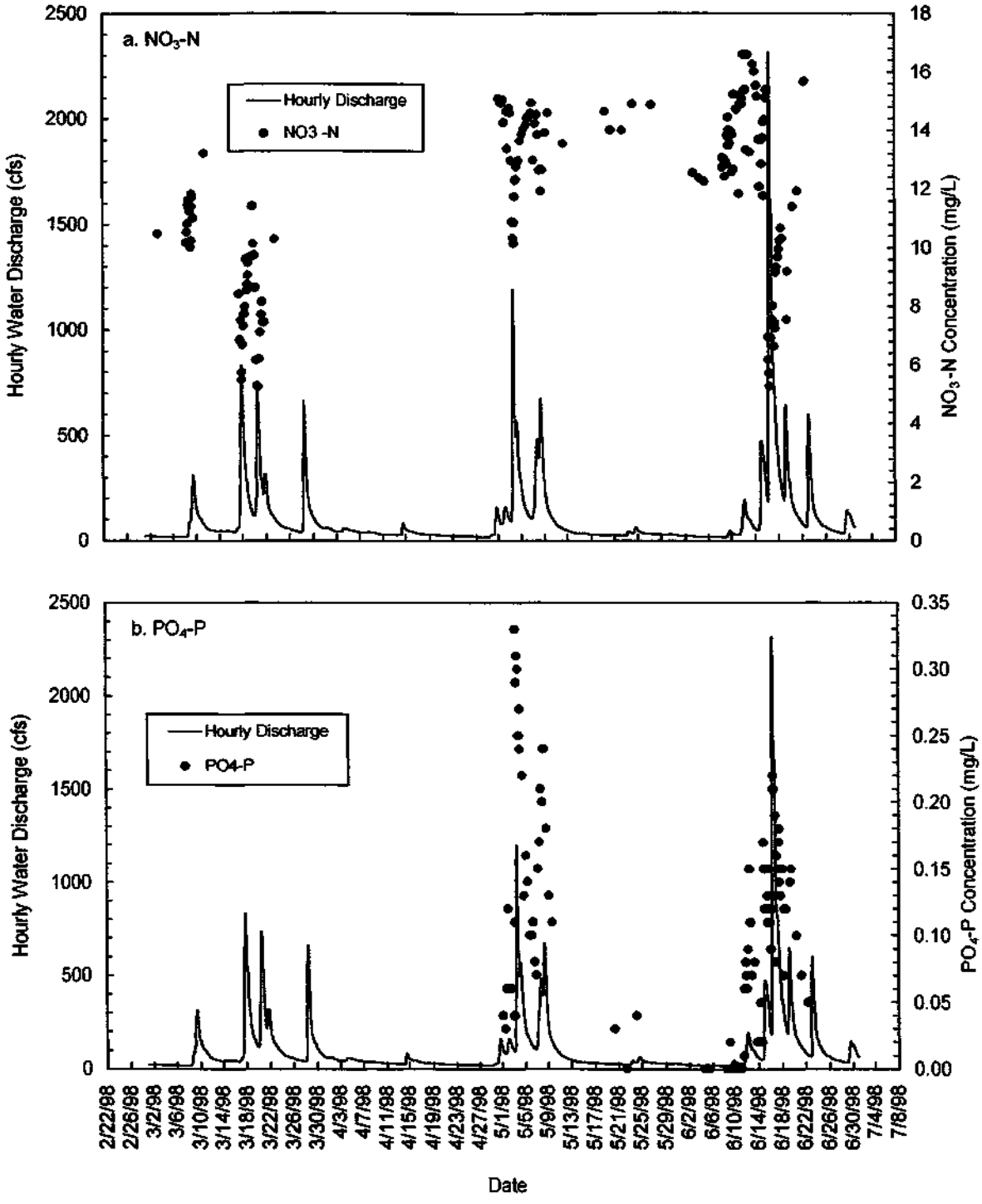

Figure 7. Observed data at Big Ditch monitored during the Spring 1998 storms:
(a) hydrograph and concentrations of nitrate-nitrogen and
(b) hydrograph and concentrations of phosphate-phosphorous

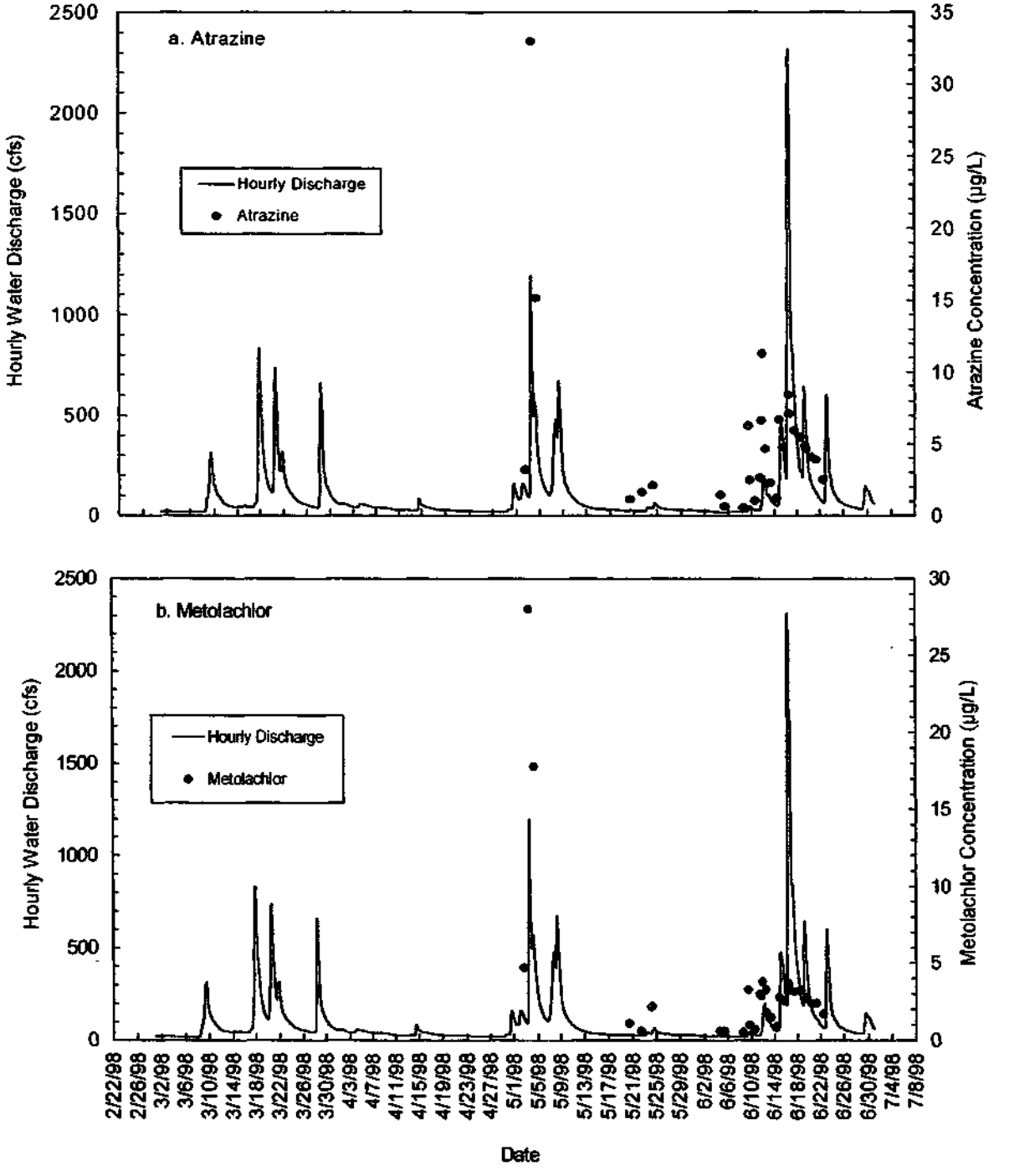

Figure 8. Observed data at Big Ditch monitored during the Spring 1998 storms:
(a) hydrograph and concentrations of atrazine and
(b) hydrograph and concentrations of metolachlor

Five additional tipping bucket type raingages with electronic data loggers were installed in the Upper Lake Decatur watershed at uniformly distributed locations. The raingage installed in April 1998 near the Big Ditch monitoring station was continued. Figure 9 shows the locations of these six raingages. Figure 10 shows the cumulative rainfall observed at these stations during the 1999 monitoring period. The raingages were installed at different times, and therefore, the records for different gages began at different times, especially Gage No. 4, which was installed on April 22, 1999 (Figure 10). As may be seen from these rainfall records, the six stations recorded noticeably variable rainfall depths, especially western stations 1 and 2 versus eastern stations 4, 5, and 6. The only intense storm recorded in all the gages was on April 15-16, 1999 (approximately 3 inches). Varying rainfall depths were observed at different gages on May 13, June 2, June 14, and June 23.

Figure 11 shows the hourly water discharges at Big Ditch, Fisher, and Mahomet along with the daily rainfall averaged over the 3-6 operating raingages during the monitoring period April-June 1999. As may be seen in this figure, the only intense storm during the monitoring period was on April 15-16. The peak and flow duration at the monitoring stations increase as the drainage basins increase from 38 square miles for Big Ditch to 240 and 360 square miles for Fisher and Mahomet, respectively.

The varying rainfall on May 13, June 2, June 14, and June 23, shown in Figure 10 have different responses at the three stream monitoring stations shown in Figure 11. Raingages 5 and 6 in the Big Ditch subwatershed (Figure 9) had very little rain on these dates, and therefore the hydrograph for the Big Ditch station shows very little flow (Figure 11). Raingages 3 and 4 (Figure 9) had heavier rain on June 2 (Figure 10), and therefore the downstream stations (Fisher and Mahomet) had flows close to 1000 cubic feet per second (cfs) following this storm (Figure 11). the Mahomet hydrograph clearly shows the attenuation and time lag of the flood peak from Fisher. Similar phenomena may be observed clearly after the June 14 and 23 rainfalls.

Figure 12 shows the concentrations of suspended sediment and nitrate-N, both with continuous measurements of water discharges (hydrograph) at the Big Ditch station throughout the 1999 monitoring period. Intensive measurements of the constituents were done only during the storms of April and June, the remainder periodically for nitrate-N (Figure 12b). As expected, suspended sediment followed very closely with the water discharge (Figure 12a). Nitrate-N concentrations were above 10 mg/L and went as high as 18 mg/L during the rising flows of the April and June storms (Figure 12b). They went down to around 16 mg/L afterwards and remained very much constant during the recession and base flow periods. These concentrations are approximately 4 mg/L higher than pre-storm concentrations (early April), indicating initiation of nitrate-N movement throughout the watershed by the storm and transport it to the streams via surface and subsurface runoff and tile drains. The inverse relationship of nitrate-N concentration with peak flow was not as pronounced as in spring 1998 storms (Figure 7a), which may be due to lower peak flow in April 1999.

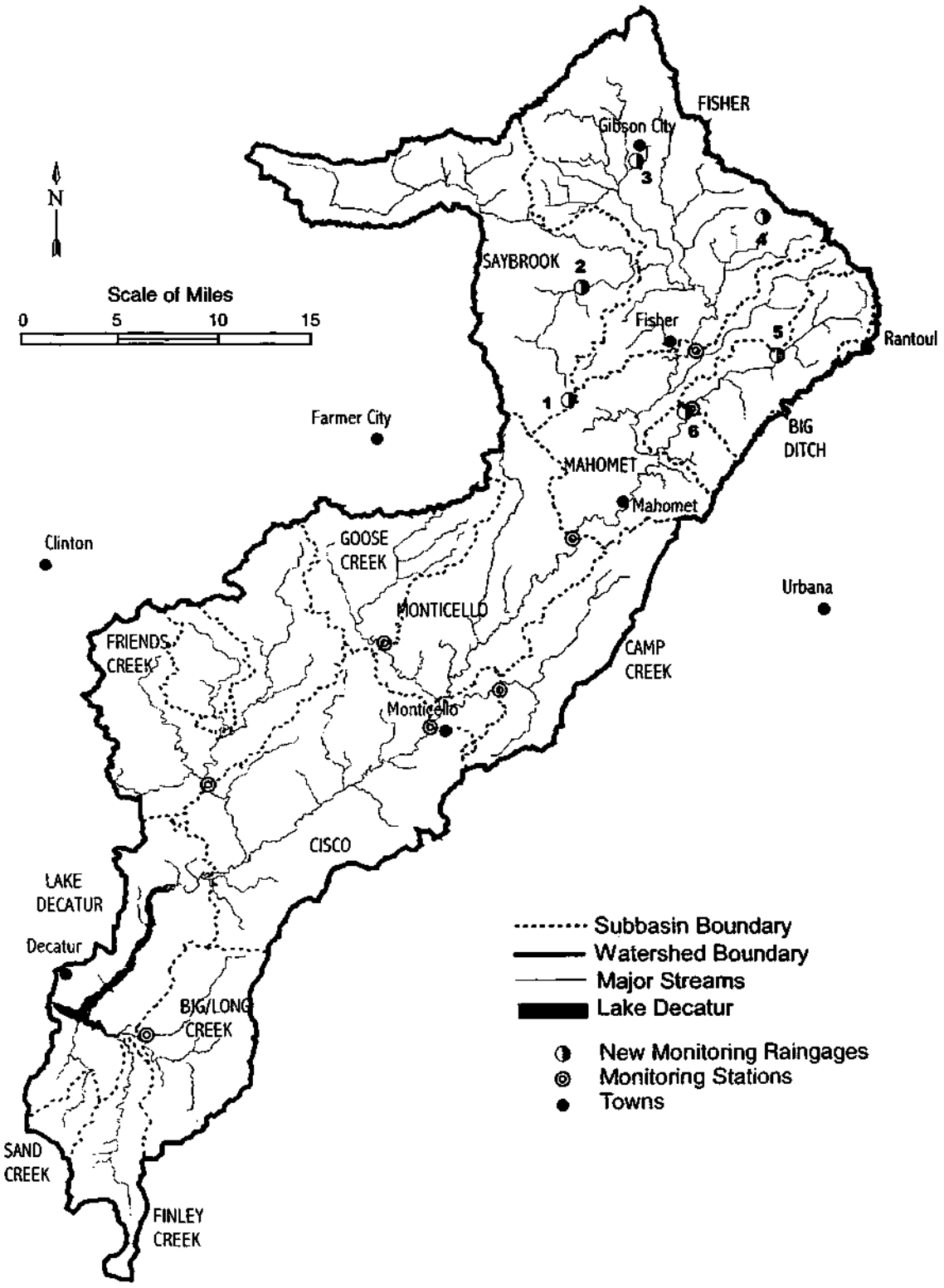

Figure 9. Locations of six new raingages above Mahomet in Lake Decatur watershed

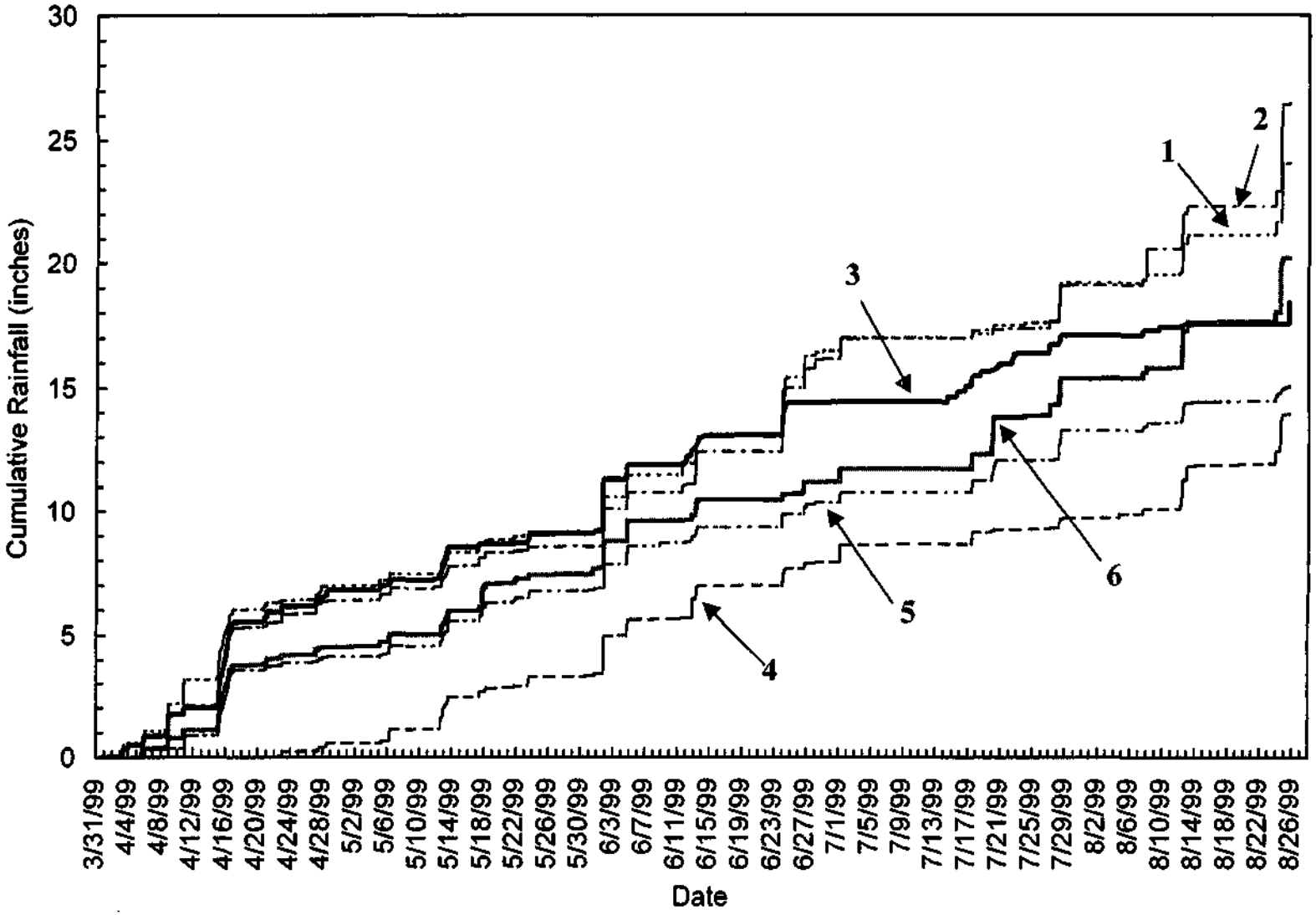

Figure 10. Cumulative rainfall observed during spring-summer 1999 at six new raingages in upper Lake Decatur watershed above Mahomet

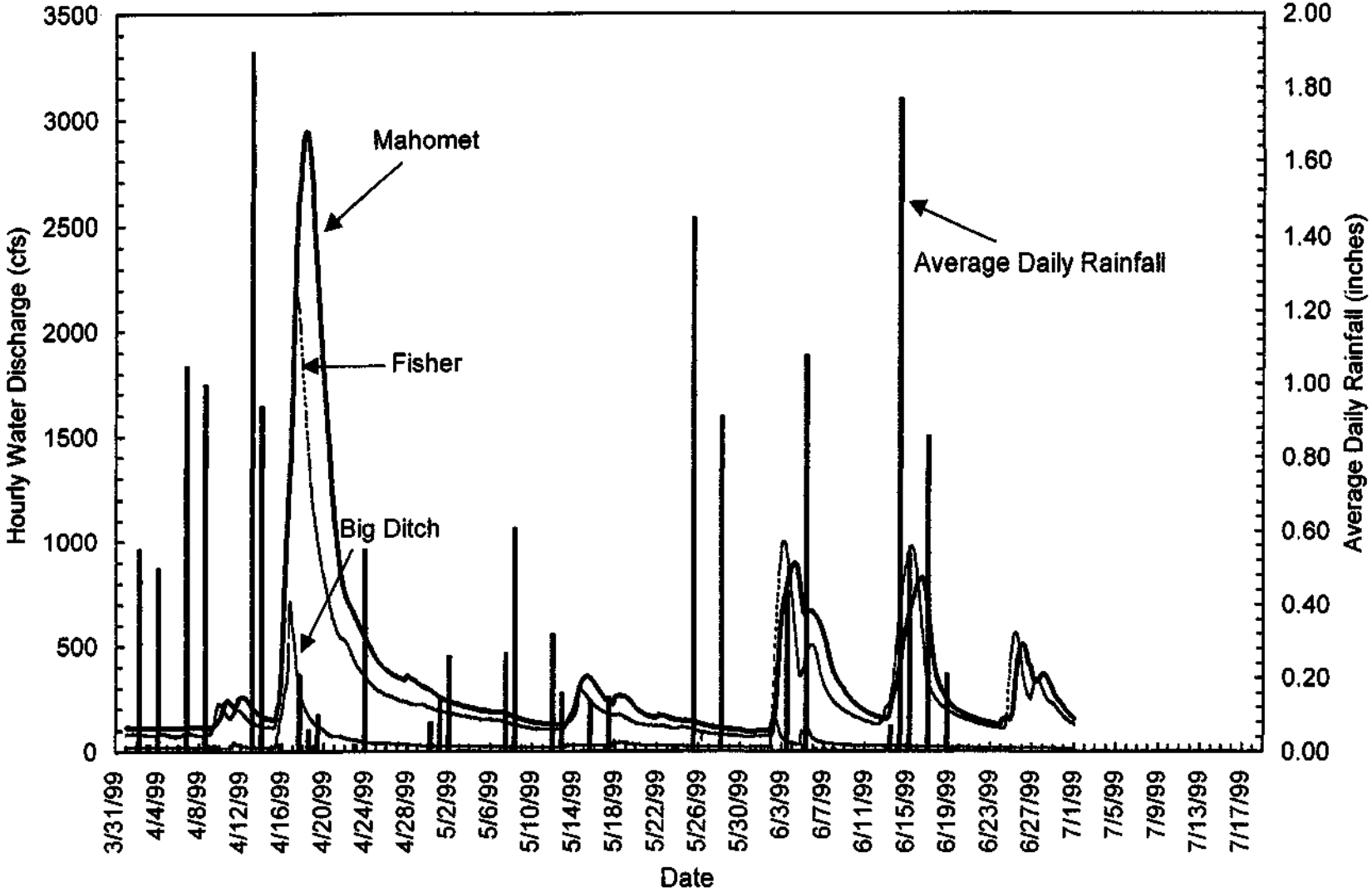

Figure 11. Observed hourly discharges at Big Ditch, Fisher, and Mahomet, and daily rainfall averages over 3-6 raingages (April-June,1999)

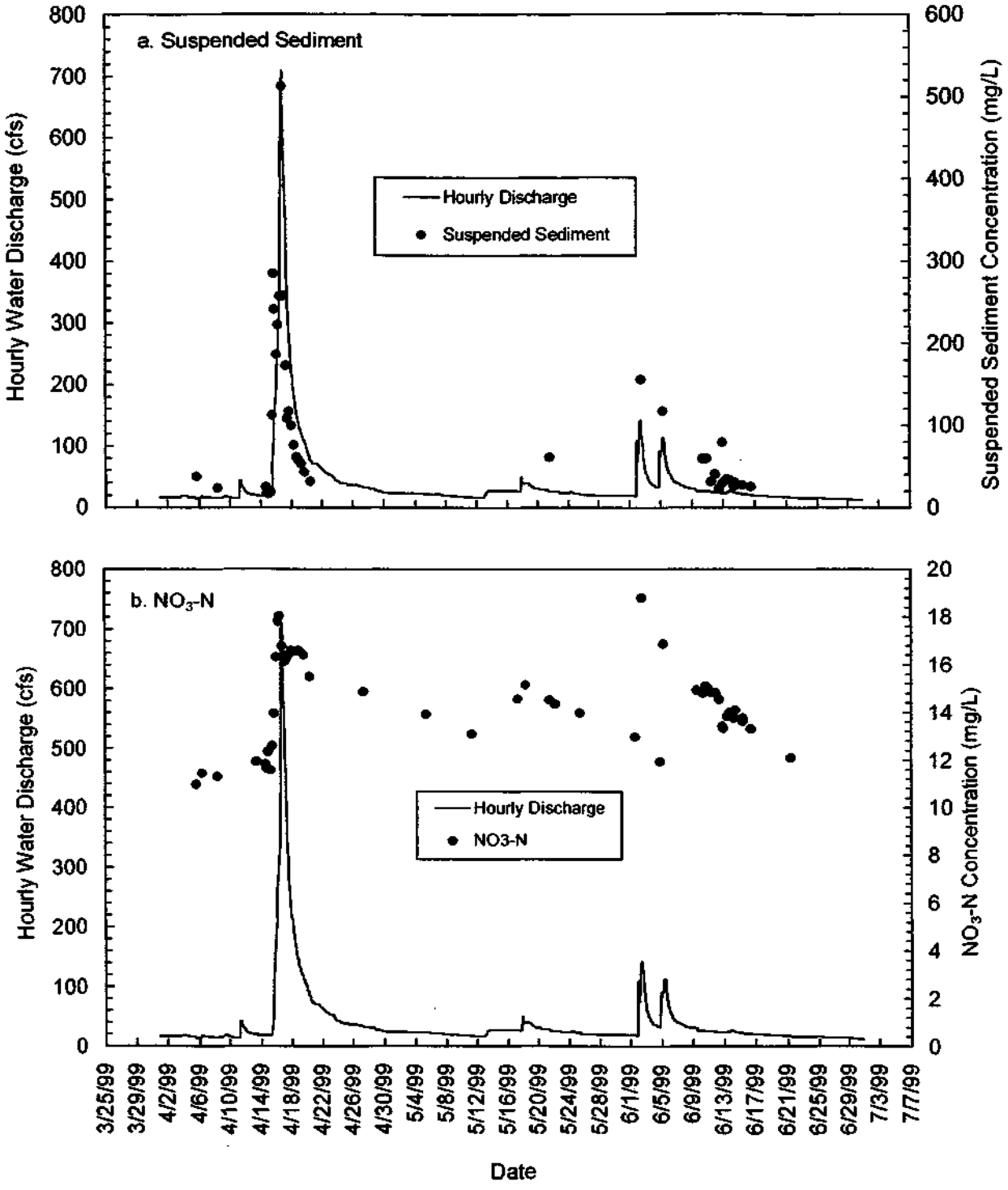

Figure 12. Observed data at Big Ditch monitored during 1999 storms:
(a) hydrograph and concentrations of suspended sediment and
(b) hydrograph and concentrations of nitrate-nitrogen

Figure 13 shows concentrations of phosphate-P and atrazine along with the hydrographs at the Big Ditch station. As shown in the graphs, both phosphate-P and atrazine followed a hydrograph similar to that for sediment. Atrazine concentrations were observed at 9 ug/L during the April peak flows and as high as 18 ug/L during the June storm (Figure 13b).

Figures 14 and 15 show all the above four constituents along with the hydrograph observed at Fisher, draining a 240-square-mile watershed. Since this station was not equipped with the automatic IS CO sampler, data points are not as intense as in the other stations. All samples were collected as grab samples. During the April storm, the peak sediment concentration appeared to precede the hydrograph peak (Figure 14a), which may be the case for a larger watershed. The peak nitrate-N concentration is around 16 mg/L (Figure 14b), approximately 2 mg/L less than for Big Ditch. Similar to Big Ditch, the difference between pre-season nitrate-N concentration (~10 mg/L in early April) and an average concentration during the rainy season is approximately 4 mg/L. Phosphate-P (Figure 15a) and atrazine (Figure 15b) concentrations followed very close to the hydrograph. Peak atrazine concentration during the April storm was near 6 ug/L, 3 µg/L less than for Big Ditch. However, the peak atrazine concentration during the June storm was near 30 ug/L.

Figure 16 shows the concentrations of sediment and nitrate-N observed at the Mahomet station, draining a 360-square-mile watershed. Figure 16a clearly shows advancement of the peak sediment concentration during the April storm by nearly 2 days from the flow peak and occurred during the early part of the rising hydrograph. Variation of nitrate-N concentration (Figure 16b) is very much similar to Fisher, a station approximately 20 miles upstream of the Sangamon River. Before the April storm, nitrate-N concentration was 9-10 mg/L, after which the concentration went up close to 16 mg/L, stayed between 12 and 14 mg/L, going down during the peak flows of the less intense storms and going up during the recession portions of these storms. This pattern of nitrate-N in response to rainfall-runoff indicates the enormous amount of nitrogen stored in the soil is ready to be dissolved by storm runoff and subsurface and tile-drained runoff, and then continued to be transported to the streams.

Figure 17 shows concentrations of phosphate-P and atrazine monitored at the Mahomet station, and, as expected, both constituents follow the hydrograph. Similar to Fisher, the maximum atrazine concentration during the April storm was approximately 6 µg/L. On June 2, the concentration went up to 11 µg/L.

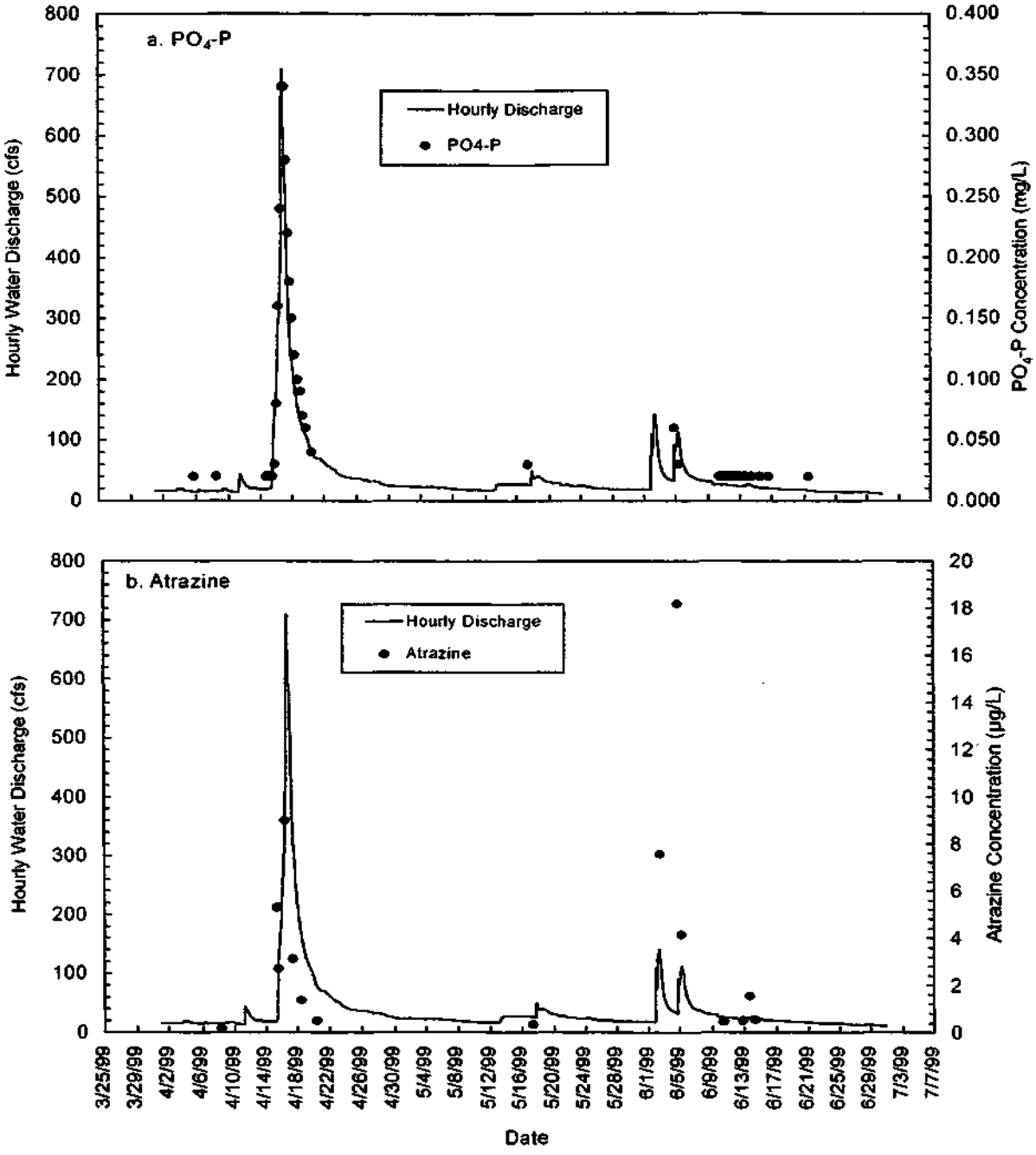

Figure 13. Observed data at Big Ditch monitored during 1999 storms: (a) hydrograph and concentrations of phosphate-phosphorous and (b) hydrograph and concentrations of atrazine

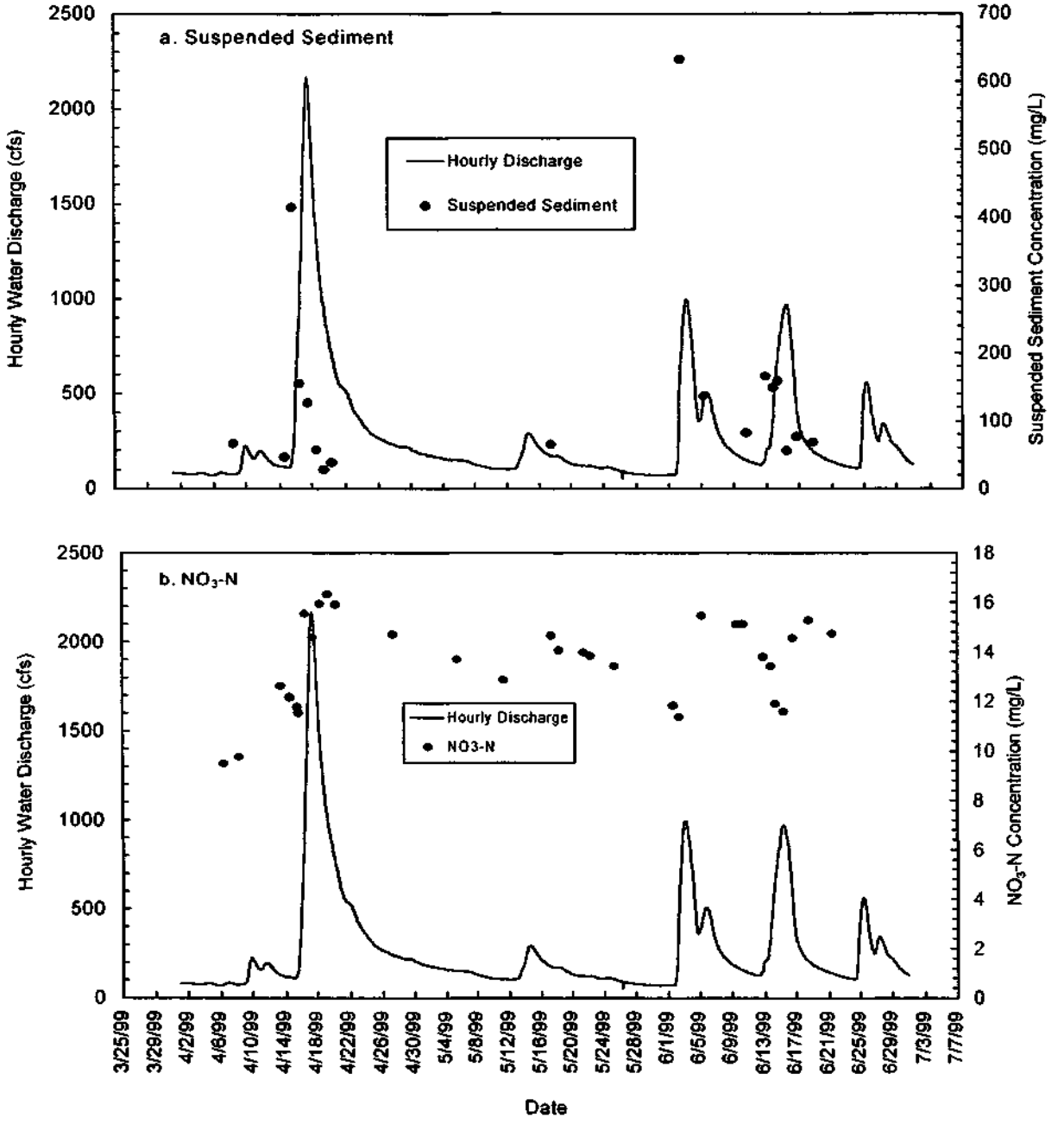

Figure 14. Observed data at Fisher monitored during 1999 storms:
(a) hydrograph and concentrations of suspended sediment and
(b) hydrograph and concentrations of nitrate-nitrogen

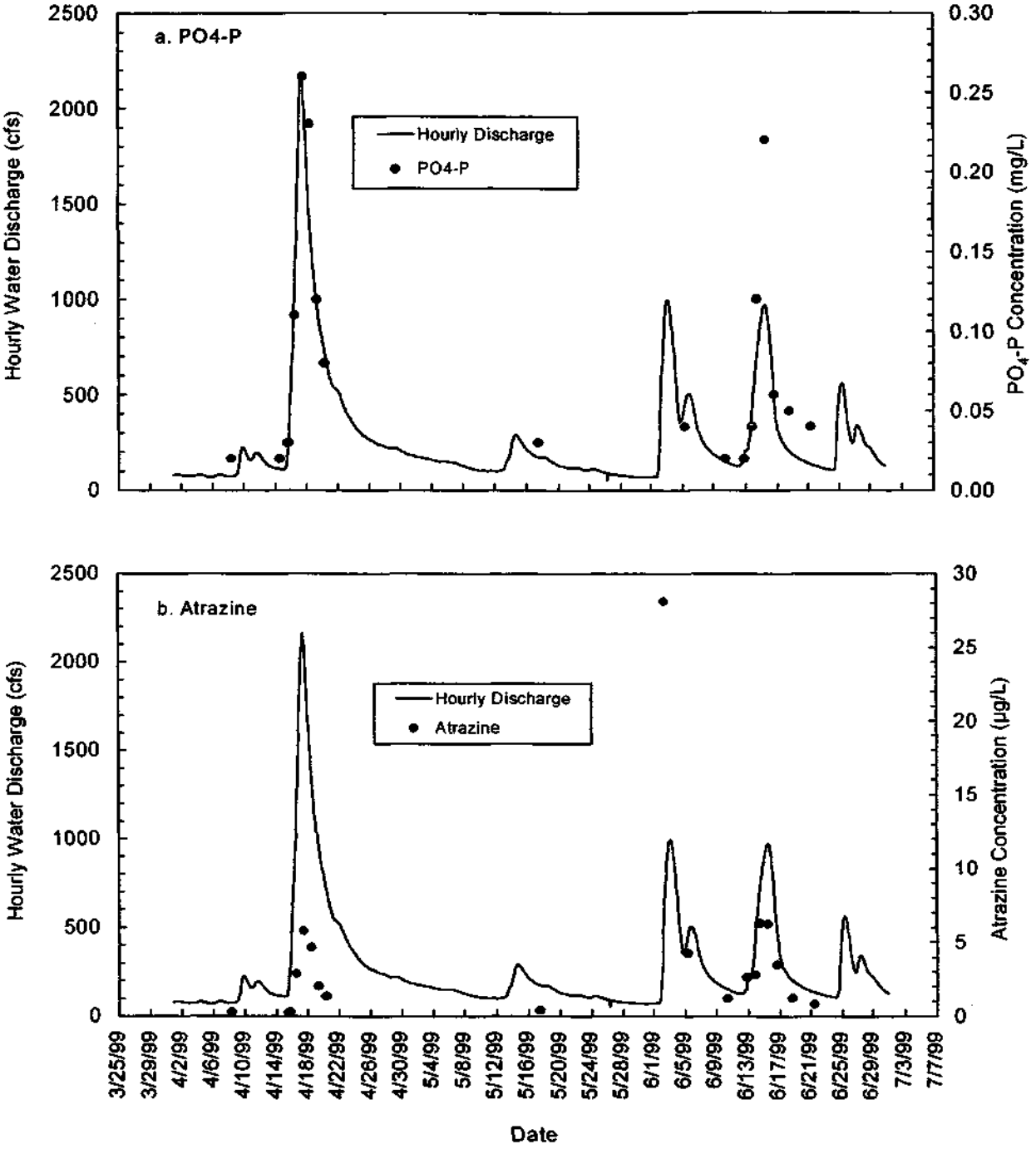

Figure 15. Observed data at Fisher monitored during 1999 storms:
(a) hydrograph and concentrations of phosphate-phosphorous and
(b) hydrograph and concentrations of atrazine

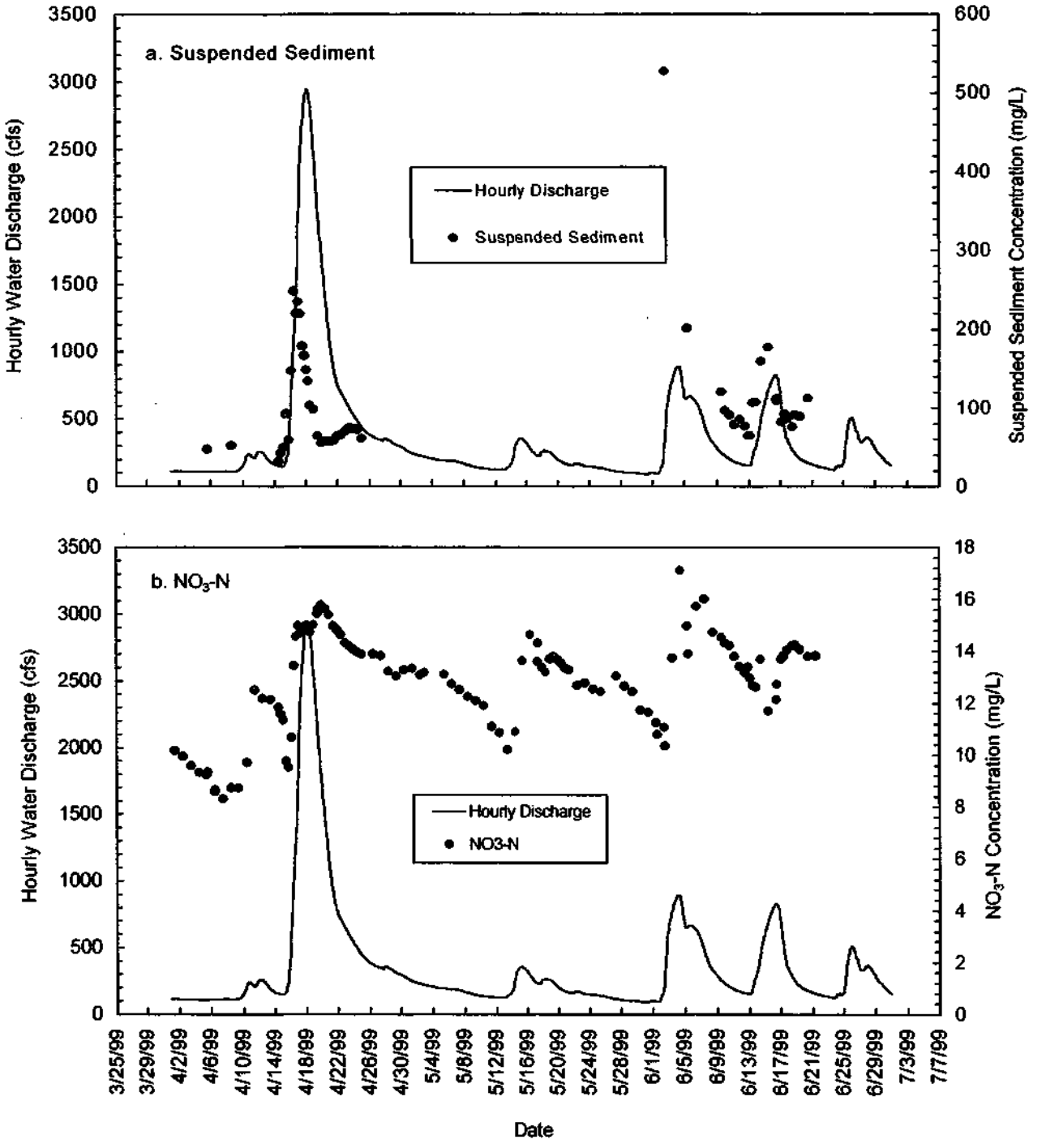

Figure 16. Observed data at Mahomet monitored during 1999 storms:
(a) hydrograph and concentrations of suspended sediment and
(b) hydrograph and concentrations of nitrate-nitrogen

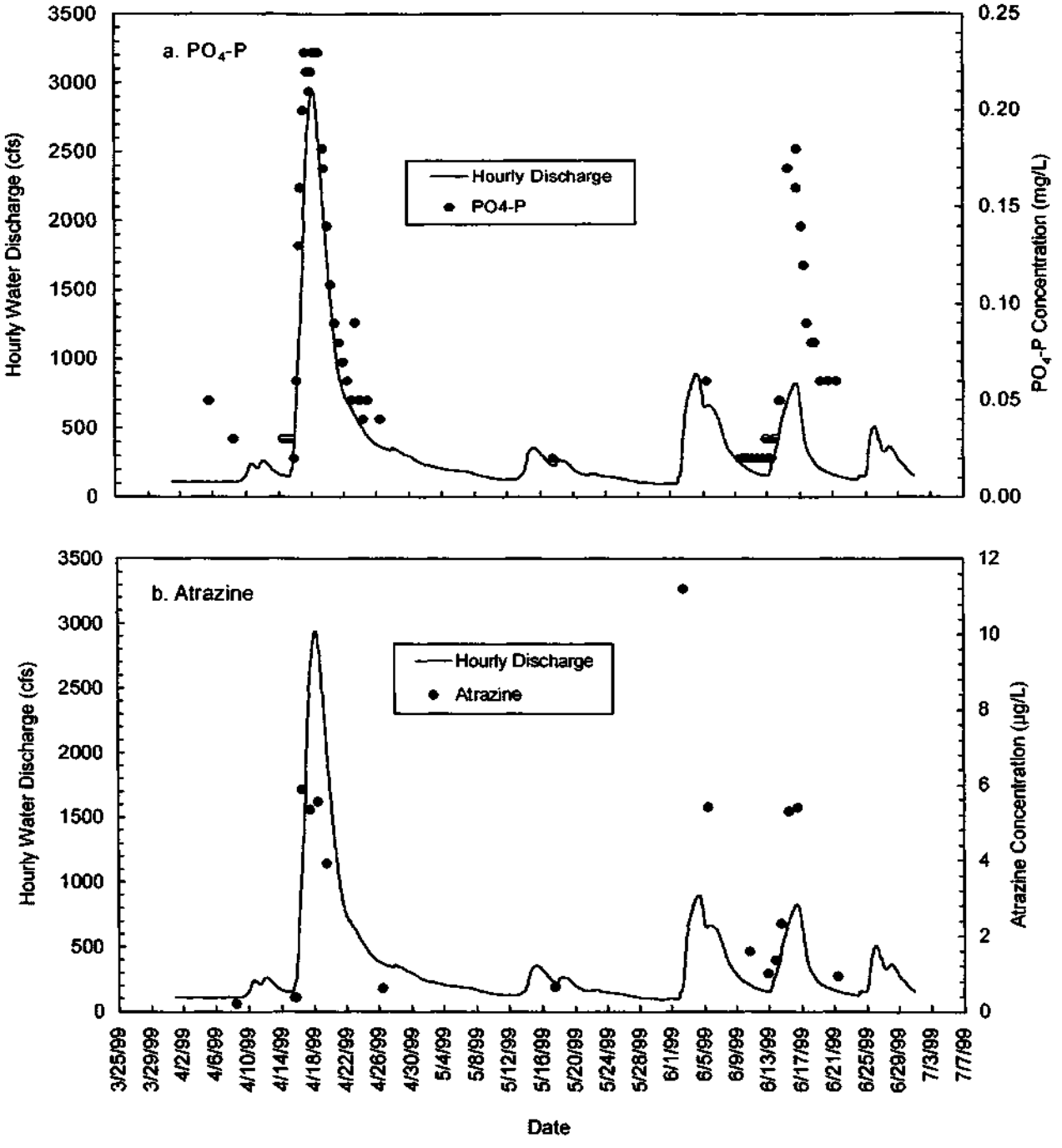

Figure 17. Observed data at Mahomet monitored during 1999 storms:
(a) hydrograph and concentrations of phosphate-phosphorous and
(b) hydrograph and concentrations of atrazine

Monitoring Tile Drain and Grassed Waterway

In April 1999, samples were collected from a tile drain, a grass waterway, and the Big Ditch station (106 in Figure 1) and were analyzed for four parameters: nitrate-N, phosphate-P, atrazine, and suspended sediment concentrations. The three sampling locations were visited on the same date and at approximately the same time to obtain samples. The tile drain, approximately 8 inches in diameter, was located about 500 feet downstream from the Big Ditch station. While sampling, the tile drain was observed fully discharging like a jet. The grassed waterway was located on road 700E just north of 2550N in Champaign County and about ¼ mile south of the Big Ditch station. It crosses under 700E and flows southwesterly until it discharges into the Big Ditch. While sampling, the grassed waterway had water approximately 4 feet wide and 1 foot deep rushing down a sinuous path. Table 3 presents the analytical results from the samples collected at these three locations.

The analytical results of the samples taken on April 15, 1999 show similarities in concentrations of nitrate-N (NO3-N), phosphate-P (PO4-P), and atrazine for the tile and stream locations. The grassed waterway concentrations were much lower for nitrate-N and atrazine. Phosphate-P concentrations were slightly higher in the grassed waterway. A sediment sample was not taken of the tile and grassed waterway on this date.

However, on April 16, 1999, it was noticed that the tile water was turbid from sediment, and, sediment samples were taken of the tile water and also of the grassed waterway. The concentration of suspended sediment was found to be high for the tile, where suspended sediment concentrations would be expected to be low because the water in the tile should be somewhat filtered by the soil before it enters the tile. It was later learned that the tile had broken when a few weeks later a crew was seen replacing the tile. Therefore, the samples taken of the tile on April 16 and 17 probably had some surface runoff mixed in with the actual tile flow and were not purely tile water. Still, the grass waterway sample showed higher or equal nitrate and phosphorous concentrations than the tile sample on these dates. Definite conclusions cannot be drawn with these limited data. Further monitoring is needed.

Table 3. Sediment and Chemical Concentrations Observed at Tile Drain, Grassed Waterway, and Big Ditch Station

Date (Time)	*Sample location*	*NO3-N (mg/L)*	*PO4-P (mg/L)*	*Atrazine µg/L)*	*Susp. Sed. (mg/L)*
4/15/99 (11:30 a.m.)	Tile	14	0.06	5.31	
	Grass waterway	0.4	0.19	0.13	
	Stream	13	0.02	5.31	113
4/15/99 (4:00 p.m.)	Tile	14	0.07	2.69	
	Grass waterway	0.5	0.15	0.09	
	Stream	14	0.03	2.72	242
4/16/99 (11:00 a.m.)	Tile	10	0.36		824
	Grass waterway	14	0.54		304
	Stream	18	0.24	9.00	257
4/17/99 (11:00 a.m.)	Tile	12	0.18		
	Grass waterway	12	0.62		
	Stream	16	0.22	3.13	109

Analyses of Monitored Data from Lake Decatur Watershed

In addition to using data to test the DWSM components, the monitored data were extensively analyzed to verify the integrity of the time-integrated automatic ISCO sampler, and to develop statistical correlation equations of the constituent concentrations with water discharge. These analyses are discussed in the following two sections.

Comparisons of ISCO Samples with Grab and Depth-Width-Integrated Samples

Most water samples for analyses of suspended sediment, nitrate-N, and phosphate-P were taken using the time-integrated automatic ISCO sampler, which pumps water samples from a point close to the water surface. Although water can be pumped from a certain depth using weights, with high velocities during intense storms, water is usually pumped from a point near the surface. This brings the question of representative samples and accuracy of the concentrations of the above constituents measured from these samples. In order to answer these quality control and quality assurance questions, additional samples were collected during field visits. Grab samples, as discussed earlier, were collected during almost all field visits, and some depth-width-integrated samples were collected using the USGS DH-59 sampler for sediment analyses.

Concentrations of different constituents measured from different sampling methods are graphically compared here to examine their consistencies. In these comparisons, linear correlation equations were derived. These correlated lines along with the scattered data points and the line with equal value are plotted for visual comparisons. Correlation coefficient (R^2) of the correlation equation is also noted in each comparison graph.

Figure 18 shows the comparisons of nitrate-N and phosphate-P concentrations measured from ISCO and grab samplers. As seen in Figure 18a, the concentrations of nitrate-N from ISCO and grab samples are almost a perfect match with R^2=0.98, and 0.99 slope of the linear fit. There seems to be an outlier in the phosphate-P comparison (Figure 18b); one of the ten data points is way off from the general trend. Even with that outlier, the correlation coefficient is 0.93, and slope of the correlation line is 1.04, indicating a good match of concentrations from the ISCO and grab samples. From these results, it can be concluded that the ISCO samples show no or negligible sample degradation for the nitrate-N and phosphate-P species.

Figure 19 shows the comparisons of the suspended sediment concentrations measured from both grab and ISCO samplers with the concentrations measured from a commonly used depth-integrated DH-59 sampler. Due to its intensive sampling procedure, depth-width-integrated sampling from the DH-59 sampler gives a more representative and accurate measurement of suspended sediment concentration than the

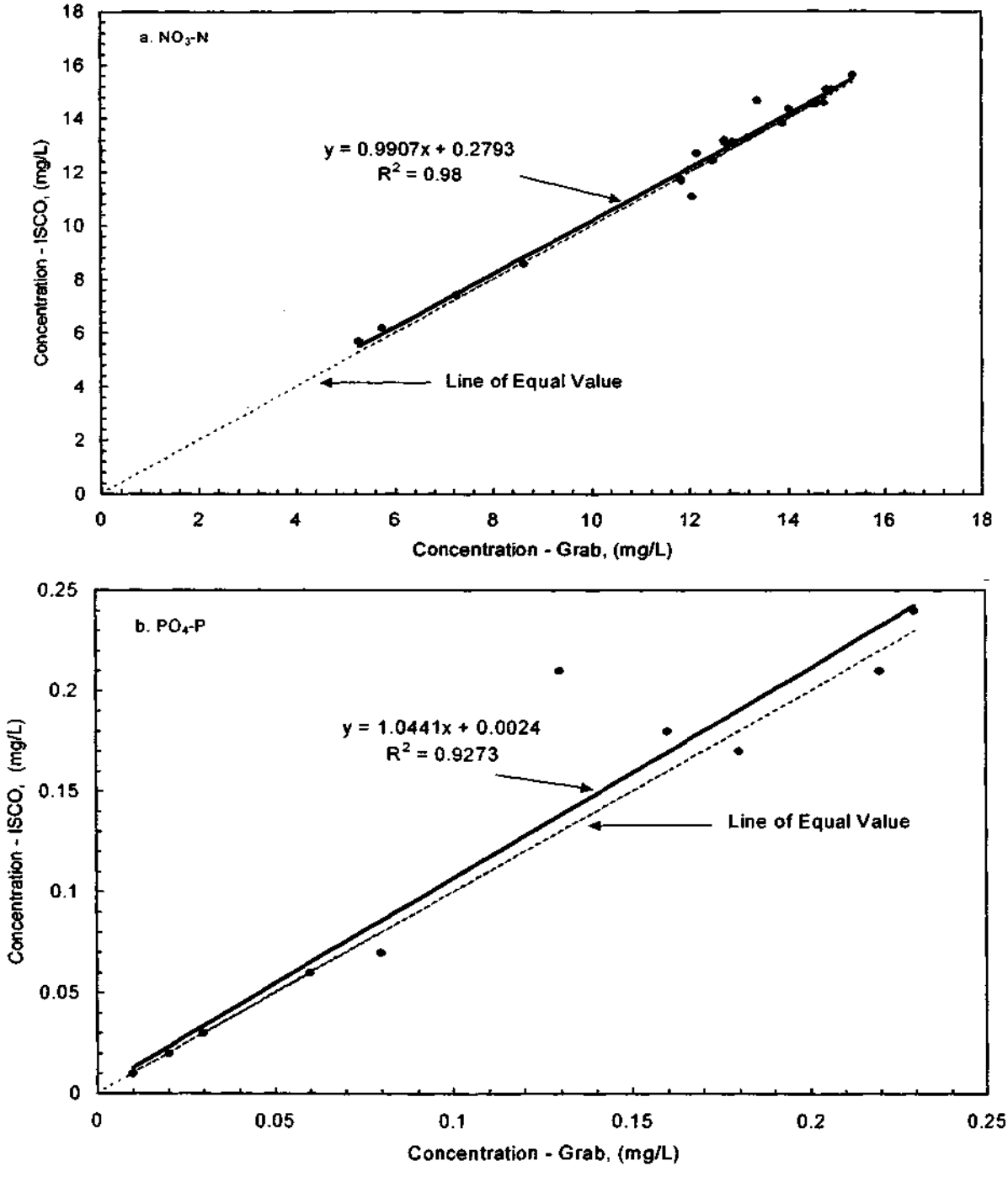

Figure 18. Comparison of concentration measurements by automatic ISCO and grab samplers for (a) nitrate-nitrogen and (b) phosphate-phosphorous

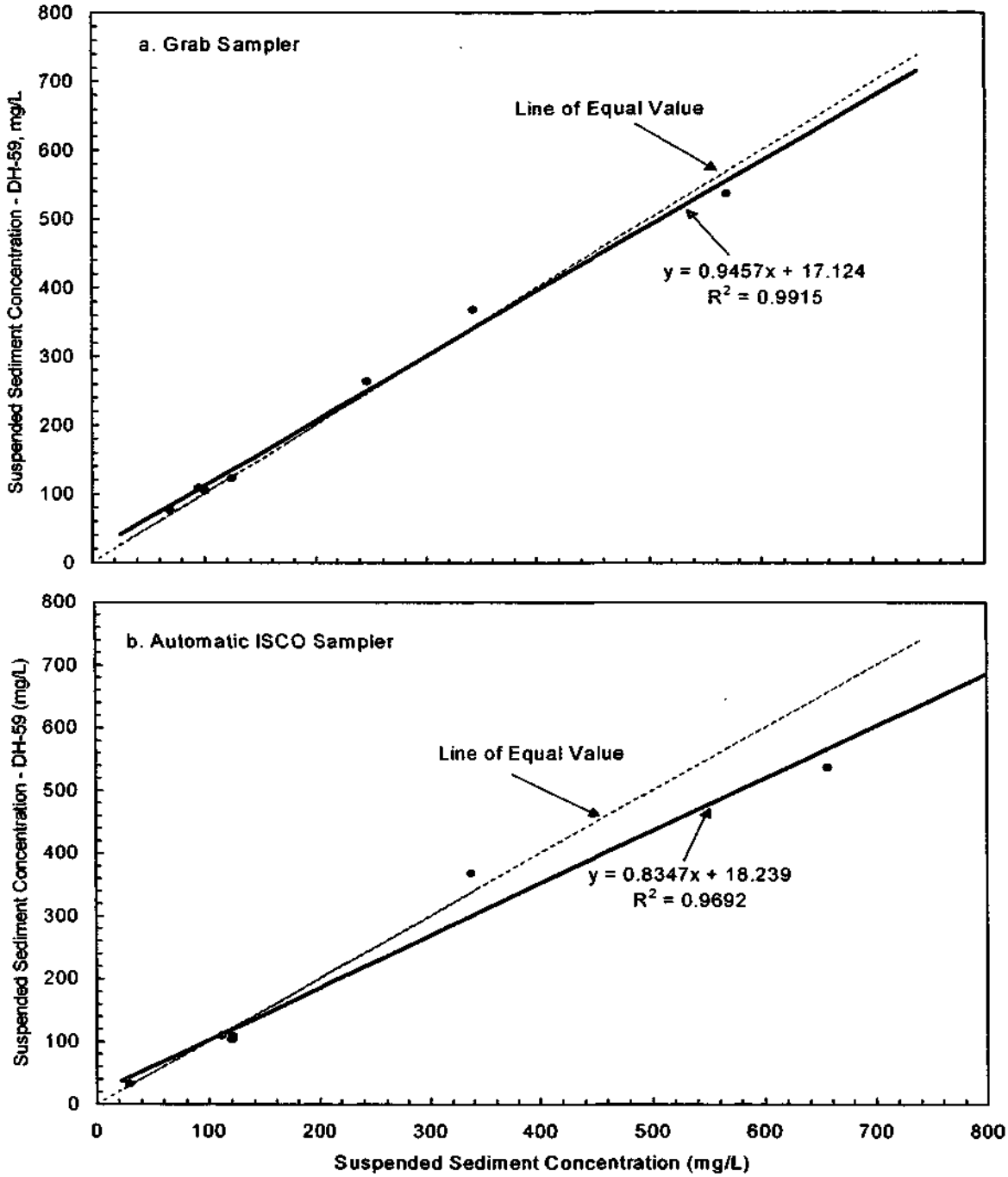

Figure 19. Comparison of suspended sediment concentration measured by depth integrated DH-59 sampler and by (a) grab sampler and (b) automatic ISCO sampler

other methods. As shown in Figure 19a, results from the grab and DH-59 samples are almost a perfect match with slope of linear correlation line 0.95 and coefficient 0.99. However, the slope and the coefficient reduced to 0.83 and 0.97 in the case of the ISCO versus DH-59 samples (Figure 19b) due to a single and the highest concentration point, with the ISCO sampler measuring almost 150 mg/L more suspended sediment. Except for this point, the comparison is very good. Figure 20 shows the comparison of grab and ISCO samples. Although the comparison is very good with slope and coefficient of 1.1 and 0.99, the highest two points show higher suspended sediment concentrations by the ISCO sampler. More data points with high concentrations of suspended sediment are required to definitely conclude such differences exist. Nevertheless, these comparisons show that the grab and the automatic ISCO samplers were producing similar concentrations to the depth-width-integrated DH-59 sampler.

From the above results, it appears that the suspended sediment was well mixed in the stream cross section during the intense storm events monitored. As a result, all the constituents were well mixed, providing the advantage of efficient point measurements in place of extensive and time- and labor-intensive depth-width-integrated measurements.

Pollutant Correlation with Flow Measurements: Statistical Models

Correlation relations were developed for all monitored constituent concentrations with the water discharge. Figures 21-23 present the relationships between concentrations of suspended sediment, nitrate-N, phosphate-P, atrazine, and metolachlor, respectively, with water discharge based on the monitored data during the spring 1998 storm events. Data collected during March, May, and June show different correlation relations, and therefore, data for each month were grouped together and an individual correlation equation for each month was developed in addition to the combined correlation equation for all data. As shown in these figures, the correlation for each constituent varies from month to month showing high dependency of constituent occurrence in water on timing during the growing season with varying climate and ground cover. Sediment concentration with respect to water discharge is the highest during March (Figure 21), which may be due to the thawing of soil from freezing conditions, and also due to very little ground cover. The sediment concentration gradually reduces in May and further reduces in June, reflecting seedling growth and establishment of crops in the field. These curves show sediment concentration increasing exponentially with water discharge.

All nutrient and herbicide concentrations are high during May (Figures 22 and 23). All chemicals, except nitrate-N, rise with respect to water discharge following a logarithmic or power relation and approaching a point of saturation or a constant value. Nitrate-N follows exponential decay functions with decreasing concentration with respect to water discharge and approaching a minimum value. This is due to the enormous storage of nitrogen in central Illinois soil (11,000 kilogram in the top meter per acre).

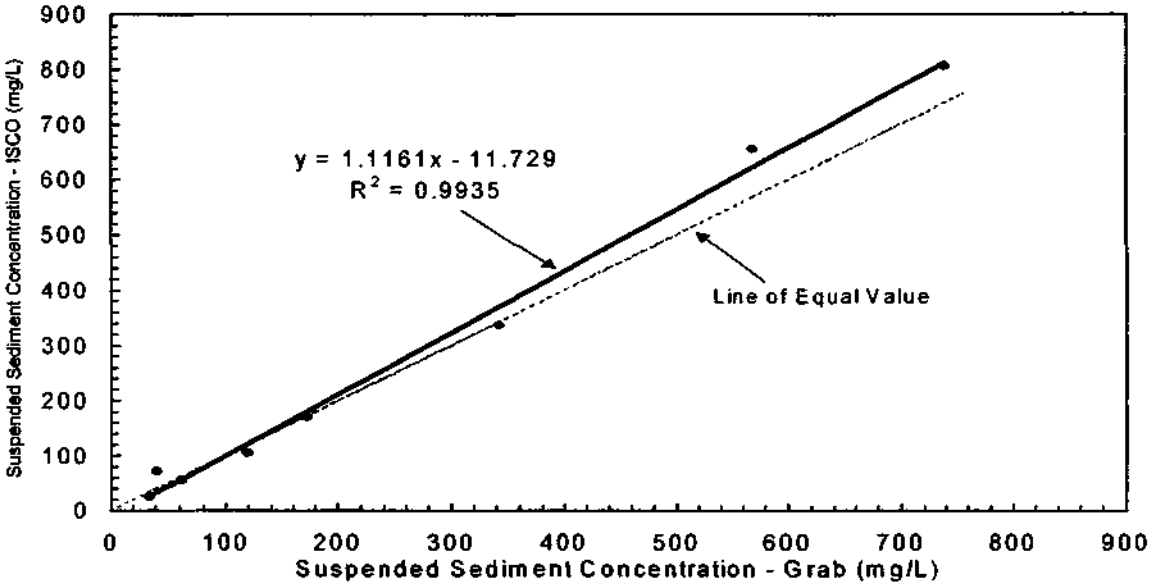

Figure 20. Comparison of suspended sediment concentration measured by automatic ISCO sampler and by grab sampler

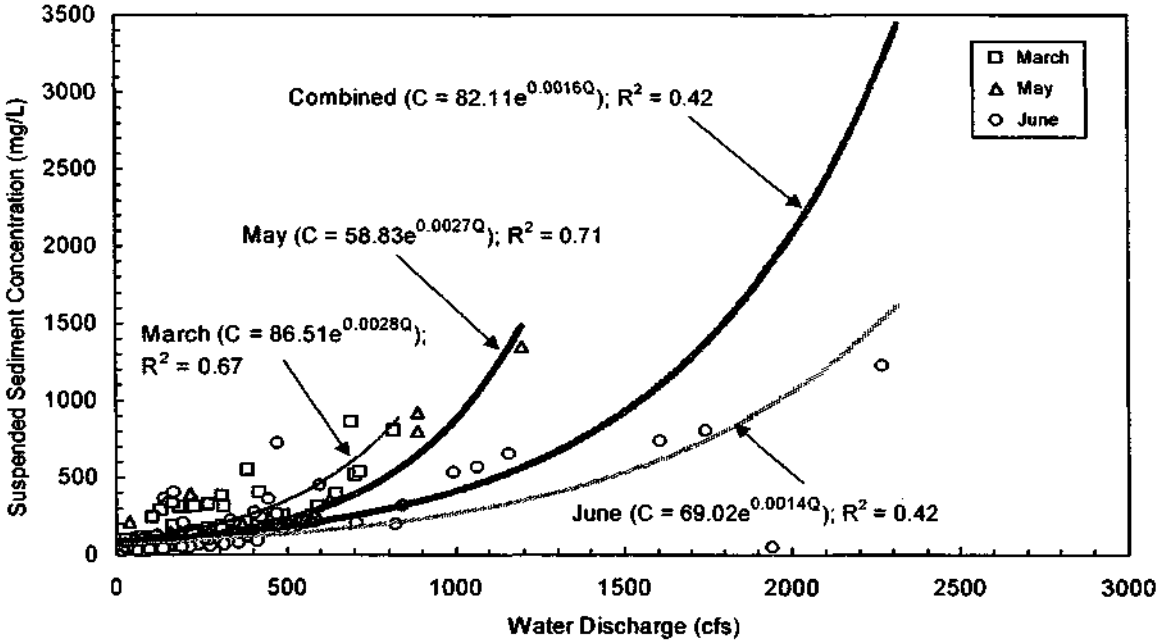

Figure 21. Correlation of suspended sediment concentration with water discharge at the Big Ditch station based on observations made during Spring 1998 storms

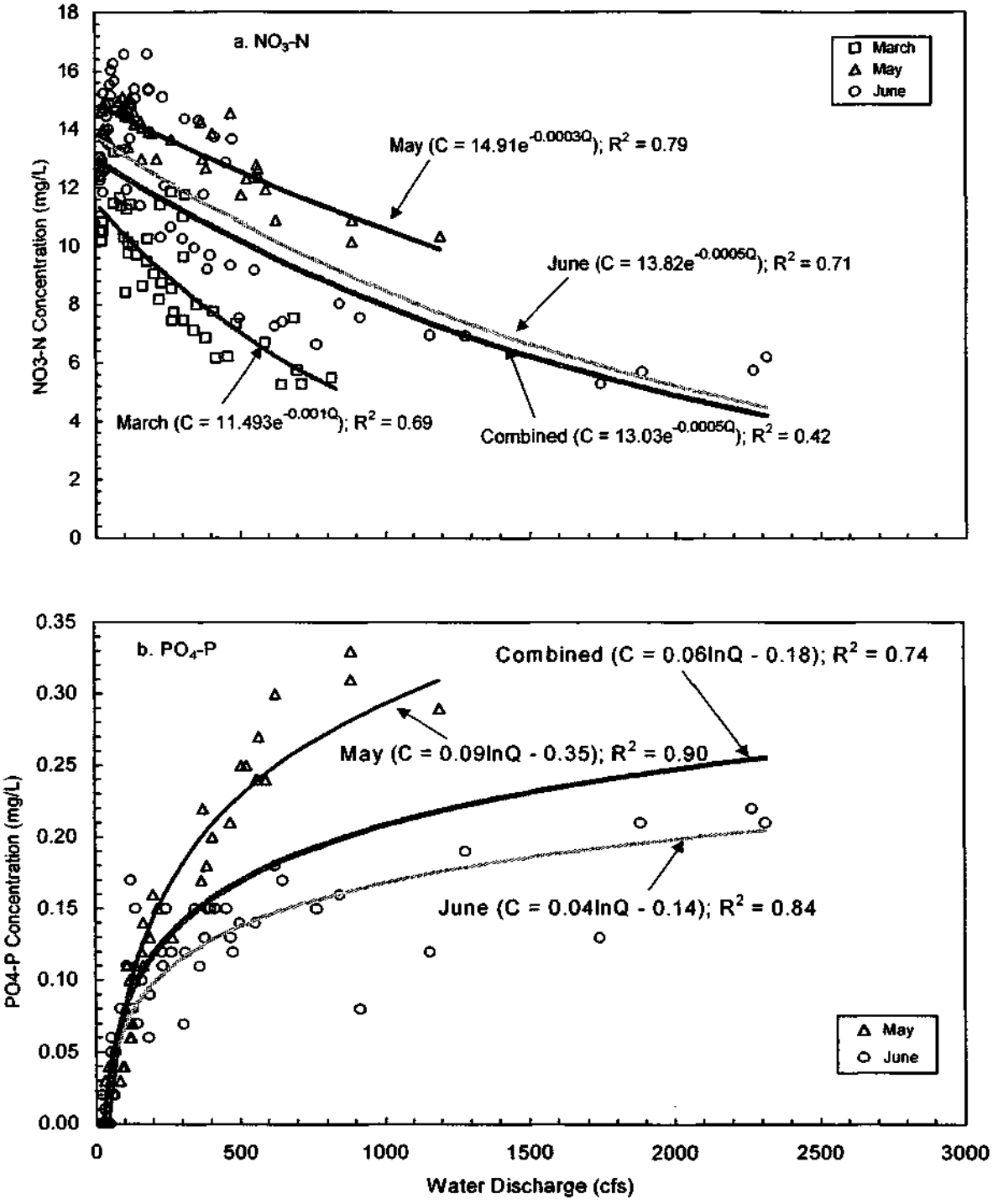

Figure 22. Correlation of nutrient concentrations with water discharge at the Big Ditch station based on observations made during Spring 1998 storms: (a) nitrate-nitrogen and (b) phosphate-phosphorous

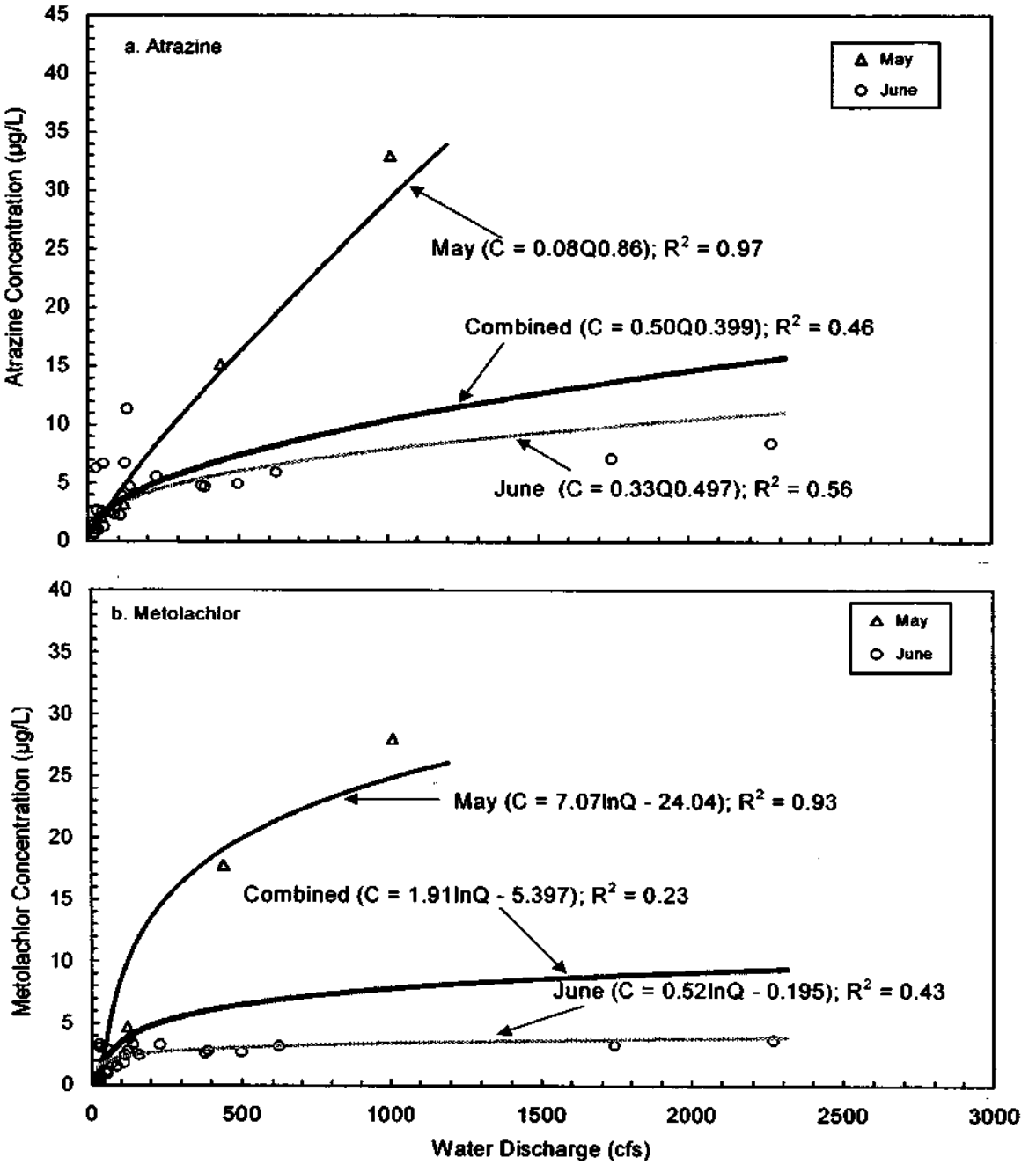

Figure 23. Correlation of herbicide concentrations with water discharge at the Big Ditch station based on observations made during Spring 1998 storms: (a) atrazine and (b) metolachlor

The correlation equations and the corresponding correlation coefficients for the constituents during individual months and for the combinations of the months are shown in the respective figures. These equations may serve as useful tools in predicting constituent concentrations in Big Ditch and similar watersheds under similar geographic, geological, climatic, and land-use conditions. These equations may also serve as useful tools in computing mass balances of the pollutants in the watershed.

Modeling Lake Decatur Watershed

Hydrologic Simulations in Lake Decatur Watershed

Figure 1 shows the boundaries of the 925-square-mile Upper Sangamon River basin (Lake Decatur watershed), and its subbasins (subwatersheds), drawn based on USGS 7.5-minute series Topographic Quadrangle maps. A schematic diagram (Figure 24) illustrates the relative sizes and positions of the subwatersheds along the Sangamon River. Larger subwatersheds, such as the Mahomet, Cisco, and Friends Creek were further subdivided. The entire watershed was divided into 20 subwatersheds. Each subwatershed is represented by two rectangular overland elements contributing to a channel or stream element laterally from each side. Areas of the two overlands and length of the channel were measured from which lengths of the overlands were computed by dividing the respective areas by the channel length. Channel cross-sectional measurements were used to estimate the coefficients and exponents of wetted perimeter versus cross-sectional area relations (Equation 14) for the channels. Representative slopes of the overlands and channels were measured from the topographic maps. Representative curve numbers for the overlands, and Manning's roughness factors for the overlands and channels were based on the earlier Lake Decatur watershed modeling study (Demissie et al., 1996). These values were adjusted during model calibration. A Lake Decatur stage-storage relationship table was prepared based on a lake cross-sectional survey by ISWS (Fitzpatrick et al., 1987). A stage-discharge table was prepared using weir formula (Chow, 1959) with a weir coefficient of 3.6. A computational sequence of flow elements and a data management array were prepared using the procedure outlined in Borah et al. (1981).

All the above data constituted the basic input data file for the model. For hydrologic simulations, the remaining data needed were the breakpoint rainfall records for the storms simulated.

Simulation of September 14, 1993 Storm: Model Calibration

The rainfall event of September 14, 1993, beginning at 10:00 a.m. and ending at 9:00 p.m., was selected to calibrate and test performance of the current hydrologic component of DWSM. Hourly flows resulting from this storm at four tributary stations (Big Ditch, Camp Creek, Friends Creek, and Big/Long Creek) were successfully monitored during the earlier ISWS study (Demissie et al., 1996). Rainfall data were obtained from National Weather Service records at stations in Urbana, Rantoul, Farmer City, Decatur, and Sullivan. No rainfall data from Rantoul were available for the above storm. Rainfall for this storm was approximately uniform at the observed stations, and thus throughout the watershed, with an average depth of 2.1 inches. The breakpoint hourly record was available and input into the model.

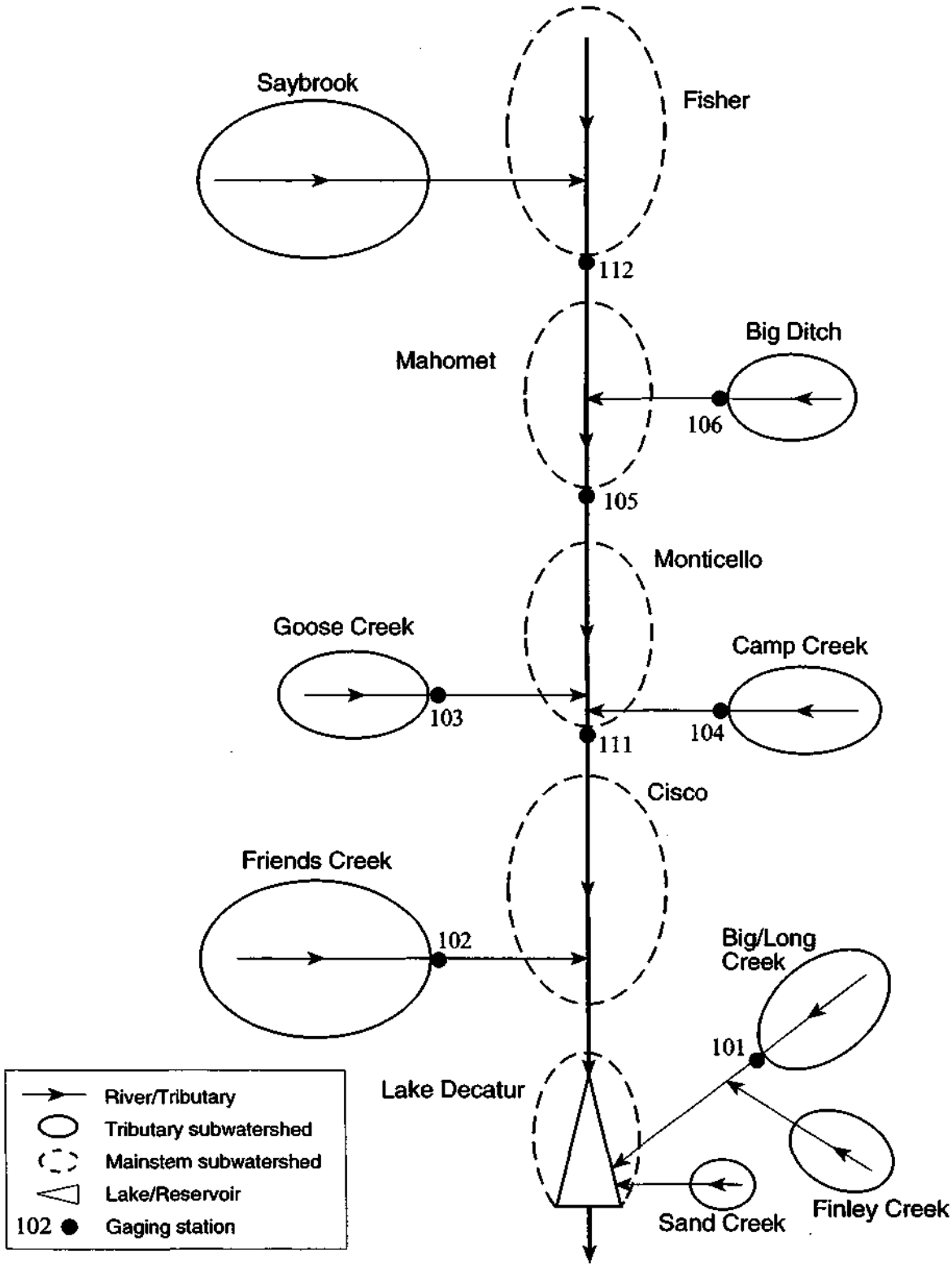

Figure 24. Schematic diagram of the Upper Sangamon River with its major tributaries and subwatersheds draining into Lake Decatur (after Demissie et al., 1996)

With a computational time step of 15 minutes, the hydrologic model was run for the above rainfall event. Predicted hydrographs at the four monitored tributary stations were compared with the monitored hydrographs. The curve numbers and the Manning's roughness factors were adjusted slightly for reasonable comparisons of the hydrographs shown in Figures 25 and 26. Predicted peak flows and time to peak flows matched very well with the observations at all four stations. However, the model underpredicted the remaining hydrographs, and thus the total runoff volumes for the storm by 19-28 percent. Such underprediction was due to the model's inability to simulate base flows. Underprediction grows with respect to basin size. For example, Friends Creek (Figure 26a) with a 112-square-mile subwatershed shows higher differences than the other subwatersheds about 40 square miles each. After deducting base flows from the observed hydrographs (Demissie et al., 1996), the difference between predicted and observed volumes of direct runoff ranged from 3 to 8 percent (overprediction). The model must be expanded to include tile drain and base flow simulations. Overall, the model performed very well during this calibration simulation. The model was calibrated easily and efficiently simply by making minor adjustments to the curve numbers and the Manning's roughness factors.

Figure 27 shows a series of predicted hydrographs from upstream to downstream at Fisher, Mahomet, and Monticello; inflows to Lake Decatur from all sources; and outflows from Lake Decatur. As expected, the model is predicting increasing runoff volumes and peak flows, except the outflow from Lake Decatur, and delayed hydrographs with increasing times to peak flows, towards downstream. The peak outflow from Lake Decatur is lower than the peak inflow to Lake Decatur due to the lake-storage effect used for flood control purposes; however, the volumes in and out are eventually the same. The hydrographs at Mahomet, Monticello, and Lake Decatur inflows show double peaks: the first peaks are the contributions from local and nearby tributaries, and the second peaks are the delayed contributions from the further upstream basins through the main stem of the Sangamon River. This figure shows model capability to simulate the dynamic behavior of flood flow and flood wave propagation in a large river basin.

Simulation of April 11-12, 1994 Storm: Model Verification

For verification purposes, the model was run for the rainfall event of April 11 (0:00 hours) - April 12 (12:00 hours), 1994. This was a major storm with a fairly uniform rainfall depth of 5.3 inches, computed based on measurements at the five stations mentioned above. Due to differences in season, ground cover, and antecedent moisture condition from the earlier storm, the curve numbers and roughness factors were revised. Figure 28 compares predicted and observed hydrographs at Camp Creek station. Similar to the earlier storm, the model predicted the peak flow and time to peak flow very well; however, it underpredicted the volume by 22 percent. When the observed base flow was separated, the volume difference reduced to 1 percent. The predicted rising limb of the

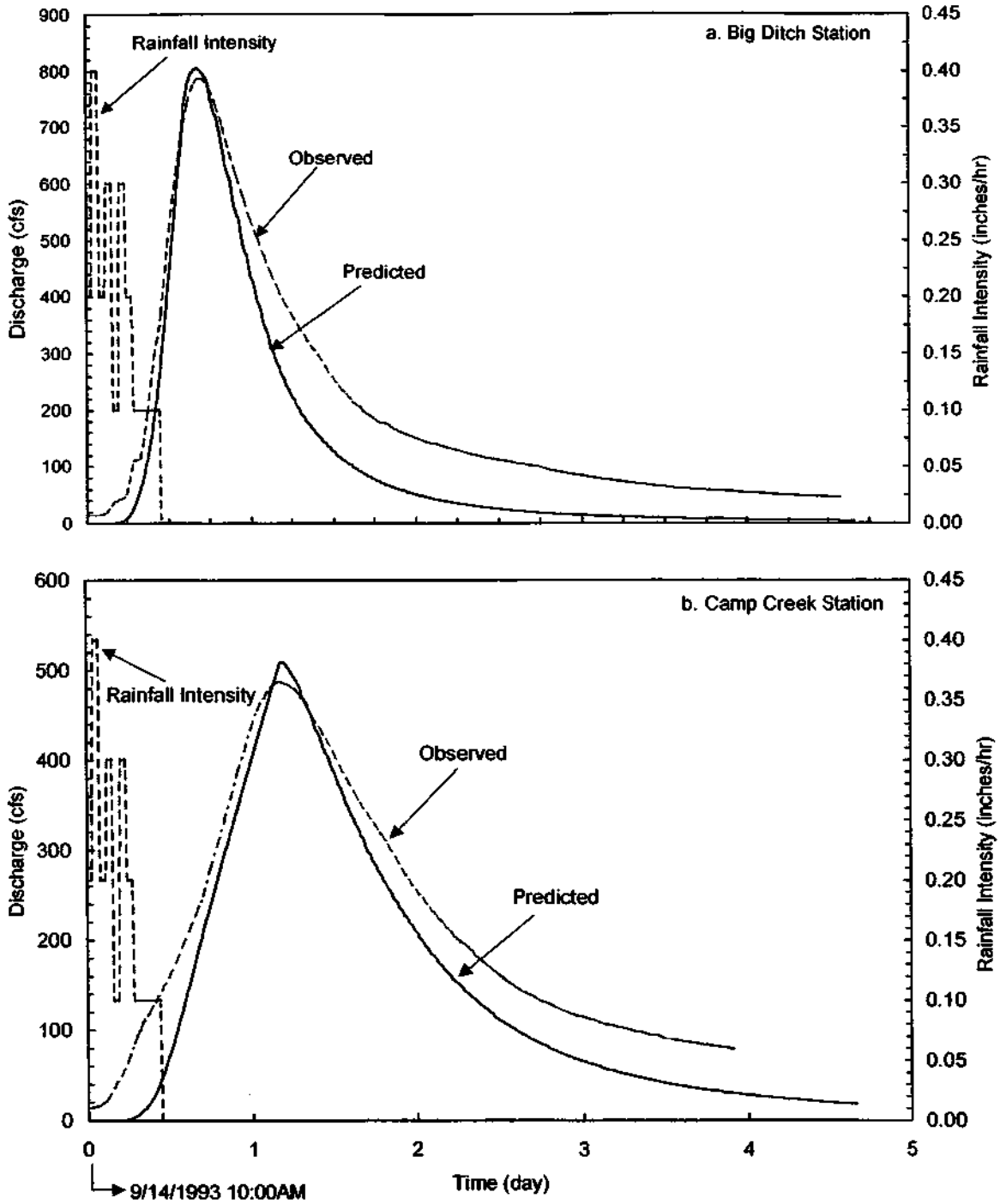

Figure 25. Comparison of hydrographs for September 14, 1993 storm at (a) Big Ditch station and (b) Camp Creek station

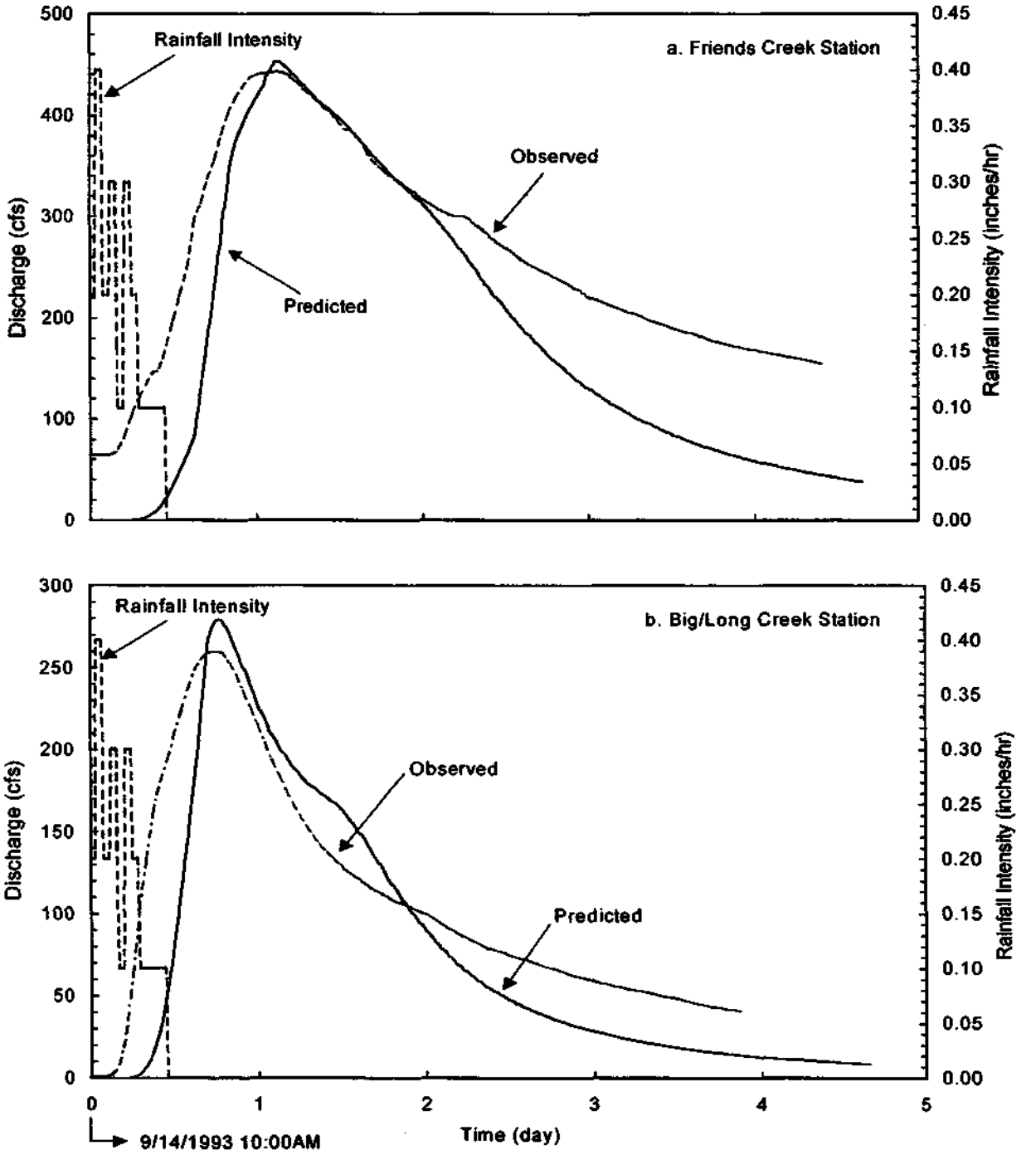

Figure 26. Comparison of hydrographs for September 14, 1993 storm at (a) Friends Creek station and (b) Big/Long Creek station

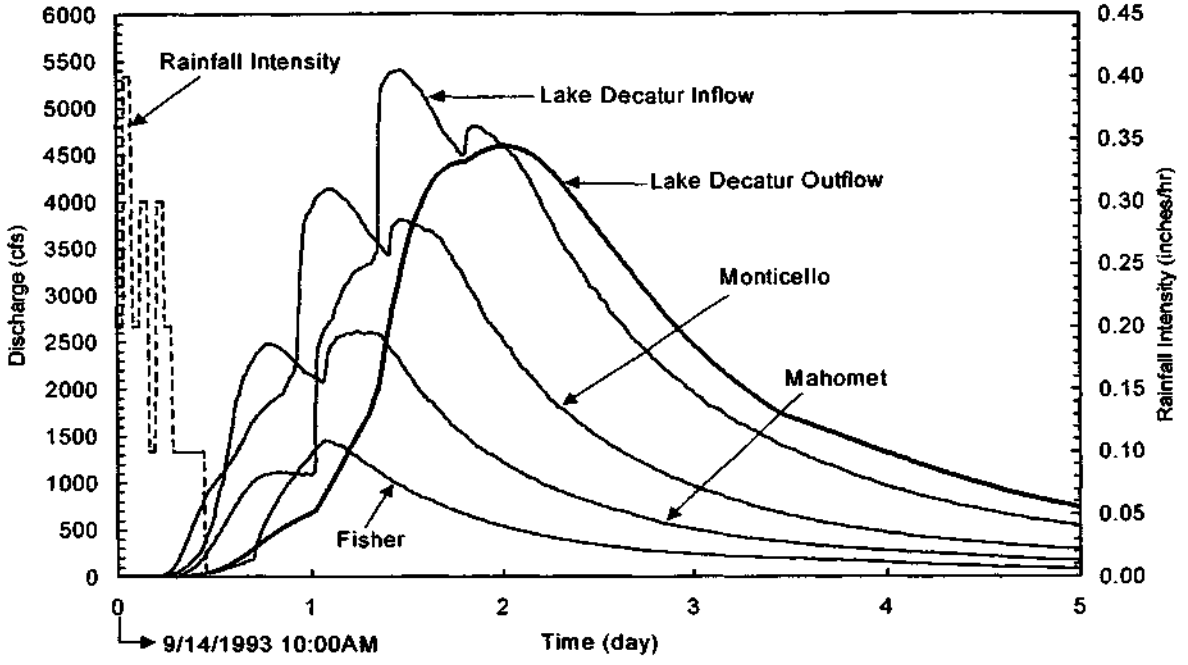

Figure 27. Predicted hydrographs along Upper Sangamon River for September 14, 1993 storm

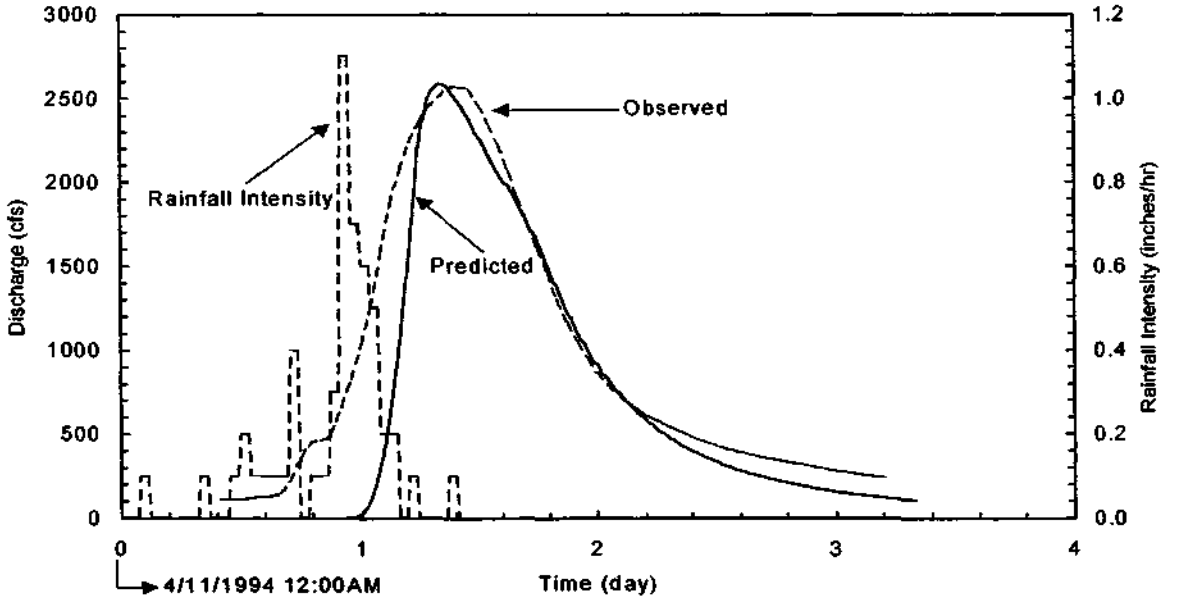

Figure 28. Comparison of hydrographs at Camp Creek station for April 11-12, 1994 storm

hydrograph is delayed by approximately 4 hours, which may be attributed to model inability to simulate tile drain flow. Overall, the model performed reasonably well for this storm as well.

Hydrologic and Sediment Simulations in Big Ditch Subwatershed

Simulations of 1998 Spring Storms

During the application of the hydrology component of the DWSM to the entire Lake Decatur watershed, described above, the basic data set for the entire watershed, including topographic and stream data, were prepared. Data were prepared for all subwatersheds, including the Big Ditch subwatershed. Using the same data for the Big Ditch subwatershed, a separate model of the Big Ditch subwatershed was developed. A new raingage station was installed in April 1998 near the Big Ditch monitoring station, and data from this gage were used in modeling the Big Ditch subwatershed.

As described earlier, the hydrology component of the DWSM has two alternative algorithms for computing rainfall excess, one using the runoff curve number and the other using an interception-infiltration procedure. The DWSM with both procedures was applied to the Big Ditch subwatershed for all storms during April-June 1998. Figure 29 compares the observed and predicted hydrographs for April-May storms and Figure 30 for June storms. Predicted results in Figures 29a and 30a used the curve number procedure, and Figures 29b and 30b used the interception-infiltration procedure. As seen in these comparisons, both procedures predicted the major storms reasonably well; however, the curve number procedure performed relatively better for small storms. Both procedures produced mixed results for the storm during days 8-10 (Figure 29), spatial variation of rainfall that was impossible to monitor with a single raingage, and inadequate accounting of antecedent moisture conditions in both the methods may be the reasons.

The DWSM with the soil erosion and sediment transport component was run on the Big Ditch subwatershed for the above storms. Predicted sediment discharges were compared with observed discharges for the storms during April-May (Figure 31a) and for storms during June 1998 (Figure 31b). As may be seen in these comparisons, the model is performing well for the major storms with high sediment discharges but poorly for small events. Better characterization of the detachment parameters may improve these predictions, which could be accomplished through extensive applications of the model in different watersheds. Tile drains also may play a very important role in these discrepancies, since tile and subsurface processes are more dominant during smaller storm events.

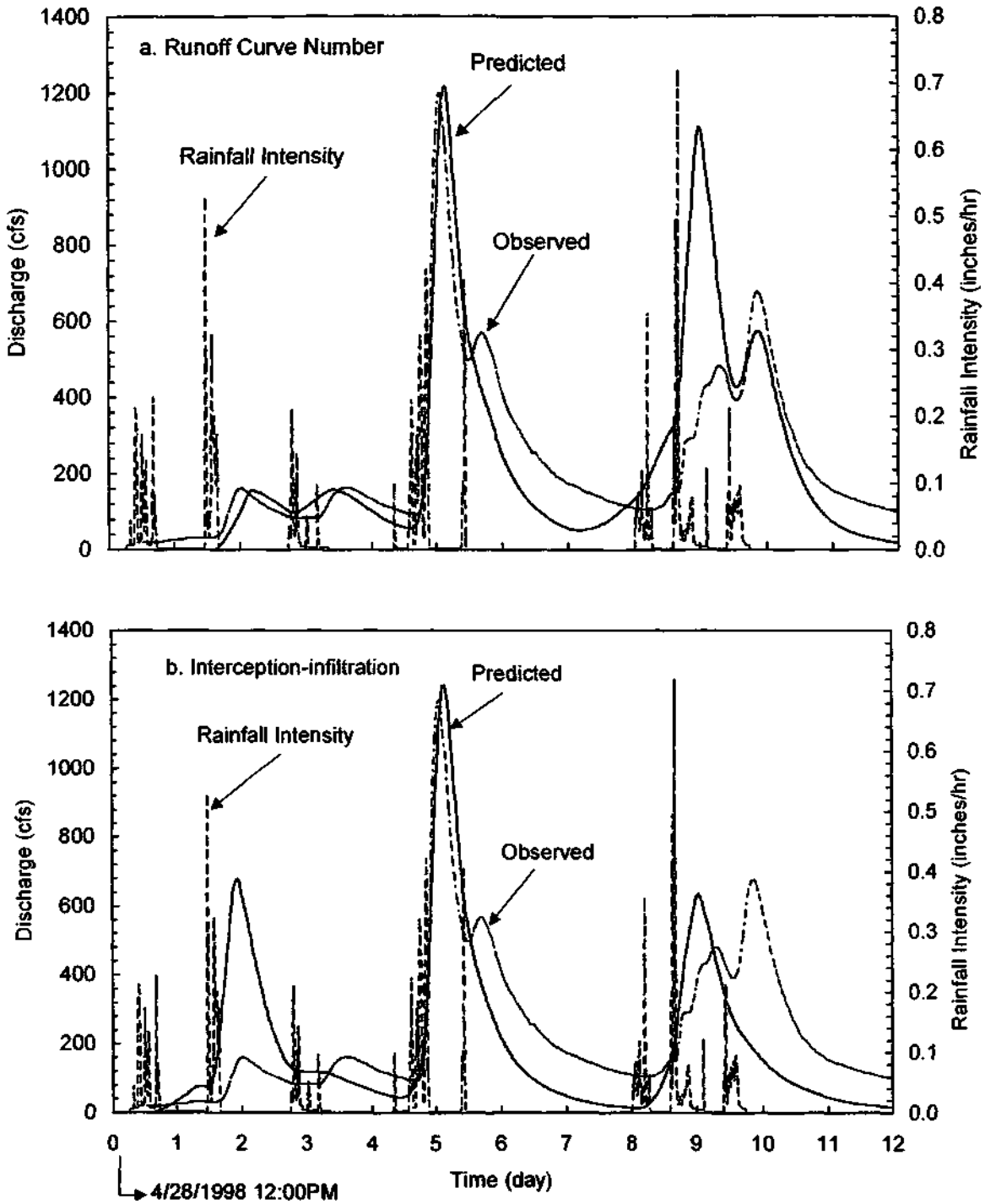

Figure 29. Comparison of observed and predicted hydrographs (using rainfall excess procedure) at Big Ditch station for storms in April-May 1998:
(a) runoff curve number and (b) interception-infiltration

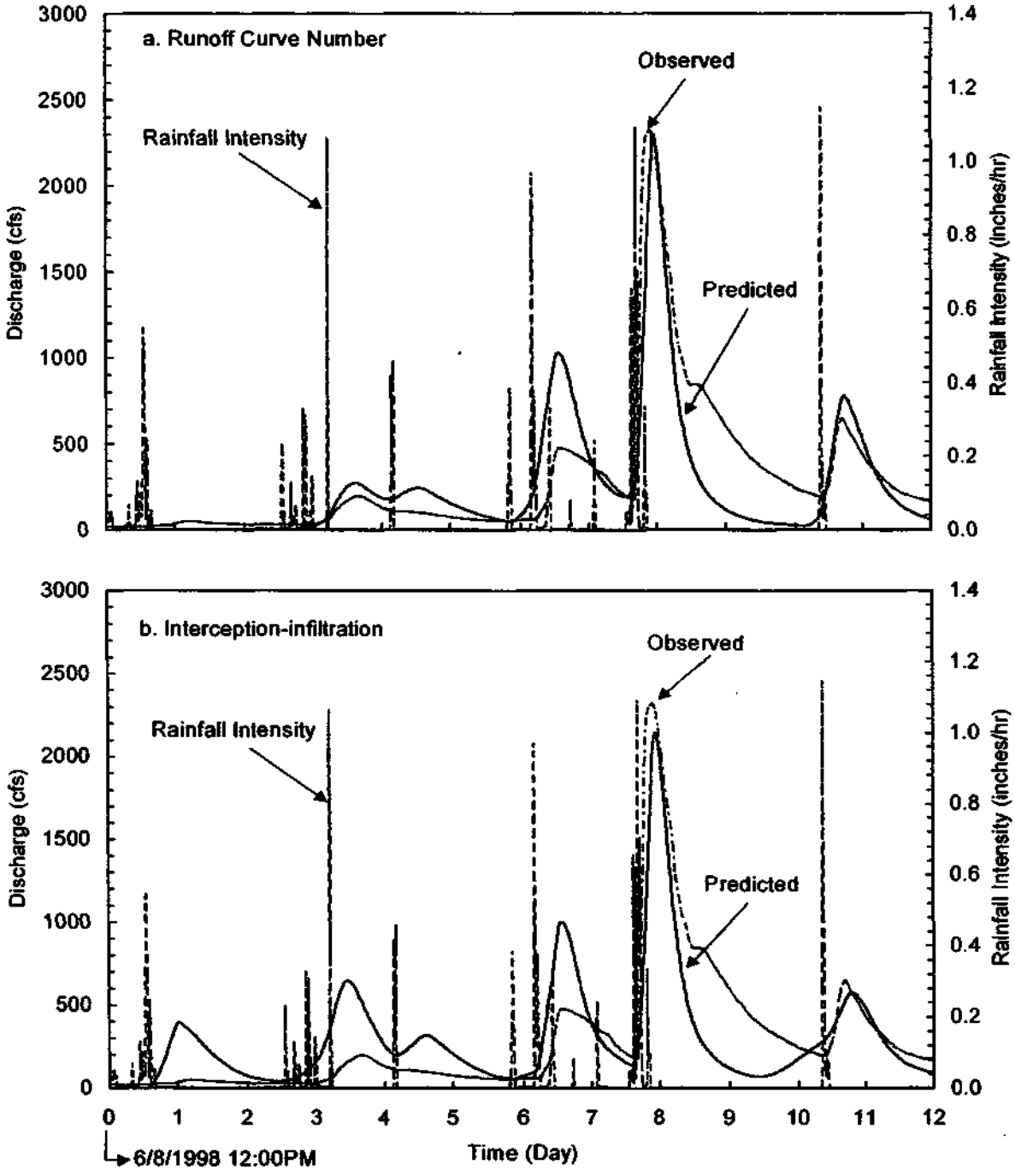

Figure 30. Comparison of observed and predicted hydrographs (using rainfall excess procedure) at Big Ditch station for storms in June 1998: (a) runoff curve number and (b) interception-infiltration

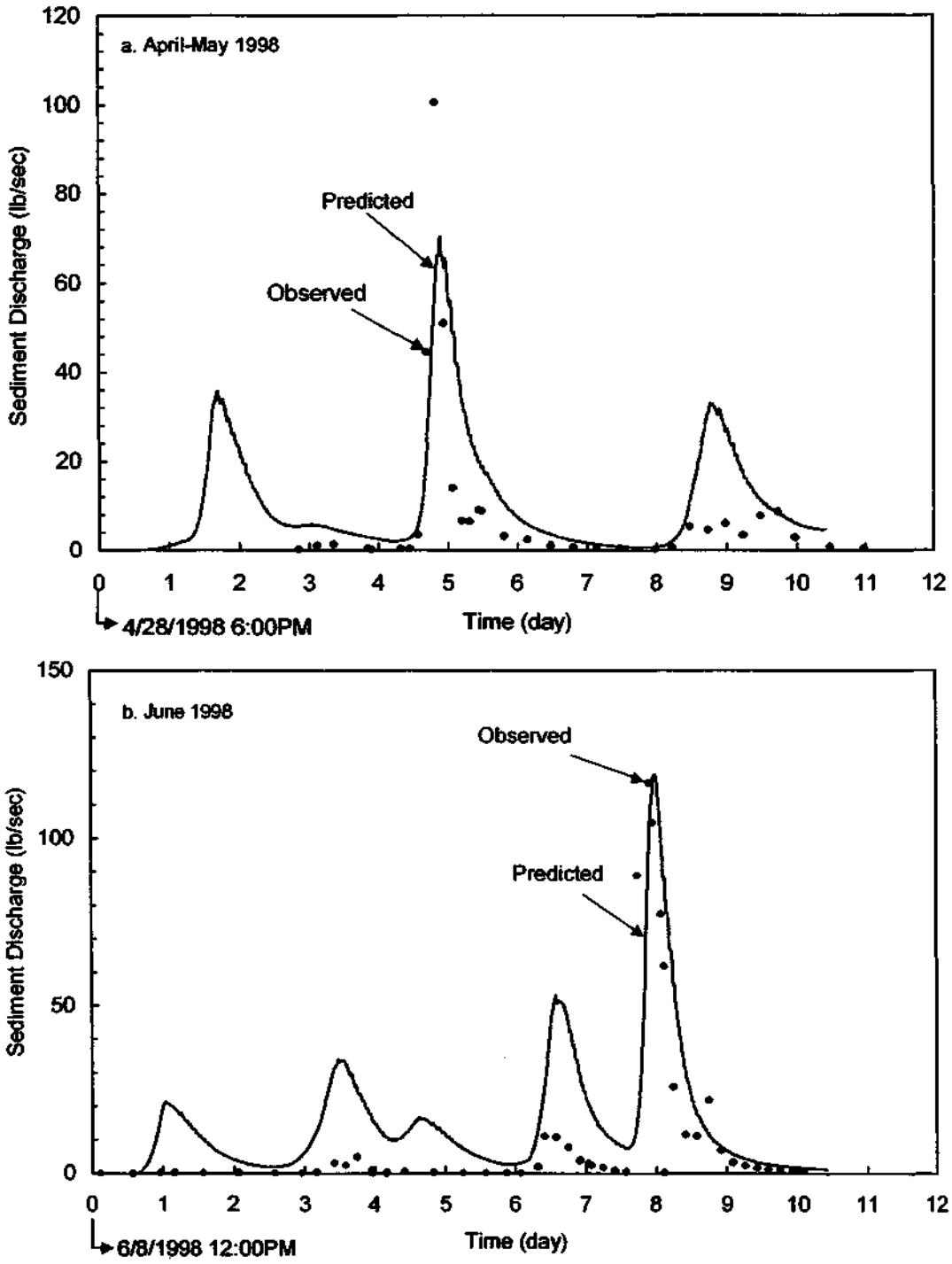

Figure 31. Comparison of observed and predicted sediment discharges at Big Ditch station for storms during (a) April-May 1998 and (b) June 1998

Simulation of April 15-16, 1999 Storm

During the 1999 monitoring period, only the April 15-16 storm generated high streamflows at the Big Ditch station. Both the hydrology and sediment were simulated for this storm. Figure 32 shows comparisons of the observed and predicted hydrographs and sediment discharges at the Big Ditch station. Due to the dry antecedent moisture conditions, both the curve number and flow detachment coefficient (FDC) were reduced by a reasonable fraction, curve number by 1 percent, and FDC from 0.003 to 0.002. As shown in Figure 32, the model predicted the peak flow and peak sediment discharge reasonably close to the observations. It predicted time to the above peaks almost perfectly. It overpredicted sediment volume, which again may be due to the lack of tile flow capability in the model. The model assumes all the flow as surface runoff predicting excess sediment.

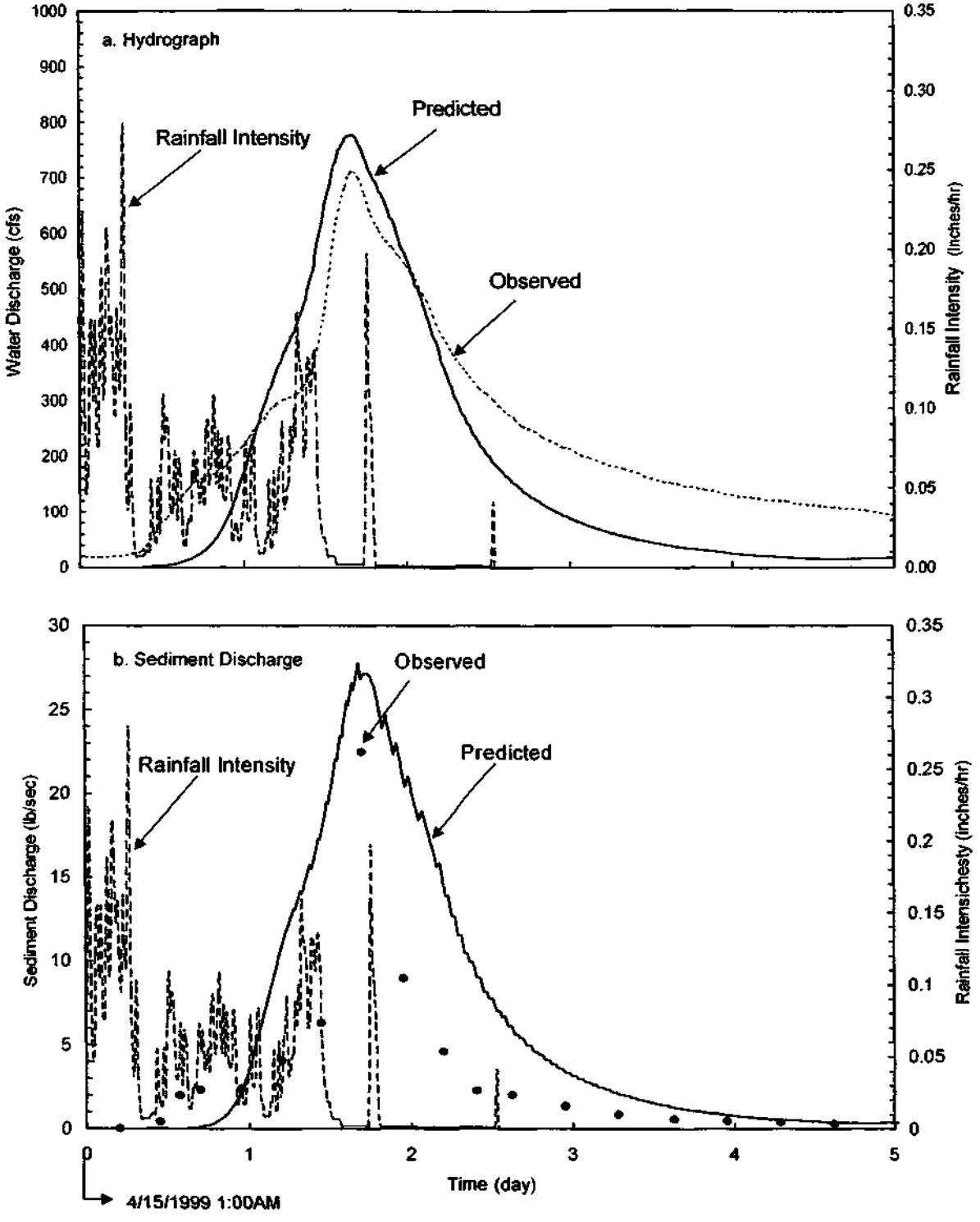

Figure 32. Comparison of observed and predicted (a) hydrograph and (b) sediment discharge at Big Ditch station for storm on April 15-16, 1999

Summary

A dynamic watershed simulation model (DWSM) is being developed at the Illinois State Water Survey (ISWS) using physically based governing equations to simulate propagation of flood waves, soil erosion, and entrainment and transport of sediment and all agricultural chemicals commonly used in agricultural and rural watersheds. The model has three major components: hydrology, soil erosion and sediment transport, and nutrient and pesticide transport. These model components, adopted from earlier work of the lead author, have efficient routing schemes based on approximate analytical solutions of the physically based governing equations, and preserving the dynamic behaviors of the water, sediment, and the accompanying chemical movements.

The hydrology component of the DWSM was tested on the 925-square-mile Upper Sangamon River basin in east-central Illinois, which drains into Lake Decatur, using data collected earlier by the ISWS. The model performed well in predicting peak flows and time to the peak flows in four monitored subwatersheds ranging in size from 38 to 112 square miles. However, the model underpredicted the recession and base flow portions of the hydrographs from larger subwatersheds due to lack of tile drain and base flow simulation capabilities.

Detailed flow and concentrations of suspended sediment, nitrate-N, phosphate-P, atrazine, and metolachlor were collected during 1998 spring storm events at the Big Ditch station, which drains a 38-square-mile subwatershed of the Lake Decatur watershed. During 1999, the same types of data, except metolachlor, were collected at Big Ditch and two other stations on the main stem of the Sangamon River: Fisher and Mahomet, which drain respectively, 240 and 360 square miles of the upper Sangamon River or Lake Decatur watershed. Rainfall data were collected from newly established raingages, one at Big Ditch during 1998 and five others in 1999 throughout the Upper Sangamon River watershed above Mahomet. Rainfall data from the six stations showed noticeable variability from station to station especially between the three eastern and three western stations. Therefore, adequate raingages are needed to record spatial variations of rainfall to adequately understand the physical and chemical processes and the associated problems in a watershed.

In the above monitored data, all the constituents closely followed the flow hydrograph except nitrate-N for which concentration varied inversely with water discharge, decreasing drastically during rising and peak flows, and increasing with the recession and base flow portions of the hydrographs. Such variations may be due to the pathways of runoff. Runoff through subsurface soil and tile drain contains more nitrate-N than runoff over the ground surface (surface runoff). Therefore, peak flows, primarily contributed by surface runoff contain less nitrate-N concentrations than water in the recession and base flows contributed by tile drain and subsurface flows through the soil matrix. Another reason could be a limited release of nitrate-N from the soil, where the

threshhold could be reached before the peak flow and beyond dilution until the flow return to a level lower than the threshhold.

The monitored constituent data were analyzed to confirm consistencies of different sampling methods, and to develop statistical relationships of suspended sediment and chemical concentrations with the observed flow. The results corifirmed consistencies of grab and automatic ISCO sampling procedures while monitoring suspended sediment, nitrate-N, and phosphate-P. Results from both grab and ISCO sampling were further confirmed using the depth-width-integrated sampling method to monitor suspended sediment.

The correlation equations of suspended sediment, nitrate-N, phosphate-P, atrazine, and metolachlor concentrations with flow are consistent with the observations made above regarding variations of the constituents with respect to the water discharge. The relations showed an exponential increase for suspended sediment, exponential decay for nitrate-N, and power and logarithmic functions for phosphate-P, atrazine, and metolachlor with respect to water discharge. In addition to a combined relation for each of the constituents with respect to water discharge, separate equations were developed for each month during the monitoring period. These relations suggested that concentrations of the constituents showed a different strong correlation with water discharge in different months representing different times in the growing season with varying climate and ground cover conditions. Therefore, a single correlation equation may not be adequate to estimate constituent concentration from water discharge during the growing season.

The flow data monitored at the Big Ditch station were used to test and compare two different hydrologic algorithms of the DWSM. Both the curve number and interception-infiltration algorithms performed well in predicting peak and time to peak flows of intense storms, but the curve number performed better in predicting the less intense storms. Sediment data monitored at Big Ditch were used to test the sediment component of the DWSM. The model performed well in predicting intense storms, but poorly for less intense storms, perhaps because of model inability to simulate tile and base flows. Testing the nutrient and pesticides component of DWSM is in progress, and will continue in foliowup studies.

The study provides a valuable database of continuous rainfall, runoff, sediment, nitrogen, phosphorous, atrazine, and metolachlor in an east-central Illinois watershed collected during storm events. These data help us understand the complex physical and chemical processes in the watershed. The study also provides the model as an advanced tool for engineers, scientists, and public policy makers to deal with watershed protection issues involving both the surface and ground waters and to make environmentally and economically sound watershed management decisions.

Due to its extensive water, sediment, and pollutant routing schemes incorporating most dynamic behaviors, the DWSM provides a sound base for further development. For Illinois hydrologic conditions, the model must be further developed with tile drain and

base flow routines, which will help improve the predictions of recession and base flow portions of the hydrographs, and also sediment discharges. The model also provides a sound base for further development in the simulations of streambank erosion and detailed stream sediment transport. Streambank erosion and sedimentation are major problems in many of the Illinois watersheds. Finally, the model must be further tested in various Illinois watersheds with different hydrologic and climatic conditions.

References

Abbott, M.B., J.C. Bathurst, J.A. Cunge, P.E. O'Connell, and J. Rasmussen. 1986a. An introduction to the European Hydrological System - Systeme Hydrologique Europeen "SHE" 1: History and philosophy of a physically based distributed modelling system. *Journal of Hydrology* 87: 45-59.

Abbott, M.B., J.C. Bathurst, J.A. Cunge, P.E. O'Connell, and J. Rasmussen. 1986b. An introduction to the European Hydrological System - Systeme Hydrologique Europeen "SHE" 2: Structure of a physically based distributed modelling system. *Journal of Hydrology* 87: 61-77.

Ahuja, L.R. 1982. Release of a soluble chemical from soil to runoff. *Transactions of the ASAE* 25(4): 948-956, 960.

Ahuja, L.R. and O.R. Lehman. 1983. The extent and nature of rainfall-soil-interaction in the release of soluble chemicals to runoff. *Journal of Environmental Quality* 12(1): 34-40.

Alonso, C.V., W.H. Neibling, and G.R. Foster. 1981. Estimating sediment transport capacity in watershed modeling. *Transactions of the ASAE* 24(5): 1211-1220, 1226.

Arnold, J.G., J.R. Williams, and D.R. Maidment. 1995. Continuous-time water and sediment-routing model for large basins. *Journal of Hydraulic Engineering* 121(2): 171-183.

Arnold, J.G., J.R. Williams, A.D. Nicks, and N.B. Sammons. 1990. *SWRRB - A Basin Scale Simulation Model for Soil and Water Resources Management.* Texas A & M Press, College Station, TX.

Ashraf, M.S., and D.K. Borah. 1992. Modeling pollutant transport in runoff and sediment. *Transactions of the ASAE*35(6): 1789-1797.

Azam, F., F.W. Simmons, and R.L. Mulvaney. 1993. Mineralization of N from plant residues and its interaction with a native soil. *Soil Biology and Biochemistry* 25: 1787-1792.

Baily, G.W., R.R. Swank, Jr., and H.P. Nicholson. 1974. Predicting pesticide runoff from agricultural land: A conceptual model. *Journal of Environmental Quality* 6(2): 159-162.

Beasley, D.B., L.F. Huggins, and E.J. Monke. 1980. ANSWERS: A model for watershed planning. *Transactions of the ASAE* 23(4): 938-944.

Bicknell, B.R., J.C. Imhoff, J.L. Kittle, Jr., A.S. Donigian, Jr., and R.C. Johanson. 1993. *Hydrologic Simulation Program - FORTRAN (HSPF) User's Manual for Release 10.* Report No. EPA/600/R-93/174. U.S. EPA Environmental Research Laboratory, Athens, GA.

Borah, D.K. 1989a. Runoff simulation model for small watersheds. *Transactions of the ASAE* 32(3): 881-886.

Borah, D.K. 1989b. Sediment discharge model for small watersheds. *Transactions of the ASAE* 32(3): 874-880.

Borah, D.K., C.V. Alonso, and S.N. Prasad. 1981. *Stream channel stability, Appendix I: Single event numerical model for routing water and sediment on small catchments.* USDA Sedimentation Laboratory, Oxford, MS.

Borah, D.K., M. Bera, S. Shaw, L. Keefer, and M. Demissie. 1999. Dynamic modeling of sediment, nutrient, and pesticide transport in agricultural watersheds during severe storm events. *Proceedings of the Ninth Annual Conference, Illinois Groundwater Consortium,* April 1, 1999, Carbondale, IL: 24-38.

Borah, D., M. Demissie, and L. Keefer. 1996a. Modeling the Lake Decatur Watershed in Illinois to evaluate effects of best management practices on nitrate loading. *Proceedings of the North America Water and Environment Congress '96,* June 22-28, 1996, Anaheim, CA, ASCE: CD-ROM.

Borah, D., M. Demissie, and L. Keefer. 1996b. Effect of best management practice locations in the Upper Sangamon River basin on nitrogen loading to Lake Decatur. *Proceedings of RiverTech96, 1st International Conference on New/Emerging Concepts for Rivers,* September 22-26, Chicago, IL, International Water Resources Association: 665-672.

Borah, D.K., M. Demissie, L. Keefer, M. Bera, and S. Shaw. 1998. Dynamic modeling of sediment, nutrient, and pesticide transport in agricultural watersheds during severe storm events. *Proceedings of the Eighth Annual Conference, Illinois Groundwater Consortium,* April 1-2, 1998, Makanda, IL: 128-150.

Borah, D.K., S.N. Prasad, and C.V. Alonso. 1980. Kinematic wave routing incorporating shock fitting. *Water Resources Research* 16(3): 529-541.

Brezonik, P.L., V.J. Bierman, R. Alexander, J. Anderson, J. Barko, M. Dortch, L. Hatch, D. Keeney, D. Mulla, V. Smith, C. Walker, T. Whitledge, and W. Wiseman. 1999. Effects of reducing nutrient loads to surface waters within the Mississippi River basin and the Gulf of Mexico. *Task Group 4 Report, Gulf of Mexico Hypoxia Assessment.* White House Committee on Environment and Natural Resources, Washington, D.C.

Chow, V.T. 1959. *Open-Channel Hydraulics.* McGraw-Hill Book Company, New York.

Committee on Watershed Management. 1999. *New Strategies for America's Watersheds.* National Research Council, National Academy Press, Washington, D.C.

Coupe, R.H., and G.P. Johnson. 1991. Triazine herbicides in selected streams in Illinois during storm events, spring 1990, pp. 343-346. In G.E. Mallard and D.A. Aronson (eds.), *U.S. Geological Survey Toxic Substances Hydrology Program - Proceedings of the Technical Meeting,* Monterey, CA, March 11-15,1991, Water Resources Investigation Report 91-4034, U.S. Geological Survey, Reston, VA.

Demissie, M., L. Keefer, D. Borah, V. Knapp, S. Shaw, K. Nichols, and D. Mayer. 1996. *Watershed Monitoring and Land Use Evaluation for the Lake Decatur Watershed.* Miscellaneous Publication 169, Illinois State Water Survey, Champaign, IL.

Demissie, M. L. Keefer, and R. Xia. 1992. *Erosion and Sedimentation in the Illinois River Basin.* ILENR/RE-WR-92/04. Illinois Department of Energy and Natural Resources, Springfield, IL.

Demissie, T.W. Soong, and N.G. Bhowmik. 1988. *Hydraulic Investigation for the Construction of Artificial Islands in Peoria Lake.* ILENR/RE-WR-88/15. Illinois Department of Energy and Natural Resources, Springfield, IL.

Doering, O.C., F. Diaz-Hermelo, C. Howard, R. Heimlich, F. Hitzhusen, R. Kazmierczak, J. Lee, L. Libby, W. Milon, T. Prato, and M. Ribaudo. 1999. Evaluation of economic costs and benefits of methods for reducing nutrient loads to the Gulf of Mexico. *Task Group 6 Report, Gulf of Mexico Hypoxia Assessment.* White House Committee on Environment and Natural Resources, Washington, D.C.

Donigian, A.S. Jr., B.R. Bicknell, and J.L. Kittle, Jr. 1986. *Conversion of the Chesapeake Bay basin model to HSPF operation.* AQUA TERRA Consultants for the Computer Science Corporation, Annapolis, MD and U.S. EPA Chesapeake Bay Program, Annapolis, MD.

Fitzpatrick, W.P., W.C. Bogner, and N.G. Bhowmik. 1985. *Sedimentation Investigation of Lake Springfield, Springfield, Illinois.* Contract Report 363, Illinois State Water Survey, Champaign, IL.

Fitzpatrick, W.P., W.C. Bogner, and N.G. Bhowmik. 1987. *Sedimentation and Hydrologic Processes in Lake Decatur and Its Watershed.* Report of Investigation 107, Illinois State Water Survey, Champaign, IL.

Foster, G.R., R.A. Young, and W.H. Neibling. 1985. Sediment composition for nonpoint source pollution analyses. *Transactions ofthe ASAE* 28(1): 133-139, 146.

Gast, R.G., W.W. Nelson, and G.W. Randall. 1978. Nitrate accumulation in soils and loss in tile drainage following nitrogen applications to continuous corn. *Journal of Environmental Quality* 7: 258-261.

Gentry, L.E., M.B. David, K.M. Smith, and D.A. Kovacic. 1998. Nitrogen cycling and tile drainage nitrate loss in a corn/soybean watershed. *Agricultural Ecosystem Environment* 68: 85-97

Goolsby, D.A., W.A. Battaglin, G.B. Lawrence, R.S. Artz, B.T. Aulenbach, R.P. Hooper, D.R. Keeney, and G.J. Stensland. 1999. Flux and sources of nutrients in the Mississippi-Atchafalaya River Basin. *Task Group 3 Report, Gulf of Mexico Hypoxia Assessment.* White House Committee on Environment and Natural Resources, Washington, D.C.

Goolsby, D.A., W.A. Battaglin, and E.M. Thurman. 1993. Occurrence and transport of agricultural chemicals in the Mississippi River basin, July through August 1993. *U.S. Geological Survey Circular* 1120-C, Denver, CO.

Guy, H.P. 1969. Laboratory theory and methods for sediment analysis. *Techniques of Water Resources Investigations of the U.S. Geological Survey.* Book 5, Chapter CI, U.S. Government Printing Office, Washington, D.C.

Guy, H.P., and V.W. Norman. 1970. Field methods for measurement of fluvial sediment. *Techniques of Water-Resources Investigations of the U.S. Geological Survey.* Book 3, Chapter C2, U.S. Government Printing Office, Washington, D.C.

Heathman, G.C., L.R. Ahuja, and O.R. Lehman. 1985. The transfer of soil applied chemicals to runoff. *Transactions of the ASAE* 28(6): 1909-1915, 1920.

Hubbard, R.K., R.G. Williams, and M.D. Erdman. 1989a. Chemical transport from coastal plain soils under simulated rainfall: I. Surface runoff, percolation, nitrate, and phosphate movement. *Transactions of the ASAE 32{A):* 1239-1249.

Hubbard, R.K., R.G. Williams, and M.D. Erdman. 1989b. Chemical transport from coastal plain soils under simulated rainfall: II. Movement of cyanazine, sulfometuron-methyl, and bromide. *Transactions of the ASAE* 32(4): 1250-1257.

Illinois Department of Agriculture (IDOA). 1987. Division of Marketing, *Bureau of Agricultural Statistics*, Bulletin 87-1, IDOA, Springfield, IL.

Imhoff, J.C., B.R. Bicknell, and A.S. Donigian, Jr. 1983. *Preliminary application of HSPF to the Iowa River basin to model water quality and the effects of agricultural best management practices.* EPA-600/3-83-068. U.S. EPA Environmental Research Laboratory, Athens, GA.

Ingram, J.J. and D.A. Woolhiser. 1980. Chemical transfer into overland flow. In *Proceedings Symposium Water Management,* 21-23 July 1980, Boise, ID, ASCE: 40-53.

Instrumentation Specialties Company (ISCO). 1975. *Instruction Manual: Model 1680 Sampler with L.E.D. Readout.* ISCO, Lincoln, NE.

Jordan, T.E., D.L. Correll, and D.E. Weller. 1997. Effects of agriculture on discharges of nutrients from coastal plain watersheds of Chesapeake Bay. *Journal of Environmental Quality* 26: 836-848.

Jordan, T.E., D.L. Correll, D.E. Weller, and N.M. Goff. 1995. Temporal variation in precipitation chemistry on the shore of the Chesapeake Bay. *Water Air Soil Pollution* 83: 263-284.

Julien, P.Y., and B. Saghafian. 1991. *A two-dimensional watershed rainfall-runoff model-CASC2D user's manual.* Civil Engineering Report CER90-91PYJ-BS-12, Colorado State University, Fort Collins, CO.

Julien, P.Y., B. Saghafian, and F.L. Ogden. 1995. Raster-based hydrologic modeling of spatially-varied surface runoff. *Water Resources Bulletin* 31: 523-536.

Kay, J.M. and R.M. Nedderman. 1985. *Fluid Mechanics and Transfer Processes.* Cambridge University Press, Cambridge, MA.

Keefer, L., M. Demissie, D. Mayer, K. Nichols, and S. Shaw. 1996. *Watershed Monitoring and Land Use Evaluation for the Vermilion River Watershed.* Miscellaneous Publication 176, Illinois State Water Survey, Champaign, IL.

Knisel, W.G. (ed.). 1980. *CREAMS: A field-scale model for chemicals, runoff, and erosion from agricultural management system.* Conservation Research Report 26, USDA-SEA, Washington, D.C.

Lane, L.J. and M.A. Nearing (eds.). 1989. *USDA - water erosion prediction project: hillslope profile model documentation.* NSERL Report No. 2, USDA-ARS National Soil Erosion Research Laboratory, West Lafayette, IN.

Laursen, E. 1958. The total sediment load of stream. *Journal of the Hydraulics Division,* ASCE 54(HY 1): 1-36.

Leonard, R.A., W.G. Knisel, and D.A. Still. 1987. GLEAMS: Groundwater loading effects on agricultural management systems. *Transactions of the ASAE* 30(5): 1403-1428.

Lighthill, M.J., and C.B. Whitham. 1955. On kinematic waves, 1, flood movement in long rivers. *Proceedings of the Royal Society,* London, **Ser.** A(229): 281-316.

Liszewski, M.J., and P.J. Squillace. 1991. The effect of surface-water and groundwater exchange on the transport and storage of atrazine in the Cedar River, Iowa, pp: 195-202, In G.E. Mallard and D.A. Aronson (eds.) *U.S. Geological Survey Toxic Substances Hydrology Program - Proceedings of the Technical Meeting,* Monterey, CA, March 11-15, 1991, Water Resources Investigation Report 91-4034, U.S. Geological Survey, Reston, VA.

Lowrance, R. 1992. Nitrogen outputs from a field-size agricultural watershed. *Journal of Environmental Quality* 21: 602-607.

Mitchell, J.K., A.S. Felsot, and M.C. Hirschi. 1994. Agricultural practices for water quality improvement. *Proceedings of the Fourth Annual Conference, Illinois Groundwater Consortium,* March 23-24, 1994, Makanda, IL: 13-24.

Mitsch, W.J., J.W. Day, J.W. Gilliam, P.M. Groffman, D.L. Hey, G.W. Randall, and N. Wang. 1999. Reducing nutrient loads, especially nitrate-nitrogen, to surface water, groundwater, and the Gulf of Mexico. *Task Group 5 Report, Gulf of Mexico Hypoxia Assessment.* White House Committee on Environment and Natural Resources, Washington, D.C.

Parr, A.D., C. Richardson, D.D. Lane, and D. Baughman. 1987. Pore water uptake by agricultural runoff. *Journal of Environmental Engineering, ASCE* **113(1):** 49-63.

Patni, N.K., L. Masse, P.Y. Jui. 1996. Tile effluent quality and chemical losses under conventional and no tillage: I. Flow and nitrate. *Transactions of the ASAE* **39:** 1665-1672.

Pike, D.R. 1985.*1985 Illinois major crop pesticide use and safety survey report.* College of Agriculture, Department of Agronomy, University of Illinois at Urbana-Champaign, Urbana, IL.

Rajagopal, R. 1993. *Herbicides in water resources during the Great Midwestern Flood of 1993.* University of Iowa, Department of Geography, Iowa City, IA.

Ray, C, T.W.D. Soong, G.S. Roadcap, and D.K. Borah. 1998. Agricultural chemicals: effects on wells during floods. *Journal of American Water Works Association* 90**(7):** 90-100.

Roseboom, D., R.L. Evans, J. Erickson, and L.G. Brooks. 1982. *An Inventory of Court Creek Watershed Characteristics that May Relate to Water Quality in the Watershed.* Contract Report 322, Illinois State Water Survey, Peoria, IL.

Sharpley, A.N., L.R. Ahuja, and R.G. Menzel. 1981. The release of soil phosphorous to runoff in relation to kinetics of desorption. *Journal of Environmental Quality* 10: 386-391.

Simons, D.B., R.M. Li, and M.A. Stevens. 1975. *Development of models for predicting water and sediment routing and yield from storms on small watersheds.* Colorado State University, Fort Collins, CO.

Smith, R.A., R.B. Alexander, and K.J. Lanfear. 1993. Stream water quality in the conterminous United States: Status and trends of selected indicators during the 1980's. In: National Water Summary 1990-91: Hydrologic events and stream water quality. *U.S. Geological Survey Water Supply Paper* 2400: 111-140.

Smith, R.E., and J.Y. Parlange. 1978. A parameter-efficient hydrologic infiltration model. *Water Resources Research* 14(3): 533-538.

Soil Conservation Service. 1972. Hydrology. Section 4. In *National Engineering Handbook.* SCS, Washington, D.C.

USEPA. 1983. *Methods of chemical analysis of water and wastes.* EPA-600/4-79-020, USEPA, NERL-Cincinnati, Cincinnati, OH.

USEPA. 1991. *Methods for the determination of organic compounds in drinking water.* EPA/600/4-88/039, USEPA, Cincinnati, OH.

USEPA. 1993. *Methods for the determination of inorganic substances in environmental samples.* EPA-600/R-93-100, USEPA, Cincinnati, OH.

USEPA. 1997. *Deposition of Air Pollutants to the Great Waters.* Second Report to the Congress, June 30, 1997, USEPA, Washington, D.C.

Vagstad, N., H.O. Eggestad, and T.R. Hoyas. 1997. Mineral nitrogen in agricultural soils and nitrogen losses: Relation to soil properties, weather conditions, and farm practices. *Ambio* 26: 266-272.

Wang, W., and P. Squillace. 1994. Herbicide interaction between a stream and the adjacent alluvial aquifer. *Environmental Science Technology* 28: 2336-2344.

Wiese, A.I., K.E. Savage, J.M. Chandlars, L.C. Liu, L.S. Jeffry, J.B. Weber, and K.S. Lafleurs. 1980. Loss of fluometuronin in runoff water. *Journal of Environmental Quality* 9(1): 1-5.

Williams, J.R., C.A. Jones, and P.T. Dyke. 1984. A modeling approach to determine the relationship between erosion and soil productivity. *Transactions of the ASAE* 27(1): 129-144.

Williams, J.R., A.D. Nicks, and J.G. Arnold. 1985. Simulator for water resources in rural basins. *Journal of Hydraulic Engineering* 111(6): 970-986.

Woolhiser, D.A., R.E. Smith, and D.C. Goodrich. 1990. *KINEROS, A kinematic runoff and erosion model: Documentation and User Manual.* ARS-77, U.S. Department of Agriculture, Agricultural Research Service, Fort Collins, CO.

Yalin, M.S. 1963. An expression for bed-load transportation. *Journal of the Hydraulics Division* ASCE 89(HY 3): 221-250.

Yang, C.T. 1973. Incipient motion and sediment transport. *Journal of the Hydraulics Division,* ASCE 99(HY 10): 1679-1704.

Young, R.A., C.A. Onstad, D.D. Bosch, and W.P. Anderson. 1987. *AGNPS, Agricultural nonpoint source pollution model: A watershed analytical tool.* U.S. Department of Agriculture Conservation Research Report 35, National Technical Information Service, Springfield, VA.

Young, R.A., C.A. Onstad, D.D. Bosch, and W.P. Anderson. 1989. AGNPS: A Nonpoint Source Pollution Model for Evaluating Agricultural Watersheds. *Journal of Soil and Water Conservation* 44(2): 168-173.

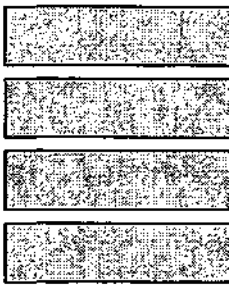


ILLINOIS
DEPARTMENT OF
NATURAL
RESOURCES